boletim paranaense
degeociências

Volume 76 (2020) 1: 1-69

A photographic atlas of the architecture, flow geometry and morphology, and facies of the Serra Geral Group (Paraná Igneous Province) in the state of Paraná, Brazil.

Um atlas fotográfico da arquitetura, geometria e morfologia dos derrames e fácies do Grupo Serra Geral (Província Ígnea do Paraná) no estado do Paraná, Brasil.

OTAVIO BONI LICHT1; EDIR EDEMIR ARIOLI2

1 PPGEOL, Universidade Federal do Paraná-UFPR, Curitiba, Paraná, Brasil; otavio.licht@gmail.com
2 Independent consultant; earioli@yahoo.com.br

Abstract
The rocks that make up the Serra Geral Group spread over approximately 100,000 km2 of the State of Paraná, which represent half of its territory and about 10% of the Paraná Igneous Province. The geologic mapping of the Serra Geral Group in the State of Paraná was carried on from 2003 to 2018, and revealed a great diversity of features and facies of basic and acidic lava flows, as well as the presence of interbedded volcaniclastic deposits. This paper presents an inventory of this geodiversity along with brief descriptions, a wealth of photographic documentation, and the georeferenced location of each outcrop, making it easy to access the documented sites, in order to assist the development of scientific research in this geologic compartment. The processes responsible for the lithologic features are interpreted in compliance to the knowledge accumulated on the various continental basaltic provinces by many researchers, including the authors of this paper, so to build up a genetic system for the Serra Geral Group more complete and coherent with the paleogeography of Gondwana in its initial breakup stage. In the early Cretaceous, during ca. 1.2 Ma with the paroxysm at 134.7 Ma, a huge magma amount, which is estimated at least in 600,000 km3, flowed over the thick sedimentary Paleozoic sequence of the Paraná Basin, stacking up a volcanic sequence. The interaction between the rising magma with the sedimentary sequence up to 7,000 m thick, gave rise also to thousands of intrusive bodies, such as sills and dikes, almost all of a basic nature. Furthermore, the ascending magma interacting with deep aquifer systems gave rise to explosive volcanism – hydrovolcanism – which produced many mafic volcaniclastic deposits (MVDs), interbedded to the basic flows. Thus, in South America, during this relatively short lapse of time, basic and acidic flows covered the Paraná Basin, being reported in Brazil, Argentina, Paraguay, and Uruguay under diverse names. In the present article, it will be referred as Serra Geral Group (SGG). The lithological inventory represented by the present photographic atlas comprises diagnostic features of basalt, andesi-basalt, rhyolite and dacite lava flows, mafic volcaniclastic deposits, and dikes of basic composition.

Keywor ds: Paraná Igneous Province, volcanism, hydrovolcanism, facies, pictures

Resumo

As rochas que compõem o Grupo Serra Geral, ocupam no Estado do Paraná, cerca de 100.000 km². Isso representa cerca de 10% de toda a Província Ígnea do Paraná. Iniciado em 2003 e finalizado em 2018, o mapeamento geológico do Grupo Serra Geral no Estado do Paraná, mostrou a grande diversidade de morfologias e fácies de derrames de lavas básicas e ácidas, e a presença de depósitos vulcanoclásticos intercalados aos derrames básicos. O presente artigo tem como objetivo, apresentar sinteticamente essa geodiversidade com breves descrições, farta documentação fotográfica e com a localização dos sítios, facilitando o acesso e contribuindo assim para o incremento das pesquisas nesse compartimento geológico que ocupa praticamente a metade do território paranaense. Os processos formadores dessas feições litológicas são interpretados com base no conhecimento acumulado nas províncias de basaltos continentais por vários pesquisadores, inclusive pelos autores deste artigo, de modo a elaborar um sistema genético para o Grupo Serra Geral mais completo e coerente coma paleogeografia do Gondwana em sua fase inicial de ruptura. No Cretáceo Inferior, durante um curto período de 1,2 Ma com paroxismo a 134,7 Ma, um gigantesco volume de magma, estimado em 600.000 km3, recobriu a sequência sedimentar paleozoica da Bacia do Paraná, dando origem à província vulcânica. A interação do magma em ascensão com a sequência sedimentar com pelo menos 7.000 m de espessura originou também milhares de corpos intrusivos, tais como diques e soleiras, quase todos de composição básica. Além disso, a interação do magma com os sistemas aquíferos profundos da Bacia do Paraná, deu origem a vulcanismo explosivo – hidrovulcanismo – responsável pela formação de muitos depósitos vulcanoclásticos máficos (MVDs), intercalados aos derrames básicos. Desta maneira, na América do Sul, durante um período geológico relativamente curto, abundantes derrames de lava básica e ácida cobriram a Bacia do Paraná, os quais recebem denominações diferentes no Brasil, Argentina, Paraguai e Uruguai. Neste artigo, esta unidade litoestratigráica é nomeada simplesmente Grupo Serra Geral (GSG). O acervo litológico representado pelo presente atlas fotográfico compreende feições típicas dos derrames de basalto, andesibasalto, dacito e riolito, depósitos vulcanoclásticos máficos, além de diques de composição básica.

Palavras-chave: Província Ígnea do Paraná, vulcanismo, hidrovulcanismo, fácies, fotografias

1. Introduction

A Large Igneous Province – LIP is "a mainly mafic (+ultramafic) magmatic province with areal extent > 0.1 Mkm2 and igneous volume > 0.1 Mkm3, that has intraplate characteristics, and is emplaced in a short duration pulse or multiple pulses (less than 1–5 Ma) with a maximum duration of < c. 50 Ma." (Ernst 2014). Thus, following this definition, in the present article the names Paraná-Etendeka Igneous Province (PEIP) and Paraná Igneous Province (PIP) are adopted as synonyms.

The Paraná-Etendeka Igneous Province occupies ca. 0.08 Mkm², in Namibia and Angola, on the west coast of Africa, and ca. 1.2 M km in Uruguay, Argentina, Paraguay and Brazil in South America, where it is known as Paraná Igneous Province (Peate et al 1992).

In the early Cretaceous, during ca. 1.2 Ma with the paroxysm at 134.7 Ma (Thiede & Vasconcelos 2010), a huge magma amount, whose estimates range from at least in 0.6 Mkm3 (Frank et al. 2009), 0.7 Mkm³ (Peate et al 1992) to 1.2 M km³ (Milner et al 1992) flowed over a thick sedimentary Paleozoic sequence represented by the Paraná Basin composing a volcanic sequence which has its maximum thickness of 1,722 m in Cuiabá Paulista, State of São Paulo, Brazil (Figure 1).

The PIP is composed of great lithological diversity that mainly comprises basic volcanic rocks (ca. 97.5%) as

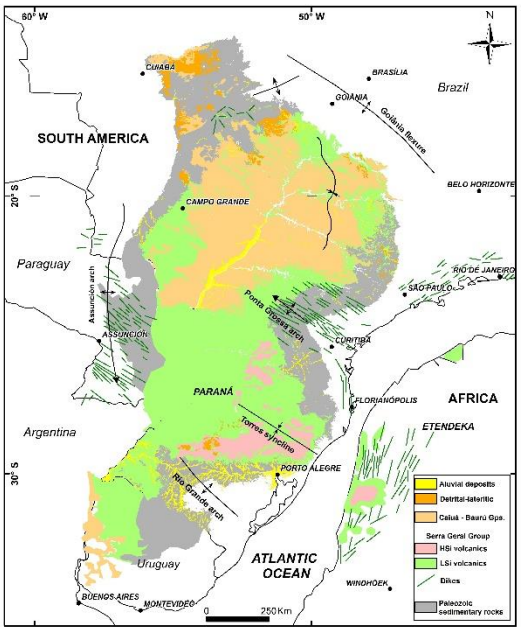

Figure 1 – South America and Africa in an early-drift position, emphasizing the basic and acidic rocks of the Paraná-Etendeka Igneous Province, the underlying sedimentary rocks of the Paraná Basin and the overlying Tertiary sedimentary rocks. The dikes, whether isolated or composing swarms, follow two main directions: parallel to the current South American and African coast lines, and SE-NW composing the well-known Ponta Grossa Arch and other of minor expression (Licht (2018), based on Peate et al. (1992), CPRM (2001), Coutinho (2008) and Nardy et al. (2011). The dikes swarm located in Paraguai and state of Mato Grosso do Sul, is based on the interpretation of aeromagnetic surveys (Druecker & Gay Jr. 1987).

basalts and andesi-basalts and acidic ones (ca. 2.5%) as dacites, trachydacites, riodacites and rhyolites.

The close interaction between the rising magma with a sedimentary sequence up to 7,000 m thick, gave rise to much more than just a thick volcanic sequence deposited on it, but also produced thousands of intrusive bodies, such as sills and dikes, almost all of a basic nature hosted by and crossing the sedimentary sequence. Furthermore, the ascending basic magma interacting with aquifer systems hosted by the sedimentary sequence, gave rise to explosive volcanism – hydrovolcanism – which pro- duced many thick mafic volcaniclastic deposits (MVDs), interbedded to the basic lows.

Dikes mainly of basalts and andesi-basalts occur frequently according to two main tectonic systems: one parallel to the South American and African coast lines and to the main structure of the occidental Gondwana's breackup, and other which follows N45W in South America and its corresponding N30E in Africa. In Brazil, this N45W dikes swarm is known as the Ponta Grossa Arch System.

Thus, in South America, during this relatively short lapse of time, basic and acidic lows covered the Paraná Basin, being reported in Brazil, Argentina, Paraguay, and Uruguay under diverse names. In the present article, it will be simply referred as Serra Geral Group (SGG) following Rossetti et al. (2017).

The present paper addresses only that portion of the Serra Geral Group, comprised by the limits of the State of Paraná (Figure 2). Approximately one half of the State of Paraná's territory, i.e., nearly 100,000 km², encompasses

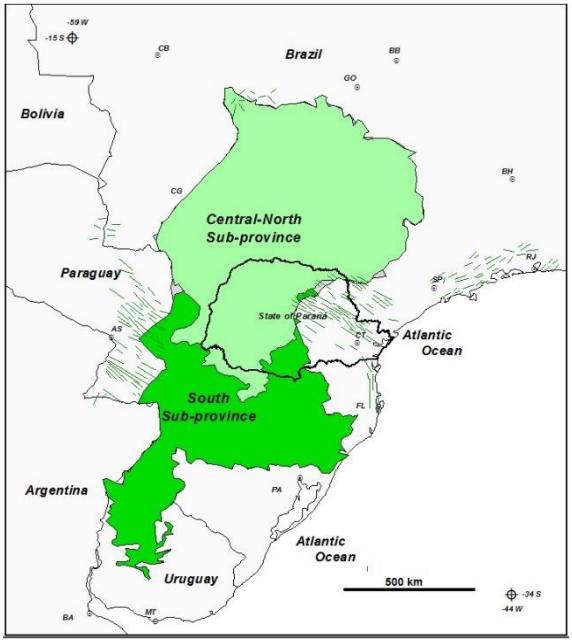

Figure 2 – Location of the State of Paraná on the Paraná Igneous Province, which is divided in two sub-provinces, based on the geochemical association of lava flows following the criteria by Licht (2018). The dikes swarm located in Paraguai and state of Mato Grosso do Sul, is based on the interpretation of aeromagnetic survey (Druecker & Gay Jr. 1987).

the Serra Geral Group. Although it appears to be a restricted region as compared to the Paraná Igneous Province as a whole, it corresponds approximately to the territory of Iceland.

Due to the large number of field stations surveyed during the 16 years of the Serra Geral Group's Geological Mapping project in the State of Paraná (Licht & Arioli 2018), the observations and conclusions can be considered as safe references for the architecture, morphology and facies arrangement in this portion of the Paraná Igneous Province. Thus, volcanological aspects of the Serra Geral Group in the State of Paraná are presented in order to facilitate the understanding of the geometry of the flow associations, the flow morphology, the internal structure and the facies of the flows and the mafic volcaniclastic deposits. Each one is exemplified by pictures obtained during the execution of the geological mapping of the Serra Geral Group in the State of Paraná.

Considering the disagreements that exist in the literature (Brooks et al 1982; Kokelaar 1982; Vincent et al. 1982; Cas & Wright 1988; Hanson & Wilson 1993; Goër de Herve et al. 1998; Batiza & White 2000; White et al. 2000; Corsaro & Mazzoleni 2002; Dadd & Wagoner 2002; Donaire et al. 2002; Mc Clintock & White. 2002; Gifkins et al. 2002; Hooten & Ort 2002; Jerram & Stolhofen 2002; Lorenz et al. 2002; Lavine & Aalto 2002; Squire & McPhie 2002; Wohletz 2002; Jutras et al. 2005; Martin & Nemeth 2007; Waichel et al. 2007; Masusili 2017; Gourgaud 2019) as to whether the term 'peperite' has a genetic or a descriptive connotation, in this article it will be written in quotation marks, 'peperite' and 'peperitic'.

2. Materials and methods

During field work performed for the Project Geological Mapping of the Serra Geral Group in the State of Paraná, from 2003 to 2016, the authors surveyed and described 3,704 sites with an average density of 1 site per 24.3 km2. (Licht & Arioli 2018). In each field station, the basalt and rhyolite flow features, such as zonality, geometry, thickness, lithological composition, relief morphology, relationships between lithologies, i.e., architecture, contact, attitudes and tectonic structures were recorded. Geometry, thickness, lateral continuity, flow structures, mineralogical composition, vesicles and amygdales with respective filling-minerals, alteration minerals and associated structures were described in the three main zones of the lava flows - base, core and top. For the deposits interspersed with flows, majorly volcaniclastic, geometry, thickness, lateral continuity, lithological and mineralogical composition, relationships between clasts and groundmass, clast statistics, stratigraphic and structural relationships with flows were described.

A photographic database was created, recording details of most of the visited outcrops, quarries, roadcuts

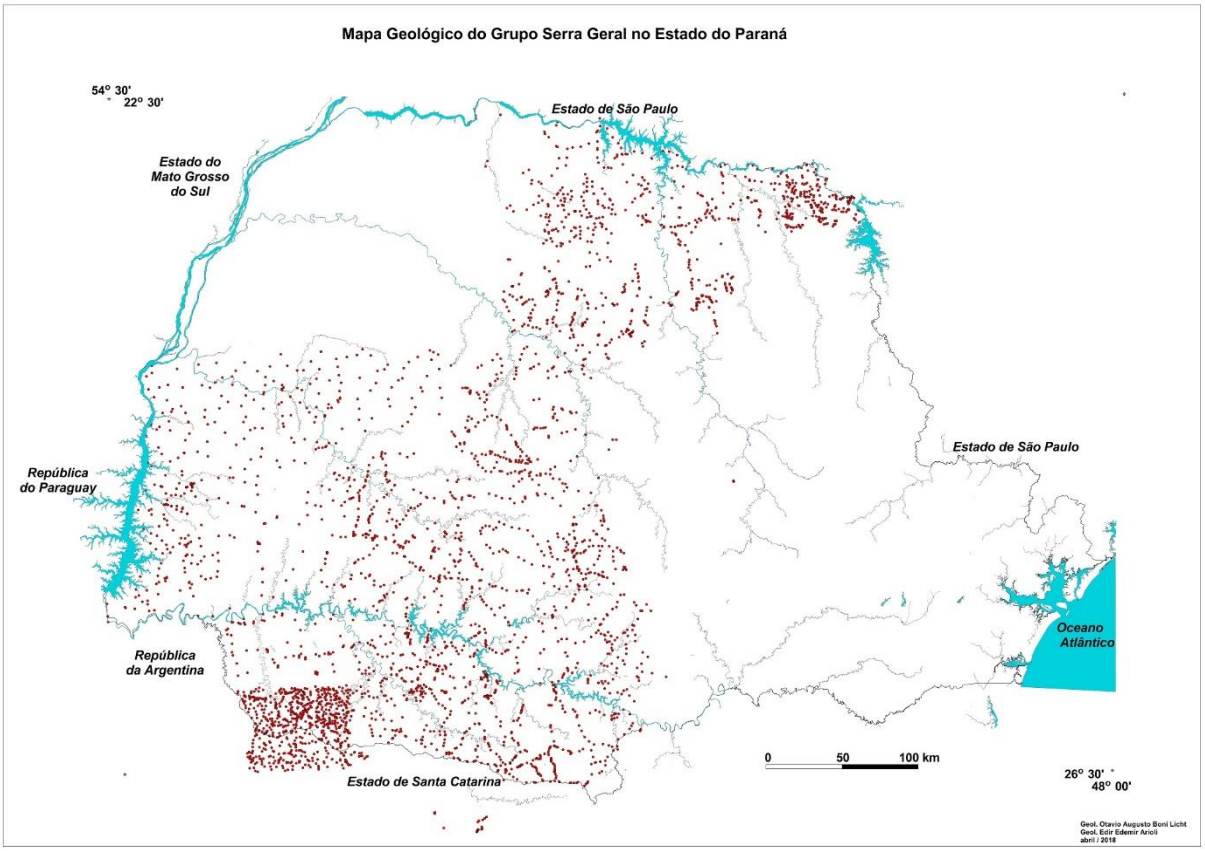

Figure 3 – The 3,704 field stations surveyed during the geological mapping of the Serra Geral Group in the State of Paraná Licht & Arioli (2018).

and river beds. From this photographic database, 276 pictures were selected representing 172 field stations. They were considered as the most representative and typical pictures of the morphologies and internal facies of basic and acidic lows, volcaniclastic deposits and dikes, to compose the 35 plates presented in this article. The emphasis was put on field aspects but, to stress small scale features, some pictures were made using a hand-held digital camera, and also at laboratory using binocular magnifying glass, petrographic microscope and scanning electronic microscope (SEM).

3. Results

In the following sections, the geometry, morphology and internal facies of the basic and acidic lows and mafic volcaniclastic deposits which compose the architecture of the Serra Geral Group in the State of Paraná will be described and exemplified with selected outcrops surveyed during geological mapping. The coordinates of almost all selected examples, exception made of two points, are provided (Annex 1), thus facilitating the selection of the field sites to compose didactic or geotouristic itineraries.

3.1 Contact between the Serra Geral flows with the Botucatu sandstones

The first flows of the Serra Geral Group, whether of basic or acidic lavas, spread over an erg, i.e., a sandy desert, currently represented by the Botucatu Formation sandstones (Plate 01 a). The contact between the Serra Geral Gp. with the Botucatu Fm. is characterized to be transitional, either for the existence of some precursor thin flows hosted by the sandstones (Plate 01 b), as for the recurrence of aeolian sandstone beds known as inter- trapp sandstones within the first lavas flows.

The style of the contact was controlled by the capacity of the erg's pavement to withstand the weight of the lava flow, the thermal contrast up to 1,100° C, as well as the presence and amount of water in that specific location. In this way, the contact can be neat (Plate 01 c), difuse (by showing a thermal halo), folded (lava flowing over a plastic but dry sediment), brecciated (lava flow encompassing masses of sand and/or fragments of the sandstone) (Plate 01 d), or 'peperitic' (an originally wet sandy matrix encompassing angular lava fragments immersed in).

The sharp contact is remarkable, as the sandstones can be friable or intensely silicified, in such case showing flow wrinkles and other drag marks imprinted during the displacement of the flow. In these cases, it is quite possible that the advance rate of the flow was enough slow and gradual, so as to have minor disturbance on the erg's sandy pavement (Plate 01 e).

All types of disturbed contact are characteristically composed by fragments of a same lava flow immersed on a sandy groundmass. It is important to stress a distinction between the brecciated contact and the 'peperitic'. In the first case, the contact consists of a disorganized mixture where the fragments of basic lava predominate with the interstices filled with sand, suggesting a faster and disturbing flow advance (Plate 01 d). In the second case, the aeolic sand matrix predominates encompassing sparse sub-angular basalt fragments, all arranged in a disorganized manner, indicating a slow and less disturbing flow advance (Plate 10 a). It seems that the sandy sediment should not be necessarily moist to form brecciated or 'peperitic' contacts, being the disturbances due only to the thermal contrast between the higher temperature of the basic flow and the "room" temperature of the sandy pavement. In some places, some evidence that the basalt lava flowed over a wet sandy pavement are observed, such as small semi-spherical blown bubbles (Plate 01 f). This type of locally explosive contact probably occured on the interdune depressions and plains, where the water table was close to or exposed at surface.

3.2 The geometry of the basic lava flows

In Large Igneous Provinces (LIPs), two main general associations of basalt flows have been recognized

Figure 4 – Scenes of modern analogues for the environmental setting of an erg, i.e., (left) a sandy desert, with depressions and interdune plains and which could also include (right) interdune lakes and oasis. It was in a similar environment that the first Serra Geral flows would be emplaced. Images from the Internet (left http://detikislam.blogspot.com/2011/12/padang-pasir-kembali-menjadi-padang.html; right http://oranbel-

air.over-blog.com/article-l-algerie-autrement-page-5-113734218.html)

Plate 01 – Contact between lava flows and the Botucatu Fm. eolic sandstones:(a) Typical channeled cross-stratification of the Botucatu Fm. sandstones. OL 3633; (b) Precursor 50-60 cm thick basalt lobe (B) interspersed with Botucatu Fm. sandstones (Ss). Even though the basalt is intensely weathered, in some places it is still possible to identify plagioclase crystals with 0.1-0.2cm long. Min. Tec. Clovis Fonseca. OL 3620; (c) Sharp contact of a basalt flow (B) covering the main body of the Botucatu Fm. sandstone (Ss). The hammer is highlighted by a white dotted ellipse. OL 3702; (d) Irregular and brecciated contact – 'peperitic'(P), between a basalt flow (B) covering a layer of the Botucatu Fm. sandstone (intertrapp sandstone) (Ss). EA -1426; (e) Streaks and drag marks, printed on the sandy pavement of the Botucatu paleoerg by the basalt flow. The arrow points the flow's direction. The sandstone is extremely endurated by silicification. OL 3752; (f) Blown bubbles (white arrows) produced by the thermal shock between the basalt flow over a wet sandy pavement of the paleoerg Botucatu. The sandstone is intensely hardened by

silicification. OL 3752.

and described according to their geometry: tabular-classic or simple, and compound-braided, lobate or compound. These features have been used to evaluate eruption rate and volume, identify terrain morphology, and also characterize the evolutionary phase of a LIP and the geotectonic regime, which has divided in three main phases, initial or onset, principal or acme, closing or waning (White & McKenzie 1989; Jerram et al. 1999; Menzies & Ebinger 2000; Menzies et al. 2002; Bondre et al. 2004; Self et al. 2008; Nelson et al. 2009; Kerr & Menzies 2012).

3.2.1 Compound lava flows

The sequences of thin flows and lobes record periods of intermittent volcanism, typical of the initial or onset phase of a LIP. Compound thin flows and lobes have a simple internal structure, consisting of a lower and an upper crust with a reddish clinker appearance, both a few millimeters thick. The core zone, measuring from few centimeters to ca. 40 cm thick, can be aphanitic in the case of thin flows or intensely vesiculated in the case of Type S lobes. They represent active flow fronts, with low volumes and low feeding rates of relatively viscous lava. They are open systems with very rapid losses of pressure and temperature, which explains why both, the lower and the upper surfaces, are made up of thin glassy crusts and a low crystallinity core (Figure 5).

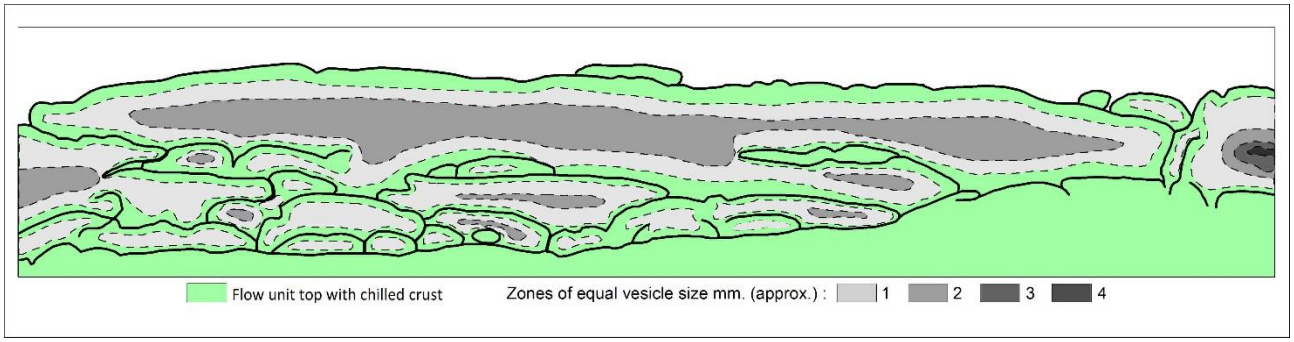

Figure 5 – Cross section of a complex composition of stacked small lobes and thin pāhoehoe flows, which defines the compound lava flows. After Walker (1989).

During this initial or onset phase, sedimentary record interspersed with the flows is abundant (White & McKenzie 1989; Jerram et al. 1999; Menzies & Ebinger 2000; Menzies et al. 2002; Kerr & Menzies 2004). However, in this early stage of most LIPs, especially those placed over a sedimentary basin, thick and continuous mafic volcaniclastic deposits (MVDs) are observed interspersed with basalt flows. These MVDs would have been produced by explosive eruptions caused by the interaction between the rising basic magma and deep aquifer systems hosted in the sedimentary sequence, as emphasized by Schminke (2004) and Ross et al. (2005). This eruptive model, known as hydrovolcanism, would be preponderant in the initial phase of the evolution of a LIP, but it would be of minor importance in the main and closing phases.

3.2.2 Single flows

Single flows represent a single cooling unit. They result from persistent eruptions of high volume and consistent feeding rates of fluid lava (Figure 6). The main reference is the pāhoehoe tabular flow, which has a complex internal structure, divided in three main zones: base, core and top, and is described below. Regional sequences of tabular and sheet flows mark periods of more persistent volcanism, typical of the syn-rift phase, with rare erosion and sedimentation periods (White & Mckenzie 1989; Jerram et al. 1999; Menzies & Ebinger 2000; Menzies et al. 2002; Kerr & Menzies 2004). Self et al. (1996; 1998) conclude that the largest lava outpourings on the Earth are tabular lava fields build with multiple tabular sheet basalt flows, and stated that in all basaltic provinces, the large lava flows were formed by inflation of sheet flows. This process develops from lobes and thin basalt flows, the interior of which is continuously fed with fluid lava.

Process of inlation (Hon et al. 1994, Self et al. 1997) which imply in continuous lava feeding within a flow, promote its thickening and widening, enabling high dispersion covering wide areas. Self et al. (1997) recognized inflation as the most fundamental and widespread mechanism in the development of CFB provinces, since it can produces tabular flows whose can easily exceed 40 m thick, reaching up to 70 m in the Columbia River Province.

3.3 Basalt flows – morphology, internal structure and facies

The basalt flows found in the Serra Geral Group follow some variations of the morphology known as pāhoehoe, ranging from thin flows, Type-S lobes, Type-P lobes, inflated-tabular to rubbly. A special variety of the pāhoehoe morphology is found exclusively on that basalt flows with hypohyaline texture.

Thick lava flows, may have been formed by filling depressions in the paleo-relief that occur either in the dunes field of the paleo-erg Botucatu, or in the relief formed by previous flows. In both cases they are called as ponded pāhoehoe lava flows (Figure 7).

To date, no flow has been identified with the A'ā morphology.

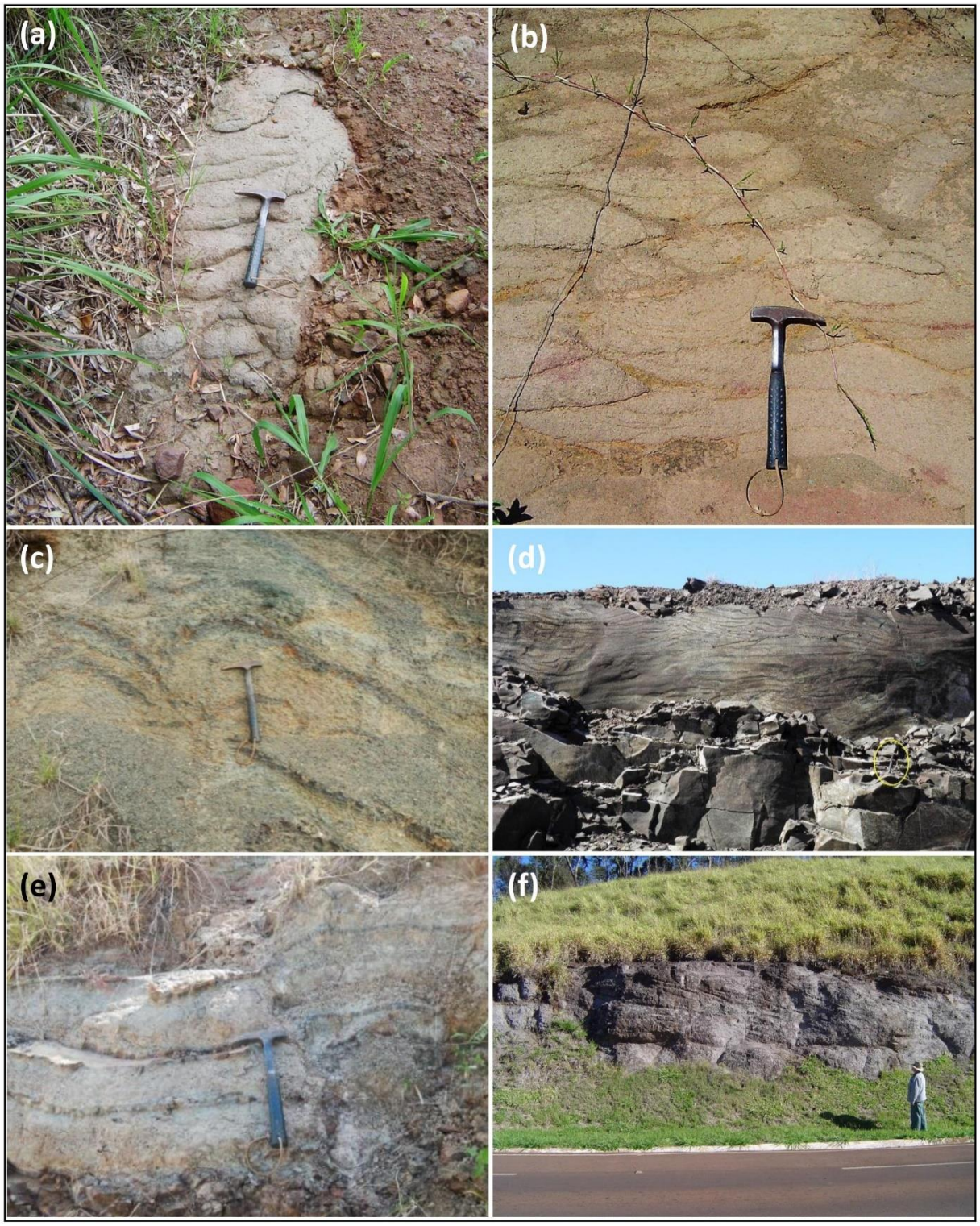

Plate 02 – Sets of basalt lobes and/or thin flows, with the typical geometry and association of compound flows: (a) Longitudinal section of thin lobes. EA-867; (b) Lenticular aspect of a thin lobes set, in cross section. EA-863; (c) Set of thin basalt flows. The dark bands are the base and top glassy crusts of each flow. The light bands are the core, slightly more vesicular and with a higher crystallinity rate. OL 3981; (d) Striped aspect given by the longitudinal section of an anastomosed thin basalt flow set. The dark bands are the base and top glassy crusts of each flow. The geologist's hammer is highlighted by the yellow dotted ellipse. OL 3162; (e) Set of thin and anastomosed basalts flows. The dark bands are the base and top glassy crusts of each

flow. OL 3889; (f) Longitudinal section of a succession of thin basalt flows, whose base and top crusts are reddened by the action of weathering. Geologist Edir E. Arioli. EA-1211c.

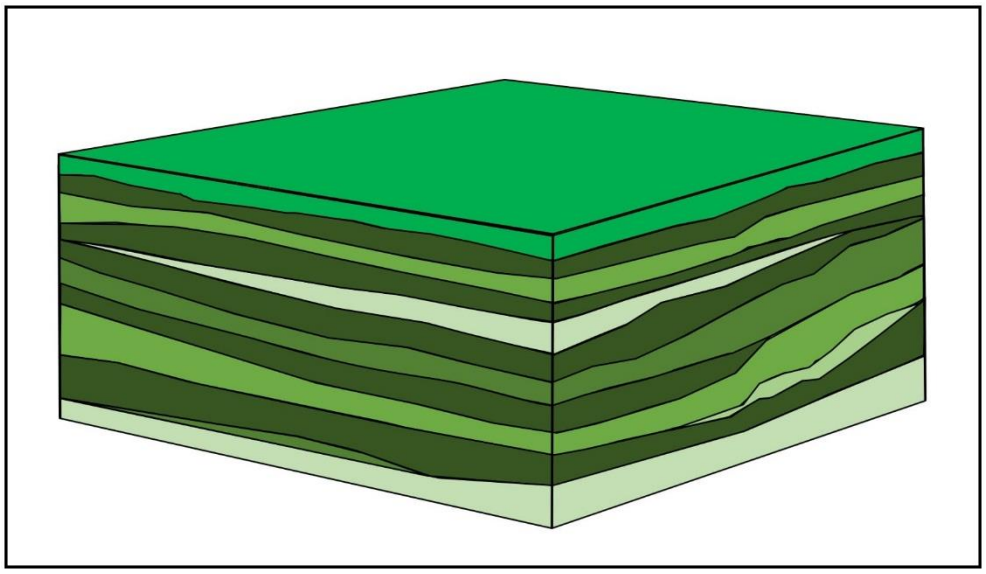

Figure 6 – Single, tabular, overlapping sheet flows produced by low to medium magma volumes at sustained eruption rates. After Jerram & Widdowson (2005)

3.3.1 Thin basalt flows

As described by Nichols (1936) pāhoehoe flows are formed by small ofshoots of very hot and highly liquid lava from the main stream driven out laterally or in advance of it in a succession of small belches. These outspreads are very thin, cool quickly, and attain a stable form before they are covered by succeeding belches of the same sort.

Thus, active flow fronts fed by very hot and liquid basic lava, produce thin tabular flows, which are no more than 10 to 15 centimeters thick, rarely occur isolated, being usually stacked as compound and anastomosed sequences of several flows up to 3 meters thick.

Two variants of this morphology have been identiied. In the first type, each flow may be a few centimeters thick, being so thin that it does not show any internal structure, and whose upper surface develops polygonal patterns due to contraction by cooling. In the same outcrop and even in the same flow, polygons can assume diferent shapes, triangular, square, rectangular or pentagonal separated by thin spaces (Plate 04 d, 04 d, 04 e). In the discontinuity plans between the polygons, or even in the contacts between the various thin flows, thinny glass sheets of a few millimeters or even masses up to 2 cm thick can be found. They seem to be late

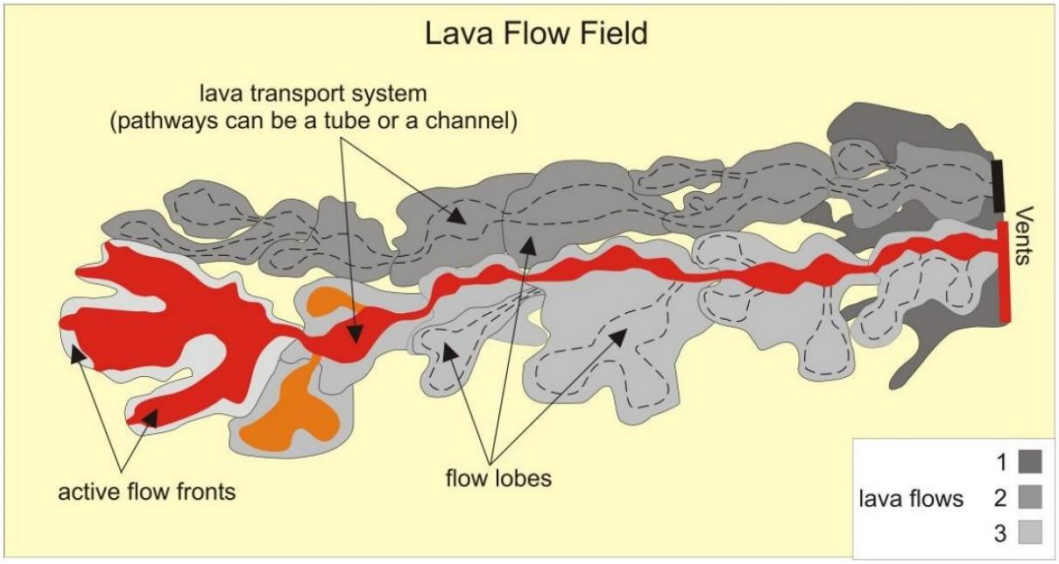

Figure 7 – Key components of a lava flow field. A flow field represents the lava produced in a single eruption. It typically consists of two or more lava flows (indicated by diferent shades of grey), which in turn comprise many flow lobes. The transport system consists of open or sealed pathways, which lava is delivered from the source vents to active flow fronts where effective growth takes place (Óskarsson 2005).

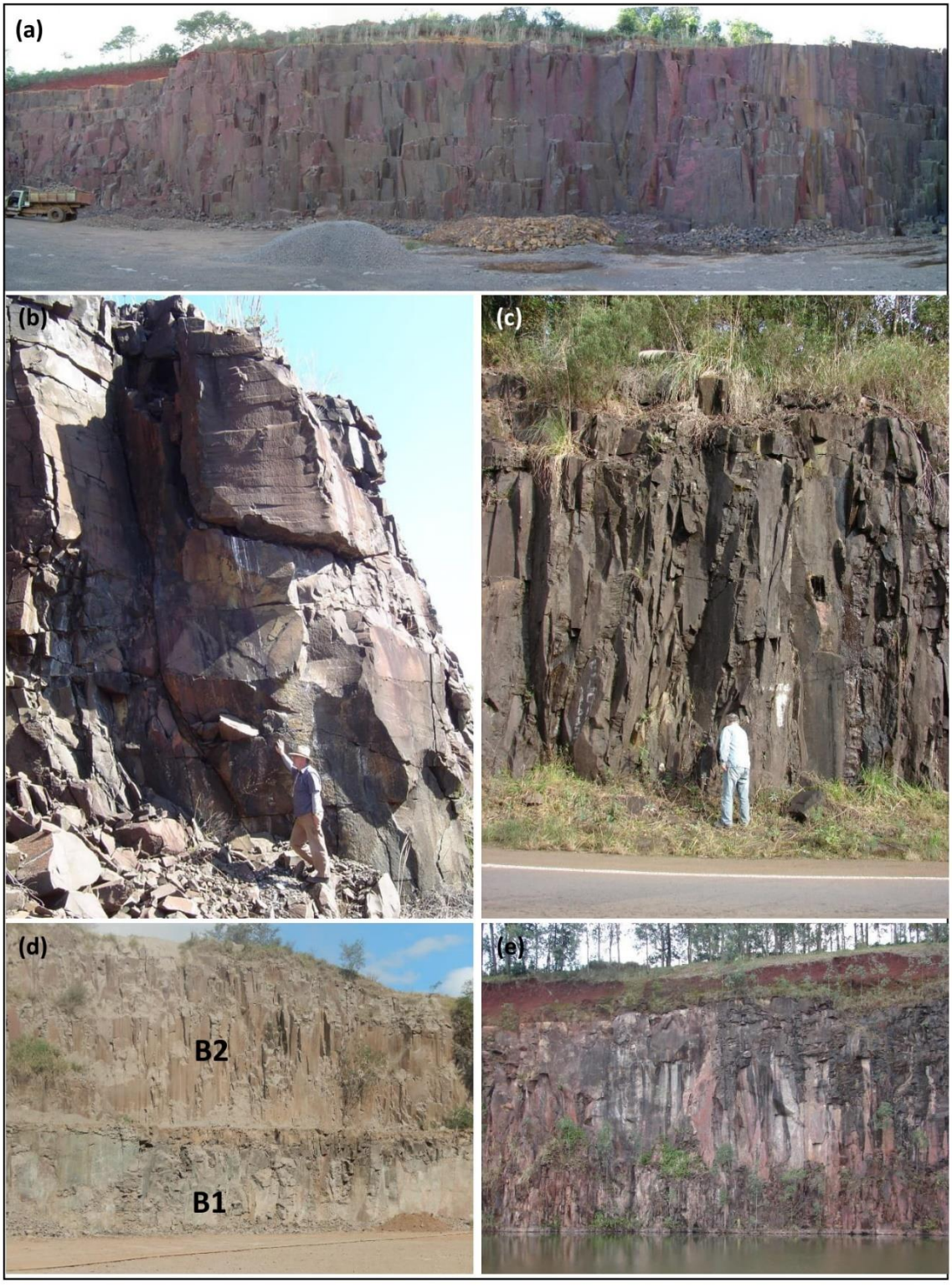

Plate 03 – Single, tabular, inflated pāhoehoe basalt flows: (a) Panoramic view of the core of an inflated tabular pāhoehoe flow. Internal shear zone due to the stress caused by the displacement of the still plastic core against the already cooled and rigid border, defines the entablature. EA-802; (b) Upper portion of the core of an inflated rubbly pāhoehoe flow, which is massive in the core and with sub-ho rizontal, plane-parallel fractures due to the diferential movement between a highly viscous topmost portion already cooled and the still fluid core. Geologist Edir E. Arioli. EA-1162; (c) Core of an inflated tabular pāhoehoe flow. The irregular, vertical fractures and joints define the entablature. Geologist Edir E. Arioli. EA-546; (d) Two inflated tabular pāhoehoe flows separated by a volcaniclastic deposit. B2 has ca. 25 m thick and B1 is

partially exposed. The vertical fractures and joints define the entablature. OL 3714 a; (e) An up to 30 m thick tabular inflated pāhoehoe basalt flow. The irregular subvertical fracturing is the entablature. EA-1695.

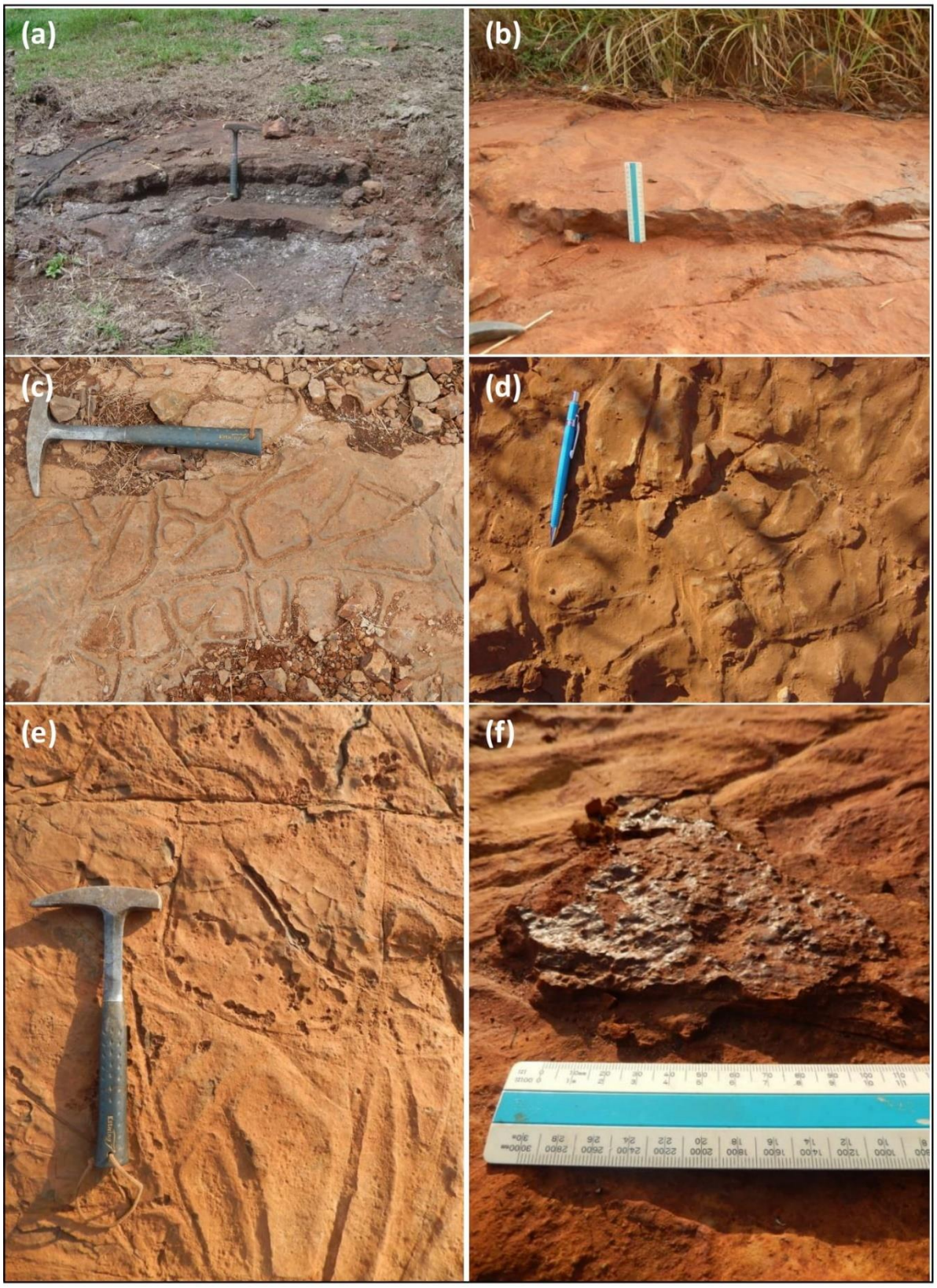

Plate 04 – Thin basalt flows: (a) Stack of thin basalt flows, 5 – 7 cm thick. EA-955; (b) Stack of thin flows, 5-7 cm thick, showing a polygonal pattern produced by quick cooling. OL 3748; (c) Polygonal pattern on the upper surface of 5 cm thick basalt flow, due to quick cooling. OL 3755; (d) Polygonal pattern on the upper surface of 5 cm thick basalt flow, due to quick cooling. EA-1375; (e) Upper surface of a 7 cm thick basalt flow, showing burst vesicles arranged according to the internal limits of the cooling polygons. OL 3748; (f) Basaltic glass sheet injected into the empty spaces between thin basalt flows, 5-7 cm thick each. OL 3748.

injections of suddenly cooled basaltic lava (Plate 04 d, 04 f).

Another variant is made up of stacks of dozens of thin flows whose longitudinal section displays a long banded section due to welding. The set may have a general sub-horizontal structure, or it may present folds due to obstacles or irregularities of the paleo-relief that hampered the progression of the ofshoots.

Each flow unit, which is no more than 10-20 cm thick, is bounded by two dark greenish gray glassy crusts, the thickest at the bottom and the thinnest at the top, with a light gray core with greater crystallinity and/or subtle vesicular structure (Plate 02 c, 02 d, 02 e).

These two variants of thin flows make up the geometry of compound and anastomosed flows and must have been produced by successive lava pulses, with low volumes, low feed rates and low volatile content.

3.3.2 S-type lobes

S-type lobes were so named by Walker (1989) because of their spongy interior due to the abundance of almost spherical vesicles. The vesicles generally comprise >40% vol. of the rock and most of them are <4 mm in diameter, with the largest ones concentrated in the core region (Wilmoth & Walker 1993, Self et al. 1998).

In longitudinal section, a S-type lobe looks like a layer with rounded edges and in cross section it has a rough ellyptical outline (Figure 8). S-type lobes have a very characteristic internal structure (Figure 8), descri- bed from bottom to top as follows:

(1) Selvage or dense glassy crust, up to 6 cm thick, black when fresh and reddish when oxidized;

(2) Vesicular area about 3-5 cm thick with abundant spherical vesicles;

(3) Vesicular area about 5-20 cm thick;

(4) Vesicular to scoriae area of about 3-5 cm thick;

(5) Selvage or dense glassy crust, black when fresh and reddish when oxidized, 1-2 cm thick.

Rarely S-type (spongy) pāhoehoe lobes are isolated and often make up a set of many overlapping flow units, each 10 to 40 cm thick. (Plate 05).

In thicker lobes, which can reach 1.5 m thick, the upper crust shows wrinkles and undulations (wrinkled surface), which indicate the direction of flow.

In some places and due to the action of subtropical weathering, the glassy crust may have been completely replaced by secondary iron oxide, thus becoming a ferruginous crust, but with the flow wrinkles still preserved (Plate 05 c, 05 e).

3.3.3 P-type lobes

The term P-type pāhoehoe was proposed by Wilmoth & Walker (1993) to designate flow units, i.e., lobes containing pipe vesicles, which can be small vertical cylinders or pipe shaped vesicles. P-type pāhoehoe lobes typically exhibit pipe vesicles in it lower part, and a dense interior and more vesicular exteriors (Figure 9). Is much less vesicular (exhibits a lower porosity) than those of S-type, but has generally larger vesicles, and pipe vesicles near the base. Pipe-vesicle bearing flows tend to be dense, probably due to bubble loss during temporary lava residence on the irregular topography of the previous flows, before final emplacement (Hon et al. 1994). The pipe vesicles grow inward from the cooling front, and although commonly seen at the lobe's base, they may also form radially around the margins (Cashman & Mangan 2014).

P-type lobes are frequent in the Serra Geral Group, especially where the flow moved over Mafic Volcaniclastic Deposits. Because they are still hot and rich in volatiles, during the cooling and degassing process, water vapor and/or gases seek to escape being partially blocked by the lobe or the overlapping flow. Thus, just in the base of the lobe or the fow, the pipes are formed.

Therefore, the amount and dimensions of the pipes depend on the volume of gases and/or water vapor. Further, the composition of the rising volatiles controls the filling of the pipes, which can be empty or lined with a film of celadonite (a phyllosilicate) generated by the alteration of the glass (Plate 06 f) or even by quartz or carbonates microcrystals.

3.3.4 Thick basalt flows

Thick lava flows may form under two major situa- tions: ponding and inflation

3.3.4.1 Ponded lava flow

Thick lava flows, may have been formed by filling depressions in the paleo-relief that occur either in the dunes fields of the paleo-erg Botucatu (Figure 11), or in

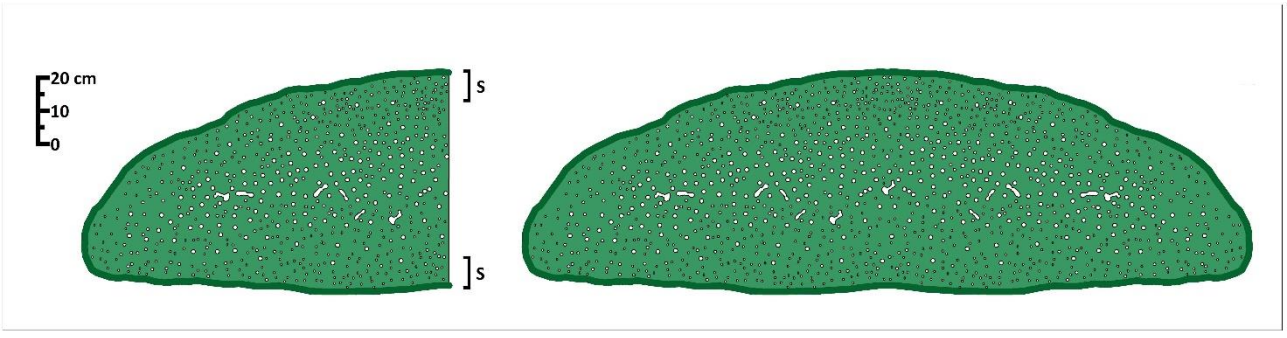

Figure 8 – Schematic sections of a S-type lobe: (left) a longitudinal section and (right) a cross section. The

internal structure is composed of a highly vesiculated (spongy) core containing evenly distributed larger vesicles, surrounded by a rim with minor vesicles. The selvage (S) is dense, glassy and ca. 2 cm thick. After Wilmoth & Walker (1993) and Self et al. (1998).

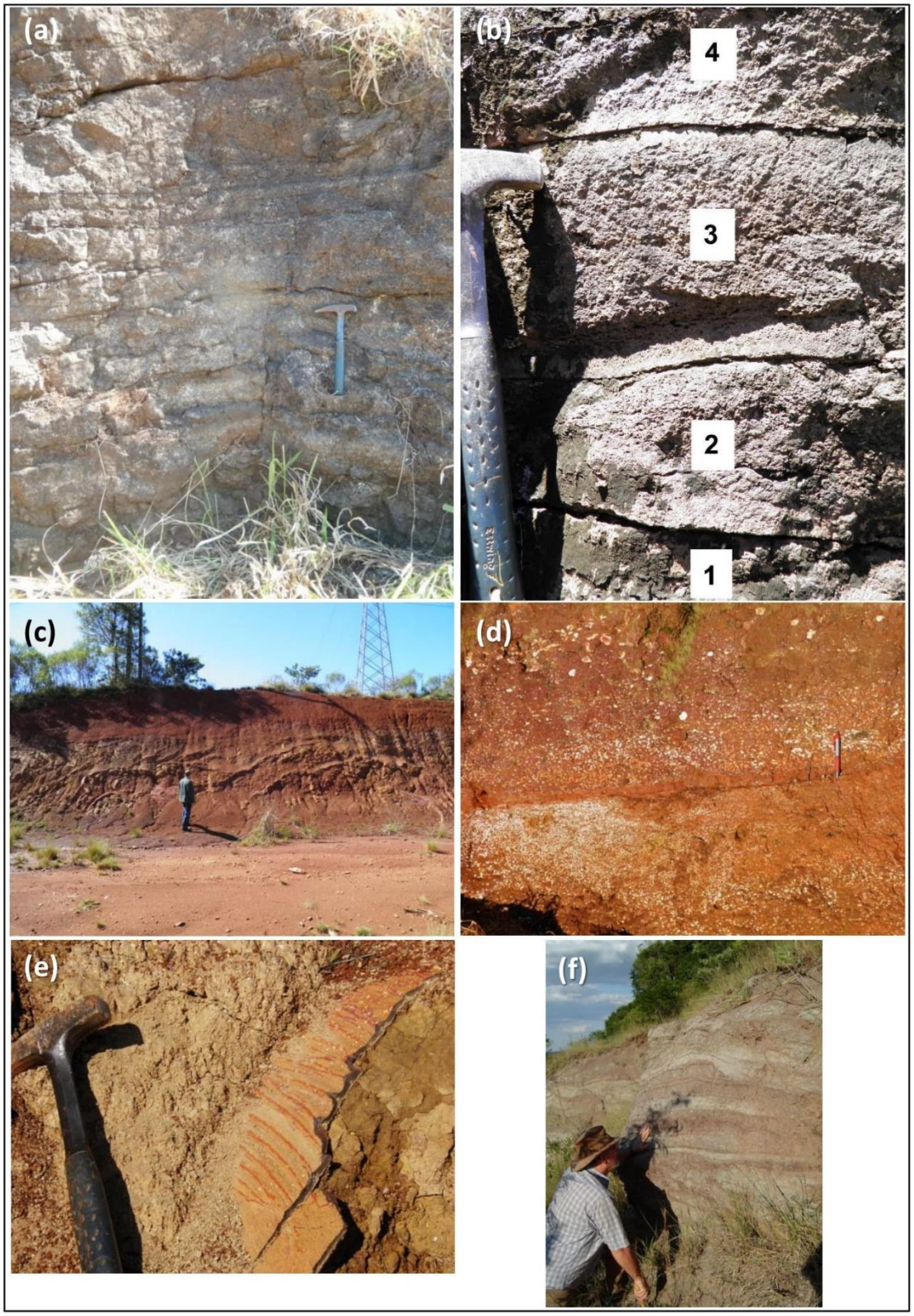

Plate 05 – Type-S lobes: (a) Stack of ca. 16 pāhoehoe Type-S lobes, each from 10 to 15 cm thick. OL 4196; (b) Detail view of picture (a). A stack of Type-S pāhoehoe lobes. The lower and upper glassy crusts are clearly shown as well the vesicular and/or amygdaloidal core. OL 4196; (c) Cross section of a stack of several Type-S pāhoehoe lobes. Both glassy crusts (upper and lower) of each lobe have been replaced by secondary iron oxides, and are highlighted in the photo as wavy planes. OL 3120; (d) Detail view of picture (c). Contact between two Type-Spāhoehoe lobes, with white amygdales, highlighted by the intense weathering. OL 3120; (e) Detail view of picture (c). Wrinkled upper surface of a Type-S pāhoehoe lobe, replaced by weathering as a Fe-oxide crust. OL 3120; (f) Longitudinal section of a stack of several 15-20 cm thick Type-S pāhoehoe lobes.

Geologist Edir E. Arioli. EA-968.

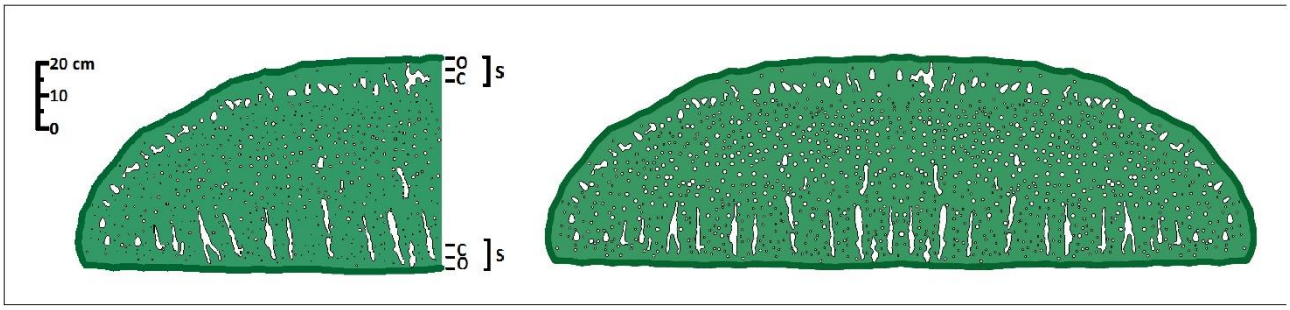

Figure 9 – Idealized sections of a thin P-type lobe: (left) longitudinal section showing selvage (S), outer rim (O) and inner rim (C) as well as the pipes tilted towards the active front of the lobe, and (right) a schematic cross section. Note the 15-20 cm. thick vesicular lower crust with pipe vesicles growing inward. The pipes can be subvertical or tilted to the active front. After Wilmoth & Walker (1993).

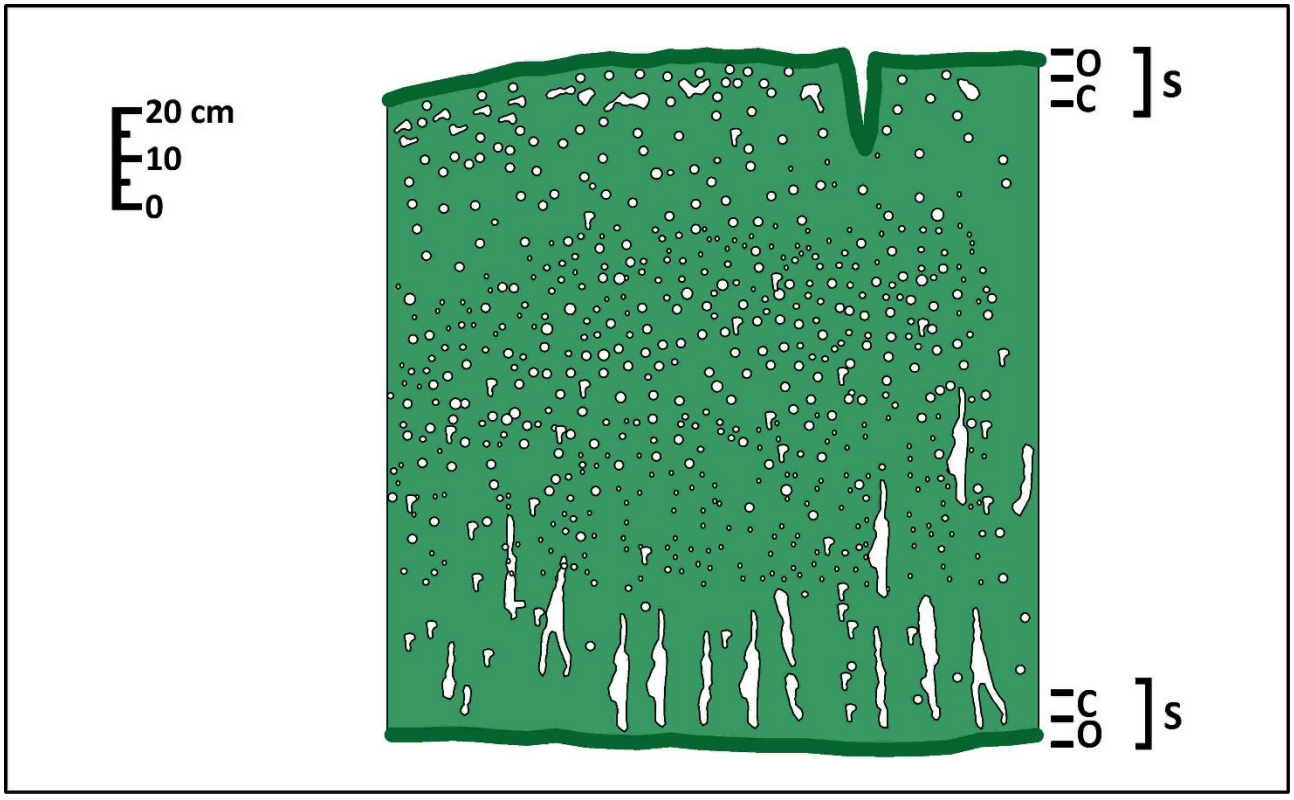

Figure 10 – Section of a thick P-type lobes from Hawaiian lavas showing selvage (S), outer rim (O) and inner rim (C); in the upper surface an inflation cleft. Note the 15-20 cm thick vesicular lower crust with pipe vesicles growing inward. The pipes can be subvertical or tilted to the active front. After Wilmoth & Walker (1993)

the hummocky relief formed by previous flows. In both cases they are called ponded pāhoehoe lava flows.

A very representative example of a ponded basic lava flow is shown in Plates 07 a and 07 b.

3.3.4.2 Inflated pāhoehoe flows

Large volumes of lava with constant feed rates and relatively low viscosity produce thick flows, which take on a tabular appearance. If the feeding is continuous and persistent, with a supply of an expressive lava volume, the flow will undergo the inflation process that produces an increase in thickness, width and length.

The flow inflation process was described in Hawaii by MacDonald (1953) and by Hon (1994) and in the Columbia River Province by Self et al. (1996).

Lava flows inflate when the transport rate of lava from the source exceeds the advance rate at the flow front. Because flows advance more slowly on low slopes than on steeper ones, flow inflation is most pronounced on low slopes. Lava flow inflation can occur either within small lobes or across large sheets (Cashman & Mangan 2014). Under these conditions and at the end of the process, flows with pāhoehoe morphology assume a tabular aspect (sheet-like flows), as occurs in the Columbia River Province, where flows up to 60 m in thickness are found

(Self et al. 1996).

Plate 06 – Type-P lobes: (a) Longitudinal section of a 25 cm thick P type pāhoehoe lobe (B1) with radially arranged pipes, growing from the cooling front towards the center. The lower pipes are tilted towards the flow direction, as indicated by the white arrow. B1 is overlapped by another P type lobe (B2) which shows the same features. EA-1163; (b) A P type pāhoehoe lobe (B), overlapping a volcaniclastic deposit (Vd). The pipes of the (B) base are tilted nearly to the upper left, towards the flow direction (white arrow). JCC 254f; (c) Contact of a P type pāhoehoe lobe (B), overlapping a volcaniclastic deposit (Vd). Geologist Edir E. Arioli. EA-1217; (d) Detail of picture (c). Lower zone of the P type pāhoehoe lobe (B); the pipes are tilted towards the flow direction (white arrow). EA-1217; (e) contact between two P type pāhoehoe lobes, B1 and B2. The base of B2 shows pipes tilted to left pointing to the flow direction (white arrow). The inner surface

of the pipes is covered with a green film of celadonite, suggesting that originally the pipes were lined with a thin glass film. EA-1163; (f) contact between two P type pāhoehoe lobes. The base of the upper flow (B2) shows many tubular and pipe vesicles. The white arrow points to flow direction. OL 4254; (g) Detail of picture (f). Hand sample of the base of the upper lobe, showing a high density of long and thick tubular pipe vesicles. OL 4254.

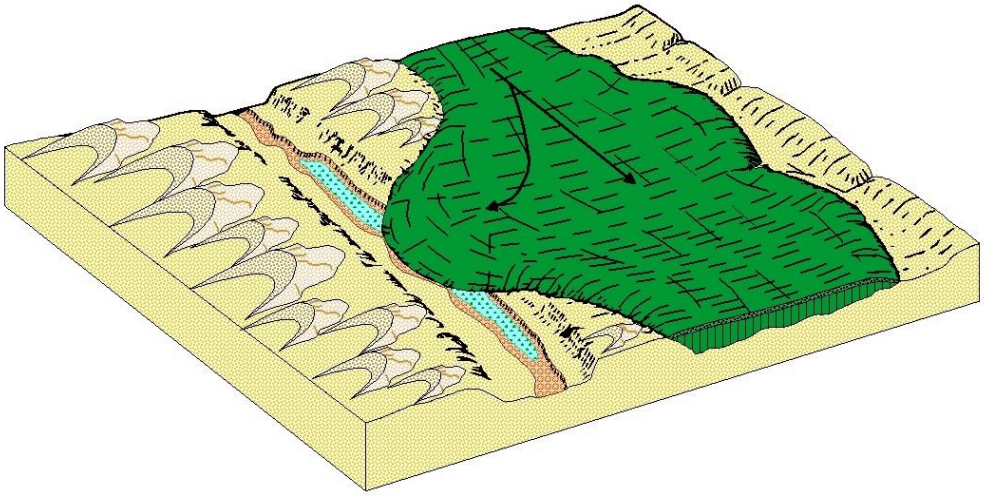

Figure 11 – Idealized picture of a ponded pāhoehoe basalt lava flow filling a depression and migrating into a valley, in the dunes field of the Botucatu erg. The thickness of a ponded lava flow can reach up to 30 meters. The direction of the flow is indicated by the arrows. After Nichols (1936).

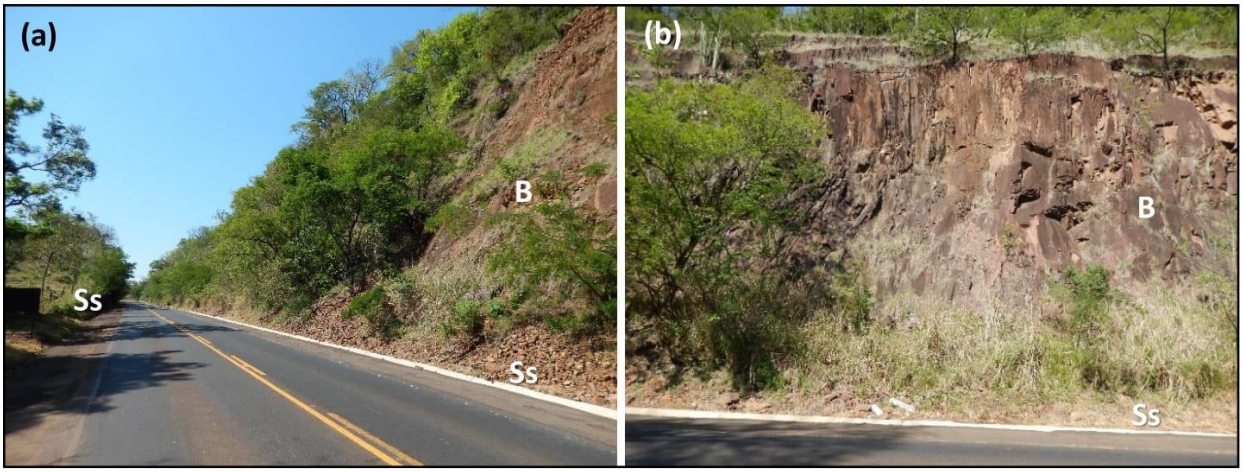

Plate 07 – Ponded pāhoehoe basalt flow: (a) In the left side of a roadcut, only the Botucatu Fm. sandstones (Ss) are exposed. In the right side, a ponded pāhoehoe basalt flow (B) lies over the sandstones (Ss). This up to 30 m thick pāhoehoe lava flow (B) accumulated and became ponded on the depressions of the dunes field of the Botucatu paleoerg. OL 3647 a; (b) Front view of the right side roadcut, where the top surface of the dunes field is exposed (Ss) over which the basalt flow (B) have moved on and ponded. OL 3647 a.

In the Serra Geral Group, the inflation process occured extensively, producing tabular flows that reach up to 30 m thick (Plate 03).

3.3.5 Hypohyaline pāhoehoe basalt flows

Some pāhoehoe basalt flows constitute a very peculiar and characteristic morphology, with a very simple internal structure, composed almost exclusively by the entablature (see item 3.4.2.b and Figure 12). It is found in basalt flows with hypohyaline texture, that is, phenocrysts immersed in an abundant vitreous matrix, in a crystals to glass ratio between 3:5 and 1:7 (Comin-Chiaramonti 1988).

Basalt is black, dense, with a vitreous aspect and resinous luster (Plate 08 f), and may be massive or show small and dispersed vesicles, without forming a well-defined vesicular zone. The vesicles can be completely empty (Plate 21 d), lined with a thin celadonite film or, in rare cases, filled with white or bluish silica (Plate 22 c).

This very peculiar and characteristic morphology is constituted almost exclusively by the entablature that can be fanned or wavy, accompanying paleo topography, with entablature elements that are many meters long and a few centimeters in diameter (Plate 08 a, 08 b, 08 c), and whose cross section has an irregular polygonal shape.

The surface of the entablature elements is marked by concave fractures, called chisel marks, which are indicative of the high glassy mesostasis content, and which have been attributed to the cooling process (Plate 08 f).

In some places, there is a basal colonnade made up of short columns with a roughly hexagonal section, which

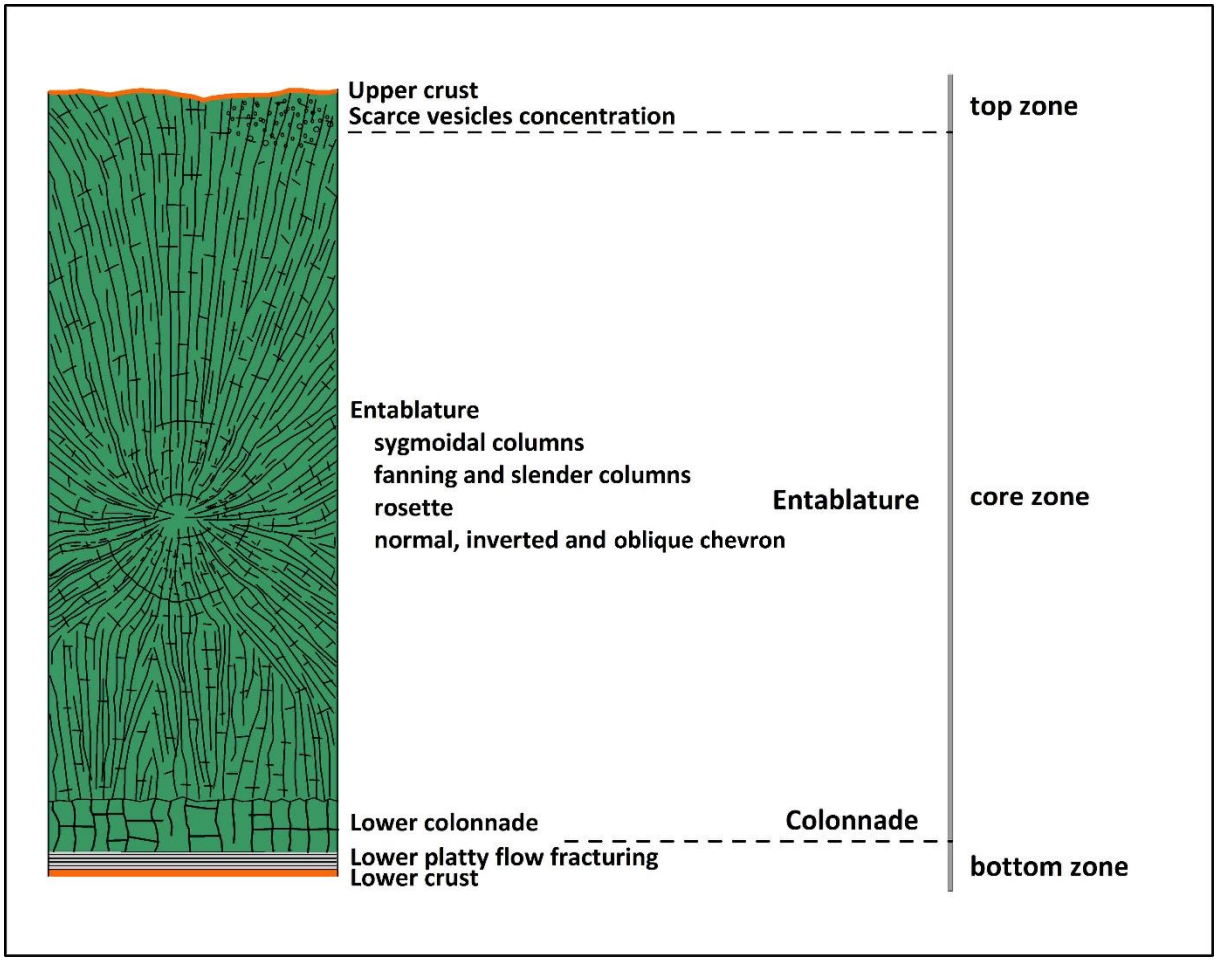

Figure 12 – Schematic section of a pāhoehoe tabular hypohyaline basalt flow.

soon subdivides into the entablature elements, meters long and a few centimeters in diameter. (Plate 08 b).

A similar morphology was described in the Columbia River Province as Type III (Long & Wood 1986) and, by Souza Jr (1992) and Sadowsky (2012) in many locations in the State of São Paulo. These authors have attributed this special type of morphology to the contact with water bodies, which would have caused its quick cooling. Forbes et al. (2014) attribute this particular morphology of pāhoehoe flows to rapid cooling by interaction with a coolant. The same conclusion was made by Forbes et al. (2014) in the basalt flows of Hreppar and those of Búrfellshraun-Þjórsárdalshraun, Iceland, for the Type III basalt flows of the Grande Ronde basalt flows, Columbia River Province by Long & Wood (1986).

Despite the presence of pillow-lavas in some sites of the Serra Geral Center North Subprovince, which points to the existence of relatively deep water bodies (Marques et al. 1981, Mano 1987, Moraes & Seer 2017), 'peperite', pillow-lavas or hyaloclastites were not observed in the base or associated to hypohyaline basalts flows.

Besides, in those locations where it is possible to observe the overlap of two or more hypohyaline basalt flows, it is matter of fact that the entablature elements are continuous, not respecting the limits of each flow, which indicates a quick and simultaneous cooling that afected all flows as if they were a single volcanic unit (Plate 08 a, 08 b, 08 c).

The contact between flows and lobes is conspicuous and notably identified by sub-horizontal or gently undulating zones, composed of continuous bundles of platy joints that represent the basal flow fracturing (Plate 12).

3.3.6 Rubbly pāhoehoe flows

This variant of the pāhoehoe flow morphology is characterized by an autoclastic top breccia, i.e., composed mostly of vesicular but also of clinkery and nonvesicular, angular to subangular clasts of the superficial crust of the flow itself, many of which retaining the festooned and ropy surfaces typical of pāhoehoe flows (Plate 09 a, 09 d, 09 f). Since they derive from a single flow, the fragments that make up the top of a rubbly pāhoehoe will have an almost identical composition.

The percentage of the breccia to rubbly surface is typically less that 30% but locally can be as much as 50% of the flow (Martin et al. 2005).

The empty spaces between the fragments of this autoclastic breccia may or may not be filled with a wind-blown sandy matrix, and can eventually be penetrated by lava fingers, which are extrusions of the fluid lava from the flow core.

3.4 Basalt flows - internal structure and facies

Since they are closed systems with slow pressure and temperature losses, pāhoehoe flows that have been ponded

or inflated, present most of the structures that are

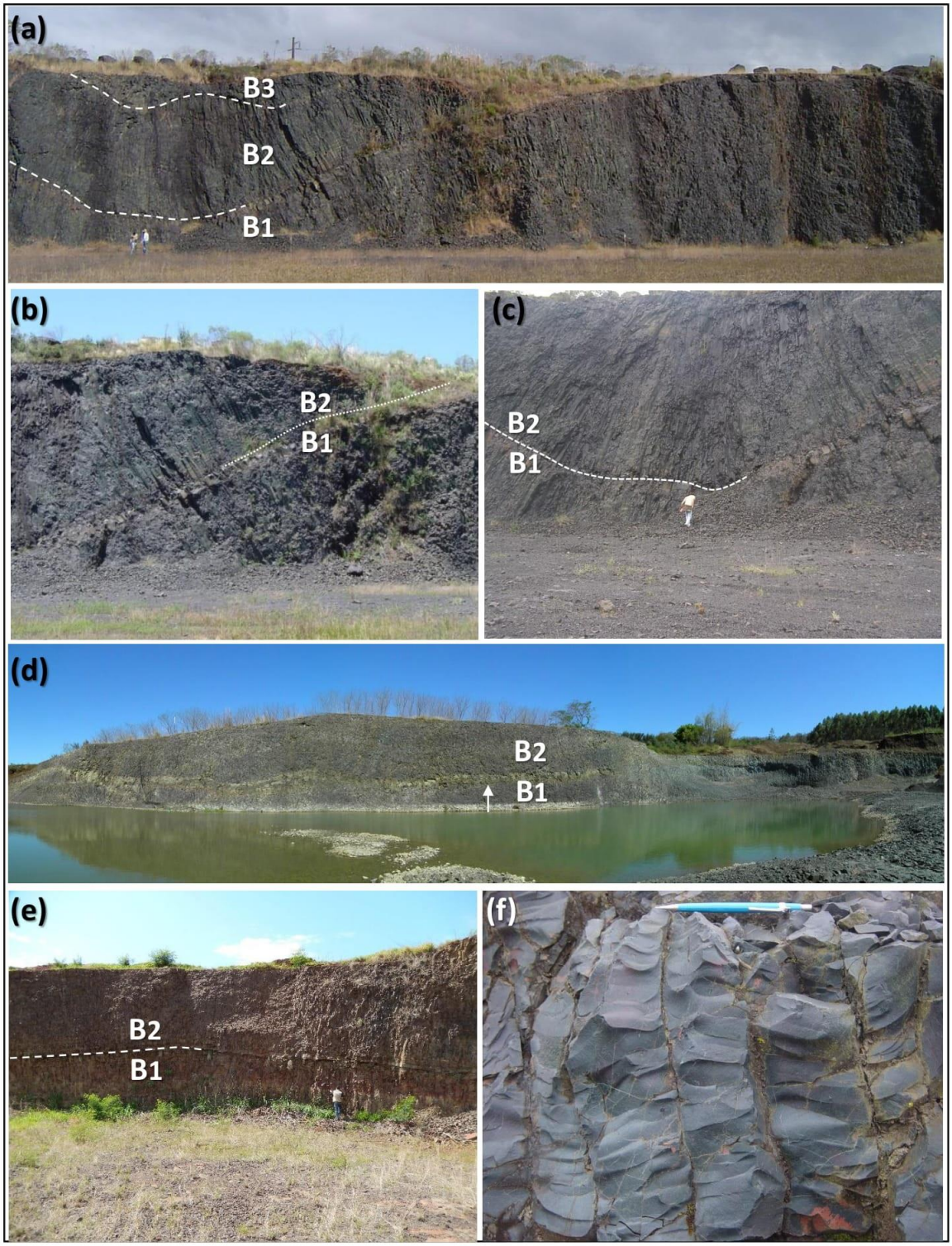

Plate 08 – Hypohyaline basalt flows: (a) Panoramic view of three hypohyaline pāhoehoe basalt flows. The sharp but waving contacts are partially highlighted by the dashed lines. The thin and long entablature elements are not interrrupted in the contacts, suggesting an almost contemporary and quick cooling. The fanning entablature of each flow is orthogonal to the irregular surface of the lower flow. EA-1073; (b) and (c). Details of picture (a) showing the contact between B1 and B2, partially highlighted by the dashed line. In addition to the long entablature elements, the parallel plane fracture zone allways found at the flow's base is the prominent feature. There is no continuous and evident vesicular zone. Millimeter vesicles are found dispersed on the flow and concentrations of these millimeter vesicles are rarely found. EA-1073; (d) Panoramic view of two hypohyaline pāhoehoe basalt flows. The contact is sharp and the base of B2 is composed of an intensely plane-parallel flow fracture zone. OL 3173; (e) Detail view of a sharp and almost horizontal contact between B1 and B2, partially highlighted by the dashed line. OL 3640; (f) Detail of the entablature elements, which are the main facies of the hypohyaline pāhoehoe basalt flows. Note the horizontal concave chisel marks, and the wavy borders of the entablature elements, all attributed to be formed by cooling steps. EA-1346.

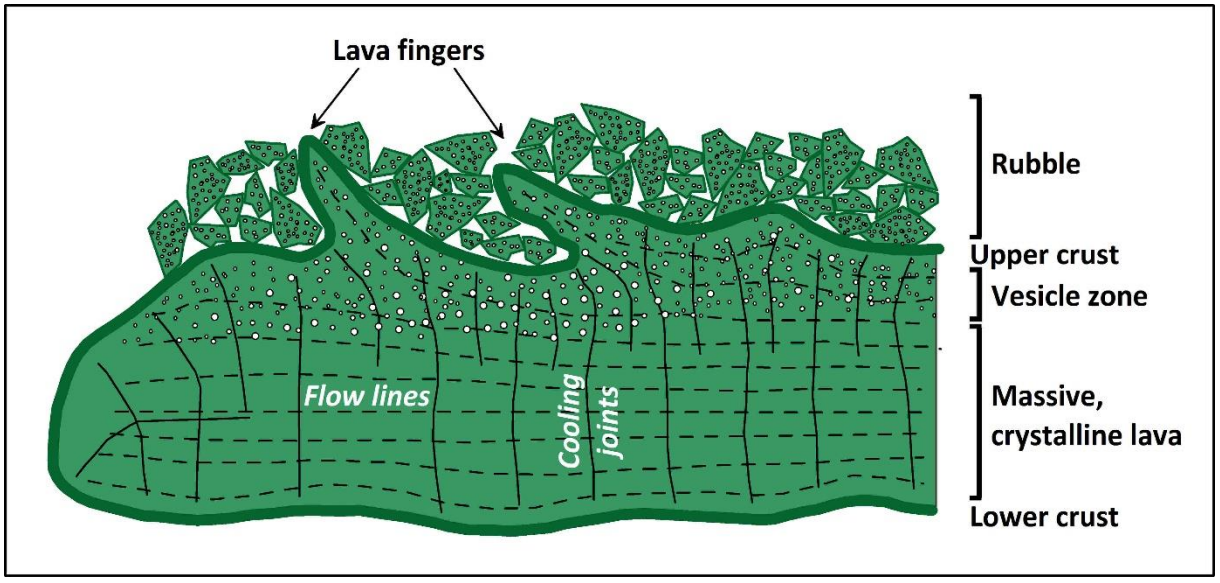

Figure 13 – Schematic longitudinal section of a flow with rubbly pāhoehoe morphology. The top portion is composed of an autobreccia made up of angular fragments, many of which maintain the ropy aspect, characteristic of the top of a pāhoehoe flow. After Tarduno et al. (2002).

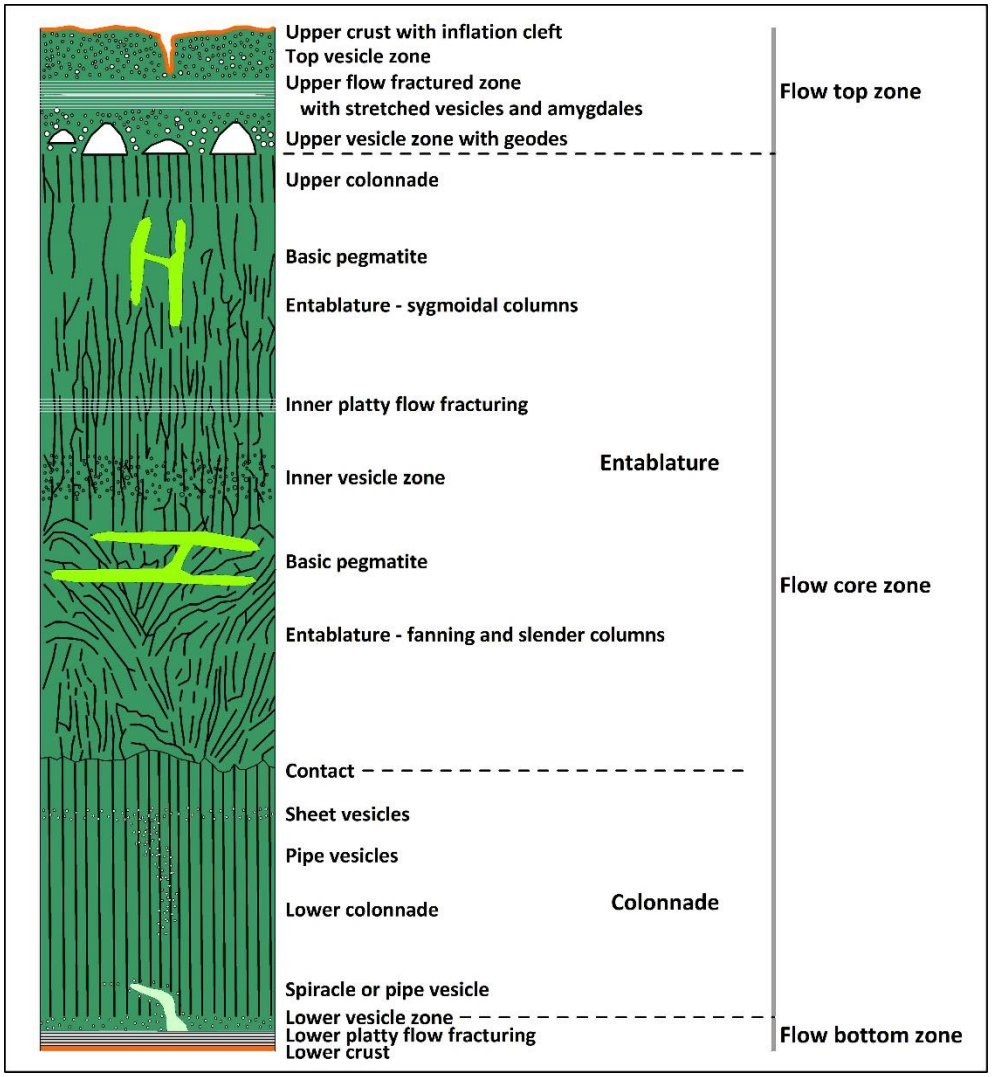

Figure 14 - Schematic internal structure of a tabular inflated pāhoehoe basalt flow, with the three main zones and its characteristic internal facies. After Martin et al. (2005), Mangan et al. (1986), Swanson & Wright

(2006), Johnston & Donnelly-Nolan (1981), Long & Wood (1986), Sem & Sabale (2011) and Forbes et al. (2014).

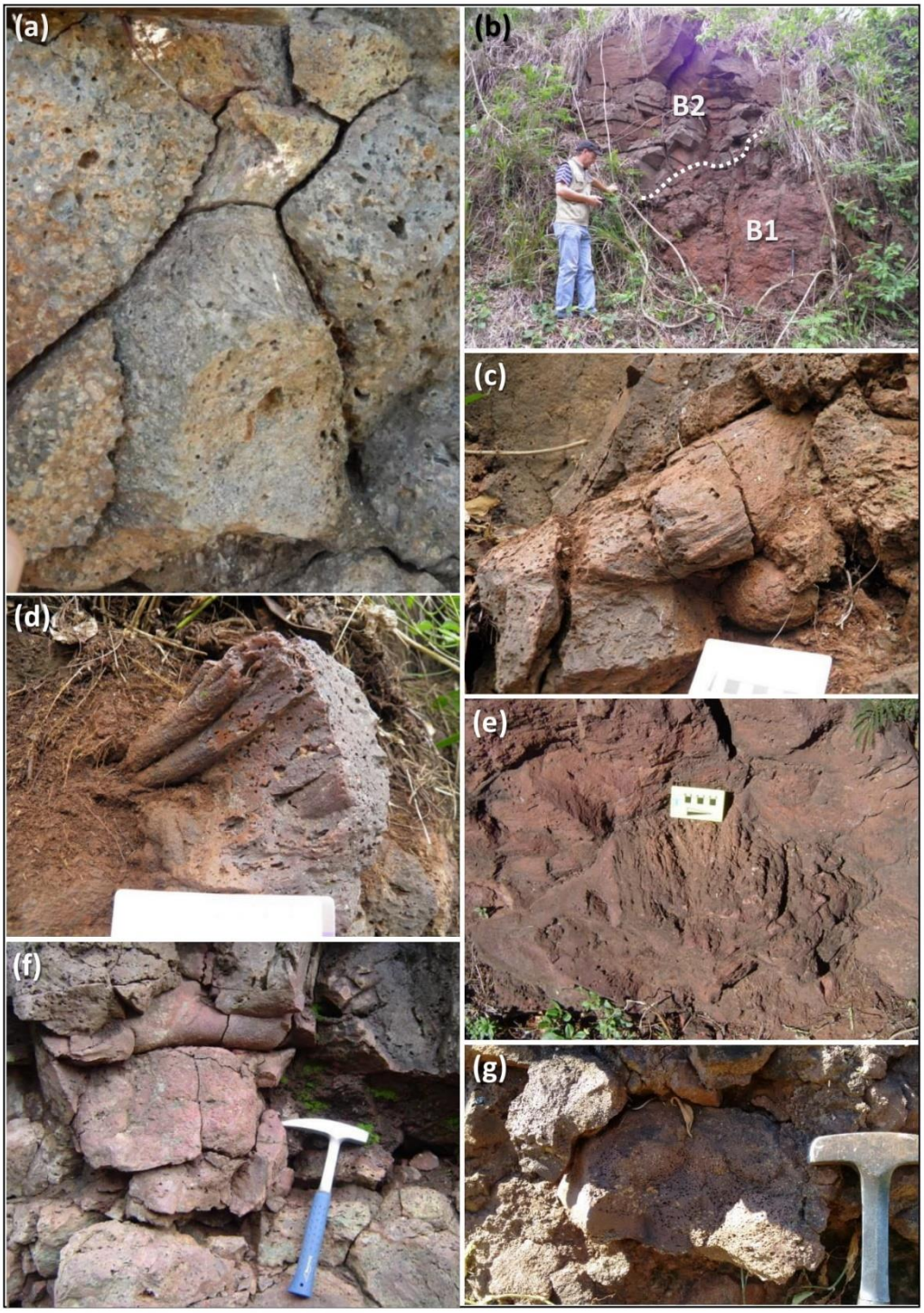

Plate 09 – Upper zone – Rubbly pāhoehoe: (a) Clast supported breccia of a rubbly pāhoehoe basalt flow. The intensily vesicular fragments are in close contact, imbricated, many showing the original filamentous surface or the ropy surface. OL 4117; (b) Sharp contact between two pāhoehoe basalt flows, highlighted by a white dotted line. B1 is typically a rubbly pāhoehoe with breccia fragments showing ropy structure. The lower zone of B2 is almost massive. B2 filled a depression in the uneven surface of B1, so the contact is irregular and plunging. Min. Tec. Clovis Fonseca. OL 3082; (c) Detail of the rubbly pāhoehoe breccia, shown on Picture (b). A small lava extrusion is in close contact with intensely vesicular fragments, many showing the original filamentous or ropy surface. OL 3082; (d) The original ropy and wrinkled structure is preserved in this lava fragment of a rubbly pāhoehoe basalt flow. OL 3082; (e) Top view of a rubbly pāhoehoe basalt flow, showing fragments with the original filamentous or ropy surface. EA-1217; (f) Detail of the rubbly pāhoehoe basalt

flow. The original ropy and wrinkled structure is preserved in the fragments. OL-2147; (g) Detail of the clast supported breccia on a rubbly pāhoehoe basalt flow top. The intensely vesicular fragments are in close contact, imbricated. OL 4161.

Plate 10 – Flow ‘peperites’ and lava toes intruded in wet sediments: (a) Flow ‘peperite’ on the contact between a thick, ponded lava flow moving on depressions of the paleoerg Botucatu dunes field. Stretched fragments of basalt lava (B) mixed with and hosted by a probable wet sand (Ss). OL 3647; (b) In the upper part of the picture, a flow ‘peperite’ (Pp) composed by stretched lava fragments (B) mixed with wet sand (Ss) is observed. This interaction possibly occured in a small salty paleolake as indicated by the many species of zeolites as well calcite lining and filling vesicles. In the lower part of the picture, a lava toe (LT) intruded the silty-sand (Ss), producing a brownish thermal halo (Th). OL 3169; (c) In the lower half of the picture, a flow ‘peperite’ (Pp) identically described as for (b). In the upper half of the picture, a lava toe (LT) intruded the silty-sand (Ss), producing a brownish thermal halo (Th). OL 3169; (d) Detail view of the intensely vesiculated lava toe (Lt) and the thermal halo (Th). OL 3169; (e) A detailed cross section of a lava toe (Lt), the thermal halo (Th) and the hosting salt lake sediment (Ss). OL 3169.

shown in the ideal flow section schemes (Figure 14). The complete and ideal vertical section of the internal structure of a pāhoehoe flow consists of three well-defined zones. From the bottom to the top, there is the bottom zone, the core zone and the top zone (Figure 14).

Each zone, e.g. Bottom, Core and Top, is characterized by several facies (Figure 14) that, depending on local conditions, may or may not develop.

3.4.1 Bottom zone

The lower zone comprises the base contact, the lower platy flow fracturing and the lower vesicular zone.

3.4.1.a Base contact

The basal portion of an inflated pāhoehoe tabular flow is ideally made up of a very fine grained, almost glassy crust, produced by the rapid cooling of the lowest portion of a flow in contact with previous flows or with

volcaniclastic or epiclastic deposits. However, the contact may take on diferent types, depending on the characteristics of the pavement on which it moves. It can be flat when flowing over a rigid, cold, dry surface, wavy when the flow moves over a ropy surface of a pāhoehoe flow, over a volcaniclastic or epiclastic deposit with a wavy top or a dune field; irregular when a flow moves over the hummocky surface with tumuli and inflation clefts of an inflated pāhoehoe flow; brecciated when the flow moves over a rubbly pāhoehoe flow or over an incoherent vulcaniclastic or epiclastic deposit; or flow 'peperite' when the flow moves over a surface composed of fine, moist, coherent material which can be volcaniclastic or epiclastic.

Flow 'peperites' are breccia-like rocks, formed by the contact between a flow and a wet sedimentary substrate or with the bottom sediment of a very shallow water body (Busby-Spera & White 1987, Hanson & Hargrove 1999). Since they originate from a single flow, the clasts are very similar in aspect and composition (oligomithic), unlike the volcaniclastic breccias whose clasts have a varied composition (polymithic). Flow 'peperite's' matrix consists of a sediment or a tufff, placed in suspension or put into on emulsion during the explosive contact between the flow with the ground surface. Thus, the sediment would penetrate and fill the voids and supports almost all clasts. Due to the thermal shock between the flow and the wet sediment, the clasts can show thermal contacts

Plate 11 – Contact of a basalt flow over a Mafic Volcaniclastic Deposit (MVD): (a) Thick basalt tabular flow (B) overlaying a Mafic Volcaniclastic Deposit (MVD). The contact is neat (white dotted line) and marked by a red clinkery crust. The hammer is surrounded by a dotted elipse. OL 3033; (b) Thick basalt tabular flow (B) overlaying a MVD. The contact is neat (white arrow) and marked by a red clinkery crust. Geologist Edir E. Arioli. EA-886; (c) Thick basalt tabular flow (B) overlaying a MVD composed by an upper tuff (T) set and a middle tuff-breccia (Tb) set. The contact is neat (white dotted line) and marked by a red clinkery crust. Geologist Otavio A.
B. Licht. OL 3029; (d) Thick tabular basalt flow (B) overlaying a MVD. The flow's base shows a conspicuous bundle of flow fractures, parallel to the contact, which is clear (white dotted line) and marked by a red clinker crust. Geologists Edir E. Arioli and Otavio A.B. Licht. EA-911; (e) The base of the flow shows

a conspicuous stack of platy flow fractures, parallel to the contact, which is clearly marked by a red clinkery crust (white dotted line); (f) Detail view of the contact between a thin tabular basalt flow and a MVD. Flow wrinkles (Fw) are stamped on top of the tuff layer (T) indicating the flow's displacement. The top of the tuff layer has many spherical vesicles suggesting the presence of fluids and moisture. OL 3029.

rim, which is not the case with the volcaniclastic breccias, since all its components, i.e., framework and matrix, comprised an isothermal system. In the state of Paraná, flow 'peperites' have been described by Waichel et al (2007), Costa (2011), Valore and Licht (2015) and Valore (2020). However, the use of the term 'peperite' is quite controversial, since even in the Auvergne region, France, which is considered the location-type of this rock, the genetic process follows two currents of interpretation (see 1. Introduction).

The contact between a basalt flow over the tuff of a volcaniclastic deposit is generally clear, but it can be wavy (Plate 11 d, 29 b), flat, welded (Plate 11 c) or even with an empty space separating both lithologies (Plate 29 a). It is common for the base of the flow to show vertical, inclined or pipe-like cylindrical vesicles, which are produced by the escape of hot and pressured fluids hosted by the tuff, and whose inclination is a safe indication for the direction of displacement of the flow (Figure 6 f).

The contact between basalt flows can be marked only by a clear dividing line between the vesicular and/or amygdaloidal zone of the lower flow's top and the upper flow's base (Plate 12 c, 12 e) or by a platy fracturing zone of the upper flow, almost parallel to the contact (Plate 12 f).

3.4.1.b Flow fracturing

The base of an inflated pāhoehoe tabular flow may show a 20 to 30 cm thick band that extends parallel to the contact, composed of a dense platy fracturing (Plate 11 d, 12 f). This platy fractured area, also called horizontal disjunction, occurs at the basalt flow's base whether phaneritic (Plate 12 b, 12 f) or hypohyaline (Plate 08 a, 08 b, 08 c, 08 e) and is produced by the differential mechanical behavior of the basal region that is already fairly solid and steady, against the core region in a very plastic state and still in displacement.

3.4.1.c Lower vesicular zone

Just above the basal contact, there is a poorly defined and diffuse vesicular and/or amygdaloidal region. The vesicles can be spherical, stretched, cylindrical or pipe-like. If they are filled, thus called amygdales, their content will reflect the composition and amount of fluids contained in the lava or which have been released from the substrate over which the flow is moving. Cylindrical vesicles are formed by the rise of volatiles as the flow solidifies (Plate 06 f, 06 g). As the flow core is still in motion, these cylinders will assume a pipe-like shape tilted and pointing to the flow direction.

Inflated pāhoehoe flows invariably have the basic characteristics of thick P-type lobes, even when they lack pipe vesicles (Cashman & Mangan 2014).

3.4.2 Core zone

The core zone is usually massive, holocrystalline, i.e., with low proportion of glass to crystals and a medium to coarse phaneritic texture. Thick pāhoehoe flows, especially those that have undergone inflation, present many characteristic structures due to slow temperature and pressure losses, a thick core under movement and the volatile escape. In the core zone of a basalt flow, the predominant intraflow structures are those zones characterized by patterns of cooling joints. These are commonly referred to as colonnade and entablature (Tomkeief 1940, in Martin et al. 2005). In the present article, the authors follow Forbes et al. (2014) and adopted the nomenclature of Spry (1962) and Long & Wood (1986) to divide flows into lower colonnade, entablature and upper collonade.

3.4.2.a Lower colonnade

The lower colonnade occurs in the basal portion of an inflated flow's core zone. It consists of columns with a polyhedral cross-section that is usually hexagonal (Plate 13 b, 13 d), but which can be also pentagonal (Plate 13 f) and quadratic.

The diameter of a column ranges between 20 and 40 cm (Plate 13 b, 13 d) and the height usually 5 m but in some cases, it can reach 10 meters (Plate 13 a, 13 c, 13 d). The colonnade is formed by the contraction undergone by the base of the core zone during lava cooling. The width and height of the columns reflect the cooling process: when columns are narrow and poorly formed, the cooling was fast, otherwise when they are thick, wide and well developed, the cooling was slow.

The columns are generally vertical, but they can be slightly and even strongly tilted. This inclination can be taken as a gross indicator of the flow's movement, but it is necessary to be very careful with this criterion since the columns develop perpendicular to the cooling surface, and so when the paleotopography is irregular, the colonnade can be smoothly fanned.

3.4.2.b Entablature

Entablature is a term firstly used by Tomkeief (1940) to describe the zones composed of columnar joints of irregular orientation or union of cubes in the upper parts of some basalt lava flows on the Giant's Causeway, in Ireland. Long & Wood (1986) describe entablature as the part of a flow that exhibits smaller column diameters and more irregular fracture patterns than those of the regular colonnade columns that may lie above and/or below the entablature tier.

Entablature is composed of irregular to regularly jointed small columns frequently less than 0.5 m in diameter. Entablature columns are commonly fractured into hackly, fist-sized fragments that can mask the columnar structure, and typically display a greater abundance of cooling joints than do colonnades. Entablature columns can be oriented vertically, exhibit regular patterns, such as rosettes and fans, or appear completely disordered (Martin et al. 2005).

The entablature is composed of columnar elements that can be vertical or in varied positions, flexed and contorted, formed during the solidification process of the flow core still in a plastic state and subjected to movement. Cooling rates in entablature are higher than in either upper or lower colonnade columns, as demonstrated by narrower striae, shorter column side widths and the presence of dendritic oxides (Forbes et al. 2014).

In some situations, entablature begins as a continuation of the flow's lower colonnade (Plate 14 e).

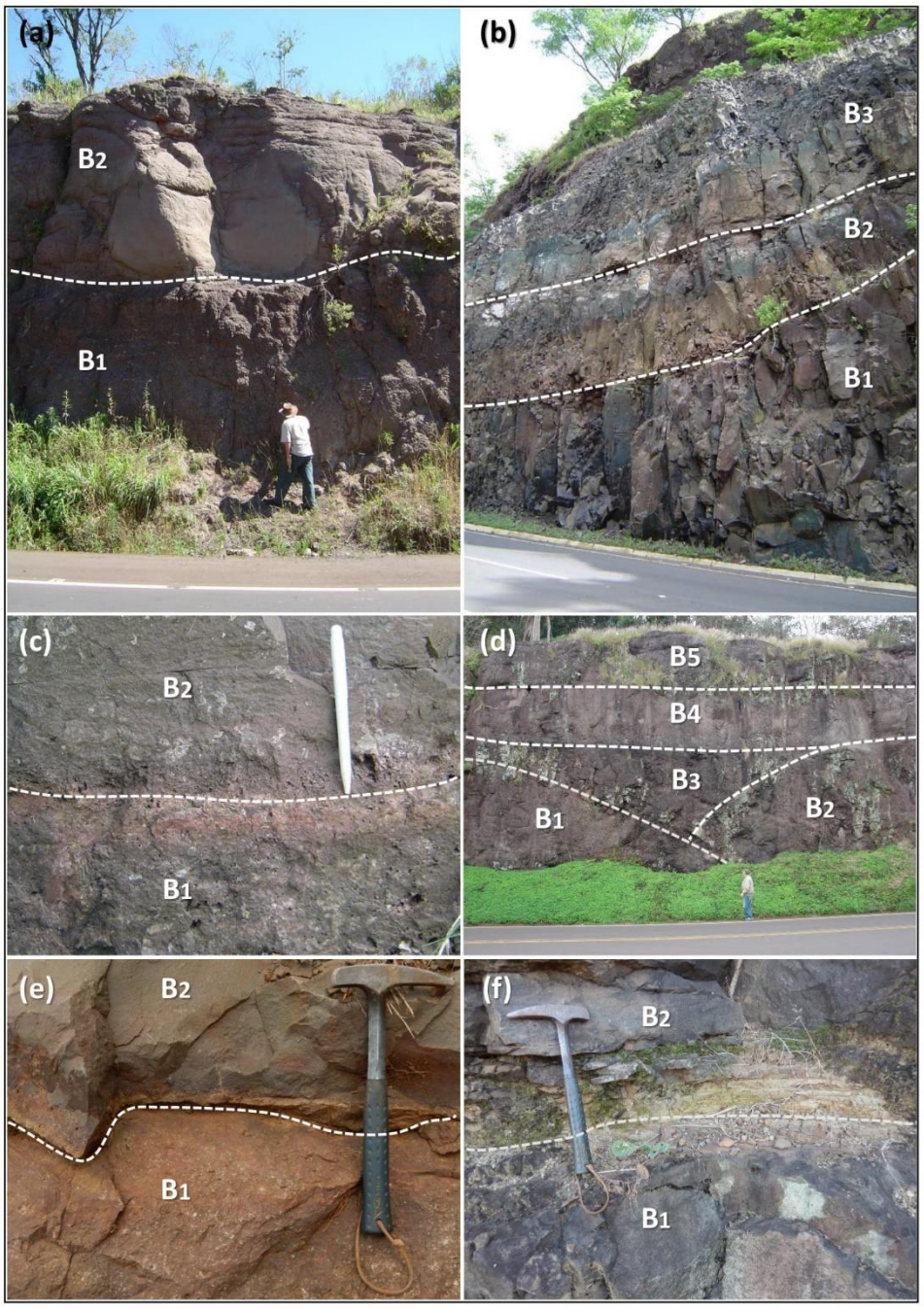

Plate 12 – Contact between basalt flows: (a) Neat contact between two basalt flows. The upper zone of the lower flow (B1) is intensely vesicular, almost scoriaceous, showing sub-horizontal levels of coalescent vesicles and/or quartz filled amygdales. The base and core zones of the upper flow (B2) show flow lamination which have been evidenced by weathering. Geologist Edir E. Arioli. EA -948; (b) Sharp contact between three basalt flows, each a few meters thick. The flows are essentially massive and do not show clear internal zoning or facies. The contacts are marked by a red clinkery crust, which is always in the upmost surface of the bottom flow. EA-1139; (c) Sharp contact between two basalt flows, each with few meters thick, marked by a clinkery red zone. The upper zone of B1 is intensely vesicular presenting some coalescent and stretched vesicles suggesting movement during lava degassing. In the B2 base some tiny spiracles are observed. EA-776; (d) Contact between five basalt flows, each a few meters thick. Flows are essentially massive and do not show clear internal zoning or facies, excepting flow fracturing. The contacts are marked by a lower reddish clinkery crust followed by a thin vesicular zone. The section appears to be transversal to the active fronts. B1 and B2 seem to be the edges of few meters thick lobes. When one lobe reaches another, a small depression was formed and filled by B3. B4 and B5 flowed on a flat and even surface. Geologist Edir

E. Arioli. EA-1617; (e) Detail view of a sharp contact between two basalt flows. The lower flow (B1) is intensely vesicular and the upper (B2) is massive. The contact is marked by a clinkery red crust, which is the B1's upmost surface. OL 4071; (f) Contact between two basalt flows. B1 do not show a vesicular zone or an upper crust, and B2 shows a 15 cm thick lower platy fractured zone, produced by the stress due to the movement of a core still plastic over an almost rigid base layer. OL 3795.

Plate 13 – Core Zone – Colonnade: (a) ‘Cambira Stones’. Lower colonnade of an inflated tabular basalt flow, composed of columns with hexagonal cross section. The front is approximately 25 meters wide and the columns are about 6 meters high. The columns located at the edges are slightly converging, inclined towards the flow axis, suggesting that the flow has displaced and filled a smooth valley on the paleosurface. Min. Tec. Clovis Fonseca. OL 4112; (b) ‘Cambira Stones’. Detailed view. Cross section of the hexagonal columns with ca. 40 cm in diameter. OL 4112.‘Cambira’ means stack of smoked fish in native language.; (c) Colonnade composed by columns with hexagonal cross section and up to 6 meters high. Geologist Otavio A. B. Licht. OL 4186; (d) Detailed view of a hexagonal column with 40 cm diameter. OL 4186; (e) Lower colonnade of a tabular inflated basalt flow. Hexagonal columns, short but well developed, measuring 40 cm side. OL 3948;

(f) Detailed view of a column with a pentagonal cross section. In the same place, columns with pentagonal and hexagonal cross sections occur together. OL 4186; (g) Cross section of the lower colonnade of an inflated tabular basalt flow. The hexagonal columns are 40-50 cm wide. EA-1188.

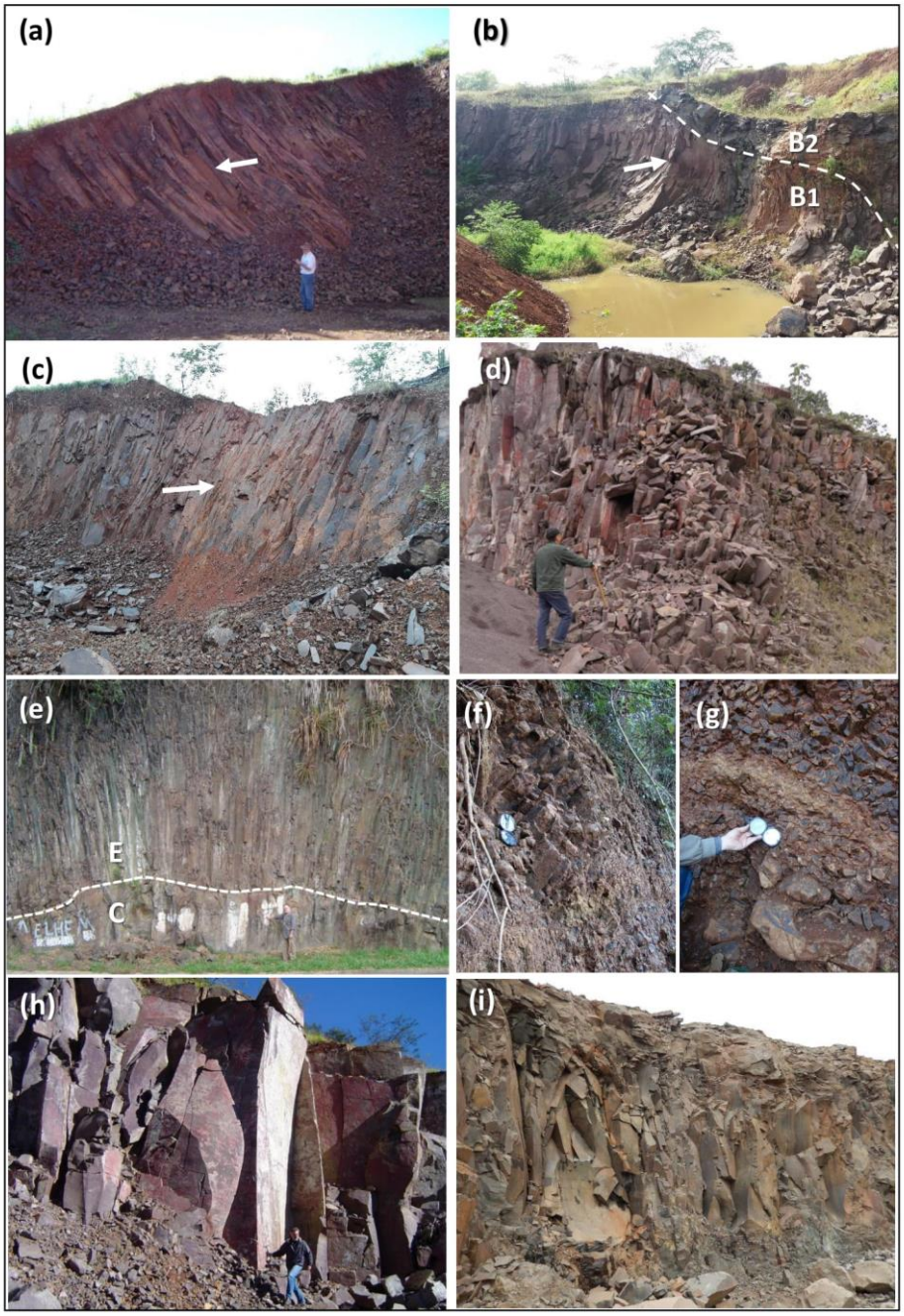

Plate 14 – Core zone – Entablature: (a) Entablature of an inflated tabular holocrystalline basalt flow. The elements with very sharp edges are hunched and tilted in the sense of the movement (white arrow). Geologist Edir E. Arioli. EA-848; (b) Entablature of an inflated tabular holochrystalline basalt flow B1, which is overlayed by B2; the dashed line marks the contact. The white arrow points to the sense of the flow. OL 4063; (c) Entablature of an inflated, tabular holocrystalline basalt flow. The curved and inclined elements in the direction of movement (white arrow), gradually change their attitude to compose a sub-horizontal flow fracturing in the base of the flow; (d) Entablature of an inflated tabular holocrystalline basalt flow. The elements with very sharp edges are almost vertical, suggesting that the flow solidified in an almost steady state. Min. Tec. Clovis Fonseca. OL 3070; (e) Transition between incipient basal collonade and a well-developed entablature marked by the white line, on a hypocrystalline basalt flow. The fan shape is due to the entablature elements are orthogonal to the paleo-topography, and solidified in an almost steady state. Geologist Edir A. Arioli. EA-1139; (f) Entablature of an hypocrystalline basalt flow. In lateral view, the elements of the entablature, resembling thin columns, are hunched and tilted in the sense of the movement, to right. EA-612; (g) A cross section of the same site of (f). The elements of the entablature are exposed as

small polyhedra. EA-612; (h) Entablature of an inflated, tabular and holocrystalline basalt flow, formed by large polyhedral blocks with sigmoidal faces, suggesting a long-term cooling in an almost steady position. Geologist Otavio A.B. Licht. EA-1210; (i) Sigmoidal and polyhedral blocks composing the entablature of the B2 flow shown in picture (b). The entablature is just over the sub-horizontal flow fracture zone. The absence of colonnade implies on a relatively fast cooling of a flow still in movement. OL 4063.

In other, especially in the hypohyaline basalt flows the entablature begins on very short, poorly developed and very fractured columns (Plate 08 a, 08 b, 08 c), forming the same cube-jointing style observed by Forbes et al. (2014) in Iceland.

Thus, one can be absolutely sure that when the entablature is exposed, this is the central zone of the flow.

In very special cases, the inclination of the entablature elements can be taken as an indicator of the direction of flow (Plate 14 a, 14 b, 14 c), but care must be taken, as the entablature elements were formed with the lava still in a plastic state, which means that the flow core was still moving producing sudden and localized changes in the shape and inclination of the entablature elements.

3.4.2.c Chisel marks

Chisel marks are observed both in the colonnade and in the entablature. The chisel marks have a concave shape, are parallel to each other and perpendicular to the axis of the column (Plate 03 b, 08 f). Since they are produced by cooling, they mirror isotherms in the cooling lava, so the carved and deeper the chisel marks are, the slower the temperature loss would have been. Thus, the depth and width of the chisel marks are much smaller in the entablature columns than in the colonnades, what indicates faster cooling (Forbes et al. 2014).

3.4.2.d Convex surfaces

Convex surfaces are isolated or bundled fractures that develop in the body of a flow and are produced by the cooling of the lava still subjected to flow in an almost rigid plastic state. Not to be mistaken for entablature.

These surfaces can develop towards the active front, i.e., indicating the direction of flow, in which case their surface is smooth (Plate 15 b, 15 f, 15 g). In complete longitudinal sections of a flow, it is possible to observe a change in the attitude of these convex surfaces to sub-horizontal, to compose the platy fracturing zone at the base of the flow (Plate 15 a). This transition, from sub-vertical to sub-horizontal, suggests that these convex surfaces actually represent relief surfaces, produced by the diferential stress that develops in the body of a flow, due to the combination of different rheological behaviors, e.g. plastic, semi-plastic and rigid, with the contraction due to cooling. Convex surfaces can also develop towards the lateral edges of a flow, marking its lateral widening. In that case, the surface will be striated, with slickensides pointing to the main active front (Plate 15 h).

3.4.2.e Degassing chimneys

Degassing chimneys are formed by the upward migration of volatiles trapped in a lava flow. They are generated by the accumulation of fluids in bubbles, the internal pressure and buoyancy of which exceeds the confining pressure and the viscosity of the lava, therefore rise slowly, assuming the shape of a subvertical chimney. Unlike vesicle pipes which occur at the base of the flow that are well defined and often empty, degassing chimneys have diffuse limits (Plate 16 c) and show a complex filling with vesicles, large glass globules and even plagioclase phenocrysts (Plate 16 b).

When the sub-vertical degassing chimney meets a sub-horizontal discontinuity surface, and the volume and pressure of the rising fluids are large enough, it can act as a feeder for a sub-horizontal layer, like a sill, that will have the same composition and grain size as the chimney (Plate 16 d).

3.4.2.f Basic pegmatites

In inflated basalt flows over than 10 meters thick and made up of fluid-rich lavas, basic pegmatites can develop, ranging in size from few centimeters to tens of centimeters in thickness and tens of centimeters to many meters in length. They have a coarse phaneritic texture composed of a network of pyroxene and/or plagioclase phenocrysts that can reach up to 10 cm in length (Plate 17).

The formation of basic pegmatites occurs by means of the segregation, migration and rise of residual fluids from the basal portions of the flow. When crossing the central zone of higher temperature, the liquid's crystalline nuclei are fused, decreasing viscosity and facilitating difusion during crystallization, forming large, fast-growing and skeletal crystals (Hartley & Thordarson, 2009).

Upon reaching the coolest upper region, the mixture of crystals and liquid is hampered and accumulates horizontally. Subsequent episodes of downward fracture of the upper barrier cause the liquid phase of the partially crystallized lava to degas and quickly cool (quench), forming glass and smaller crystals in the middle of the larger crystals (Pufer & Horter, 1993).

Because they represent special conditions of fluid escape during the final stages of consolidation of a basalt flow, the basic pegmatites can be sub-horizontal (Plate 17a), sub-vertical or even composing a stockwork (Plate 17 f). Thus, when they are tilted, they indicate the flow direction.

3.4.2.g Lava tubes

Lava tubes display a major importance in insulating flows and, thus, permitting long-distance internal transport of lava, being fundamental to the formation of pāhoehoe flow fields (Wright & Takahashi 1989, Cashman & Mangan 2014).

Basalt flows are continuously fed by tubes, true internal ducts that are responsible for the transport of the lava, ensuring the advance and the inflation process of the flow. These ducts have a semicircular (Plate 18 a, 18 b, 18 e) to elliptical section (Plate 18 c, 18 d, 18 f), its internal structure has concentric layers and a solid core (Plate 18 b, 18 c), but if the lava supply sudden stops, the tube could remain empty (Plate 16 d, 18 f). They can have different dimensions, depending on the volume of lava and the rate of feeding. There appears to be a direct relationship between the thickness of the flow and the diameter of the tubes.

3.4.3 Top zone

The top zone comprises the platy flow fracturing or lamination, may contain autoliths, the upper vesicular/ amygaloydal zone, and an upper crust that may be covered by basalt or glassy filaments, present the characteristic ropy structure of a typical pāhoehoe flow, or even an autobreccia.

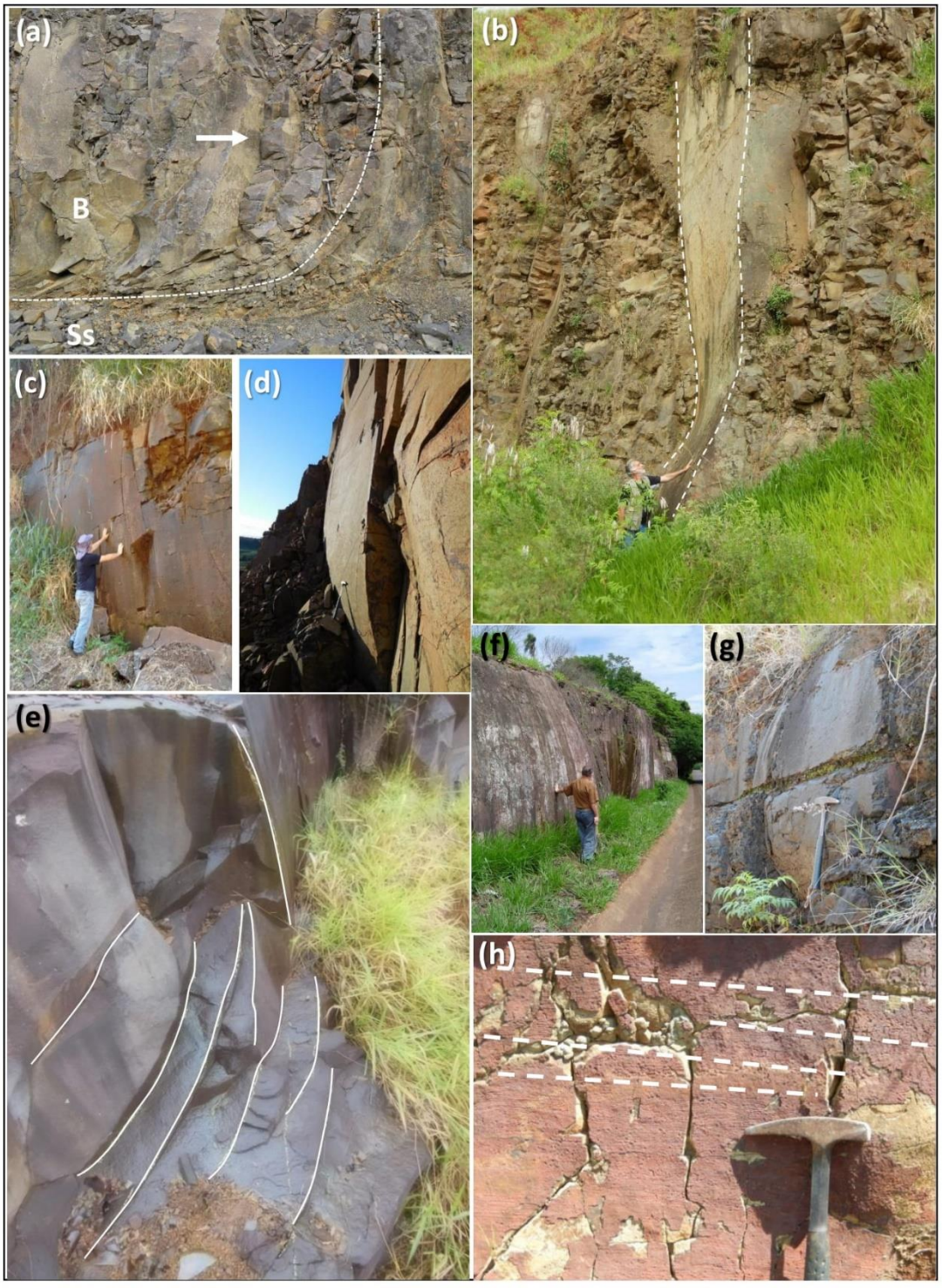

Plate 15 – Core Zone – Convex surfaces: (a) Almost parallel and vertical convex surfaces in the core of the basalt flow (B) identified by the dashed line. Do not confuse it with entablature. The arrow indicates the sense of flow. The surfaces gradually tilt and become almost horizontal planes composing the fractured zone at the low's base, just in the contact with the Botucatu Fm. sandstones (Ss). OL 3142; (b) Part of a convex surface (delimited by dashed lines), at the core of a tabular basalt flow. The curvature indicates that the movement occured to the right of the photo. Geologist Otavio. A.B. Licht. OL 4071; (c) Convex surfaces in the massive core of a pāhoehoe tabular flow, indicating the movement to the left of the photo. Min. Tec. Clovis Fonseca. OL 4160; (d) Convex surfaces in the massive core of an inflated pāhoehoe tabular flow, indicating a leftward movement. OL 3517; (e) Top view of parallel convex surfaces (highligted by white lines) in the core of a tabular inflated basalt flow, indicating movement toward the right. EA-631. Modif.

Soares (2016); (f) Convex surfaces in the massive core of a tabular inflated basalt flow, indicating movement to the right. Geologist Edir E. Arioli; (g) Convex surfaces on a flow's core, indicating movement to the left. OL 3949; (h) Sub-horizontal streaks on a convex surface; the slickensides indicate the direction of the movement. This striated surface delimits a border and is not related to the flow's frontal portion. OL 4119.

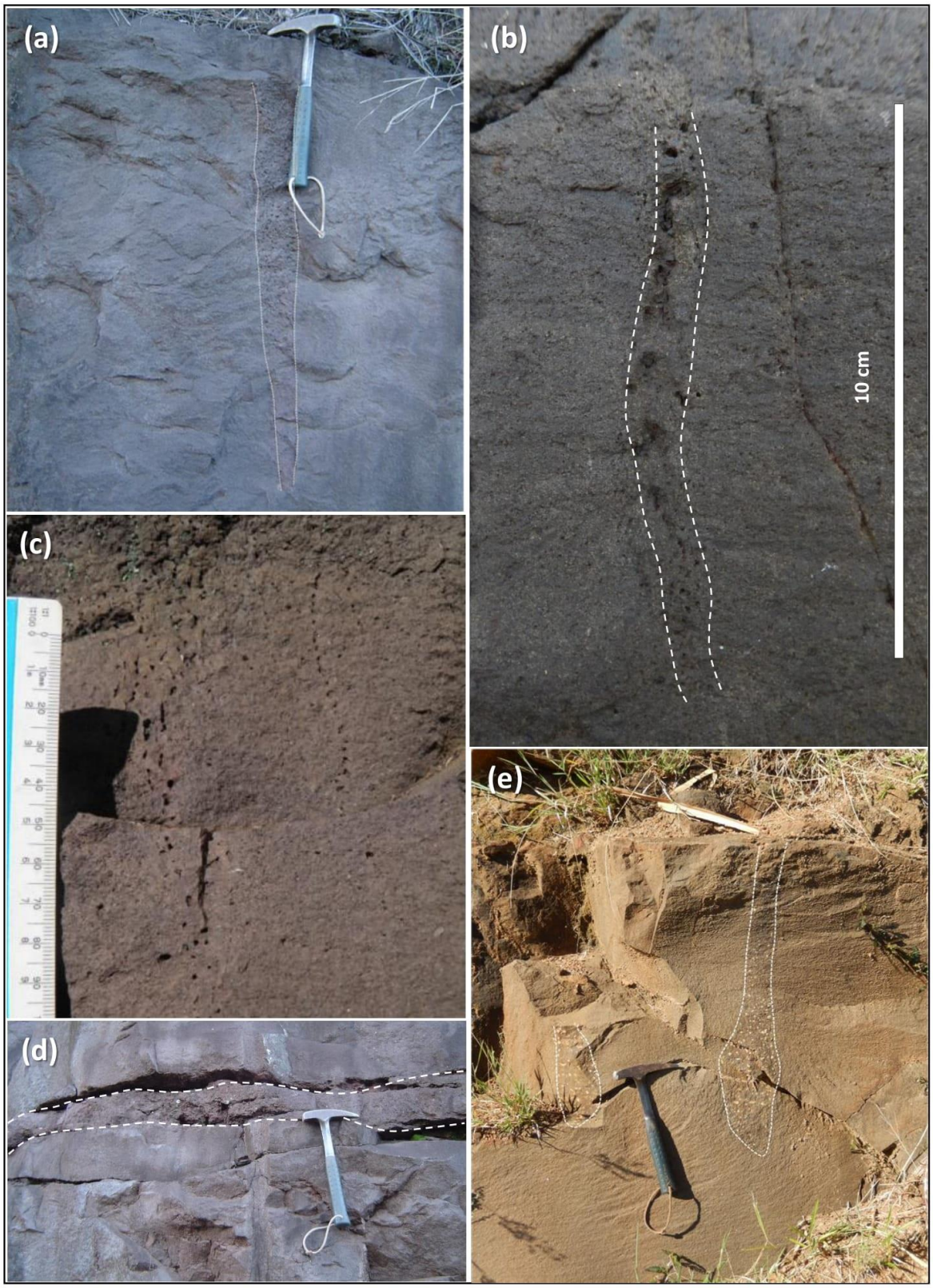

Plate 16 – Core zone – Degassing chimneys: (a) coarser than the host basalt flow, a degassing chimney is composed of empty spaces and vesicles, glass globules, and small pyroxene and plagioclase crystals. Its apparent conical shape is due to the slight dip of the section in relation to the vertical pipe. EA-1230; (b) A small, but well defined subvertical degassing chimney. The number of empty spaces indicate the ascending fluids were volatile-rich. OL 4254; (c) In case the amount of ascending volatiles is insuficient to compose a well-defined chimney, its limits will be subtly suggested by aligned vesicles. OL 3153; (d) When the pressured fluids are trying to escape from the still plastic basalt flow, they occasionally find a sub-horizontal weakness plane. Thus, they may migrate along this plane, widening the fracture to form a small sill, whose limits are highlighted by the white dotted lines. These sills are always fed by a subvertical degassing chimney, which is not shown in this picture. EA-1230; (e) Two amygdale-rich degassing chimneys formed by the releasing of volatiles from the body of the basalt flow. The limits of both are highlighted with white dotted lines. OL

4146.

Plate 17 – Core zone. Basic pegmatites: (a) A tabular, inflated basalt flow containing several sub- horizontal basic pegmatite bodies. The lower limit of some pegmatites are highlighted by white dotted lines. The quarry wall has ca. 14 m high. Geologists Carlos H. N. Ferreira and Luiz C. Silvério Jr.(Ferreira 2011). OL-2011; (b) Detail view of a basic pegmatite, to emphasize the augite crystals, each up to 8 cm long. O L- 2011; (c) Detail view of a basic pegmatite, showing the unusual association of chloritized glass globules, which fill the interstices between large plagioclase and augite crystals. O L-2140; (d) Detail view of a swallow-tail aggregate of augite crystals. Augite crystals, up to7 cm long, with corroded borders. Note the chloritized

glass globules and mesostasis. Scale bar in cm. OL-2011; (e) Basic pegmatite. Swallow-tail aggregates of augite crystals up to 7 cm long, with smaller plagioclase crystals, immersed on a chloritised glassy mesostasis (dark green globules). OL-2140; (f) A complex stockwork structure of a basic pegmatite. The general dip of the main pegmatite bodies suggests a northward flow direction (to the right of the picture). (Soares 2016). EA-1054.

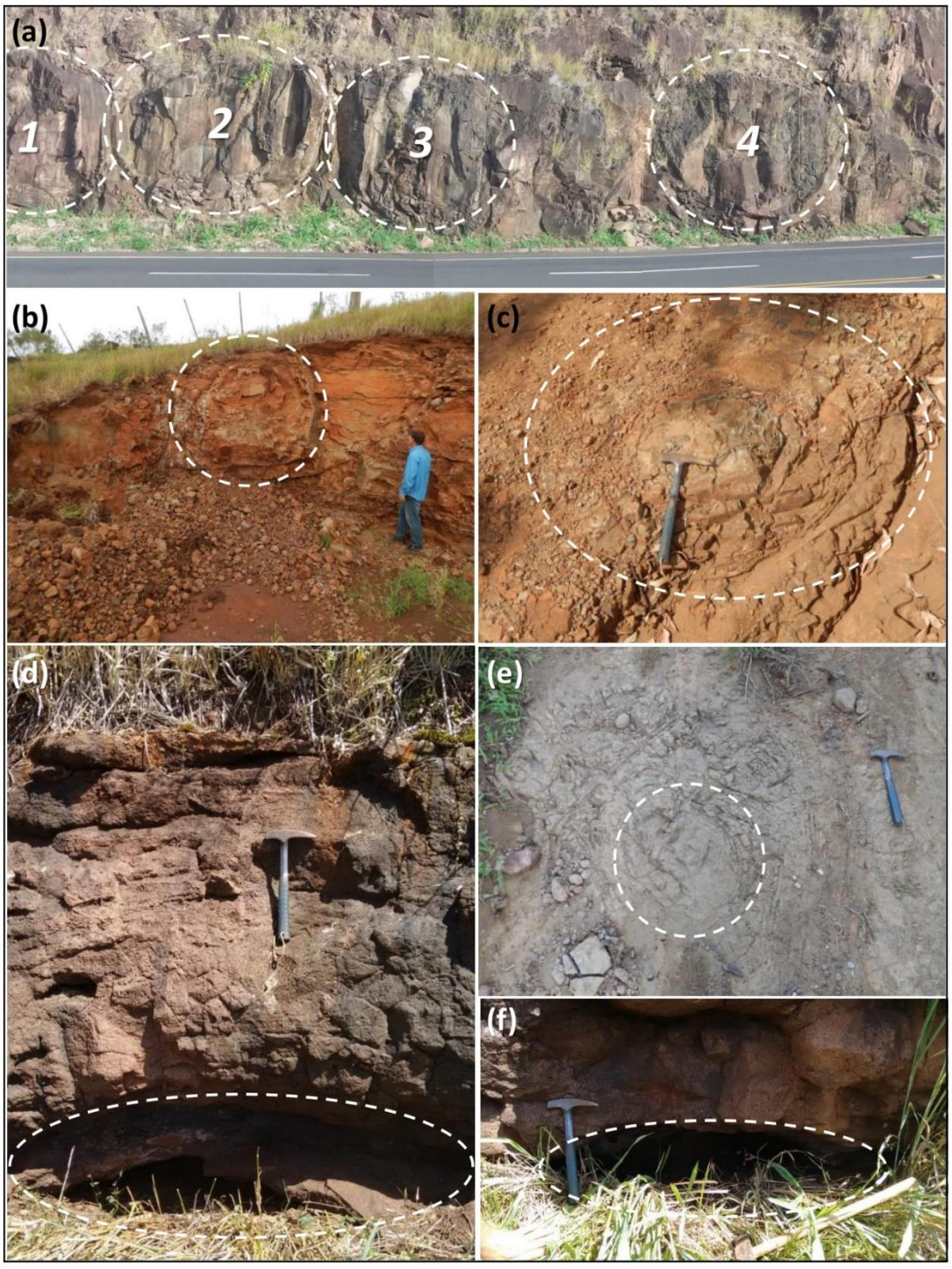

Plate 18 – Core zone – Lava tubes: (a) Cross section of four feeder tubes (outlined by the dashed lines), ca. 6 m in diameter each, of the same inflated and tabular pāhoehoe basalt flow. The edges are well marked by convex fractures and are concentric to the massive core. Based on the convergence of the edges, the lava must have flowed towards the road cut. OL 3161; (b) Cross section of a filled feeder tube (outlined by the dashed lines), ca. 4 m in diameter; the edges are marked by convex fractures, surrounding the massive core. This primary feature should not be taken for spheroidal exfoliation, which is due to weathering. Min. Tec. Clovis Fonseca. OL 4139; (c) Top view of a feeder tube (outlined by the dashed lines), ca. 1 m in diameter; the edges are marked by convex fractures, surrounding the massive core. Do not mistake with spheroidal exfoliation. OL 4107; (d) Cross section of an empty, flat feeder tube, ca. 0.3 m high and 1 m wide (highlighted by dashed lines). The edges are marked by convex fractures, which are concentric to the hollow

core. OL 4165; (e) Top view of a feeder tube (outlined by the dashed lines), ca. 1 m in diameter; the edges are marked by convex fractures, surrounding the massive core. Do not mistake with spheroidal exfoliation. OL 4126; (f) Cross section of an empty, flat feeder tube, ca. 0.3 m high and 1 m wide (highlighted by dashed lines). The edges are marked by convex fractures, which are concentric to the hollow core. OL 4165.

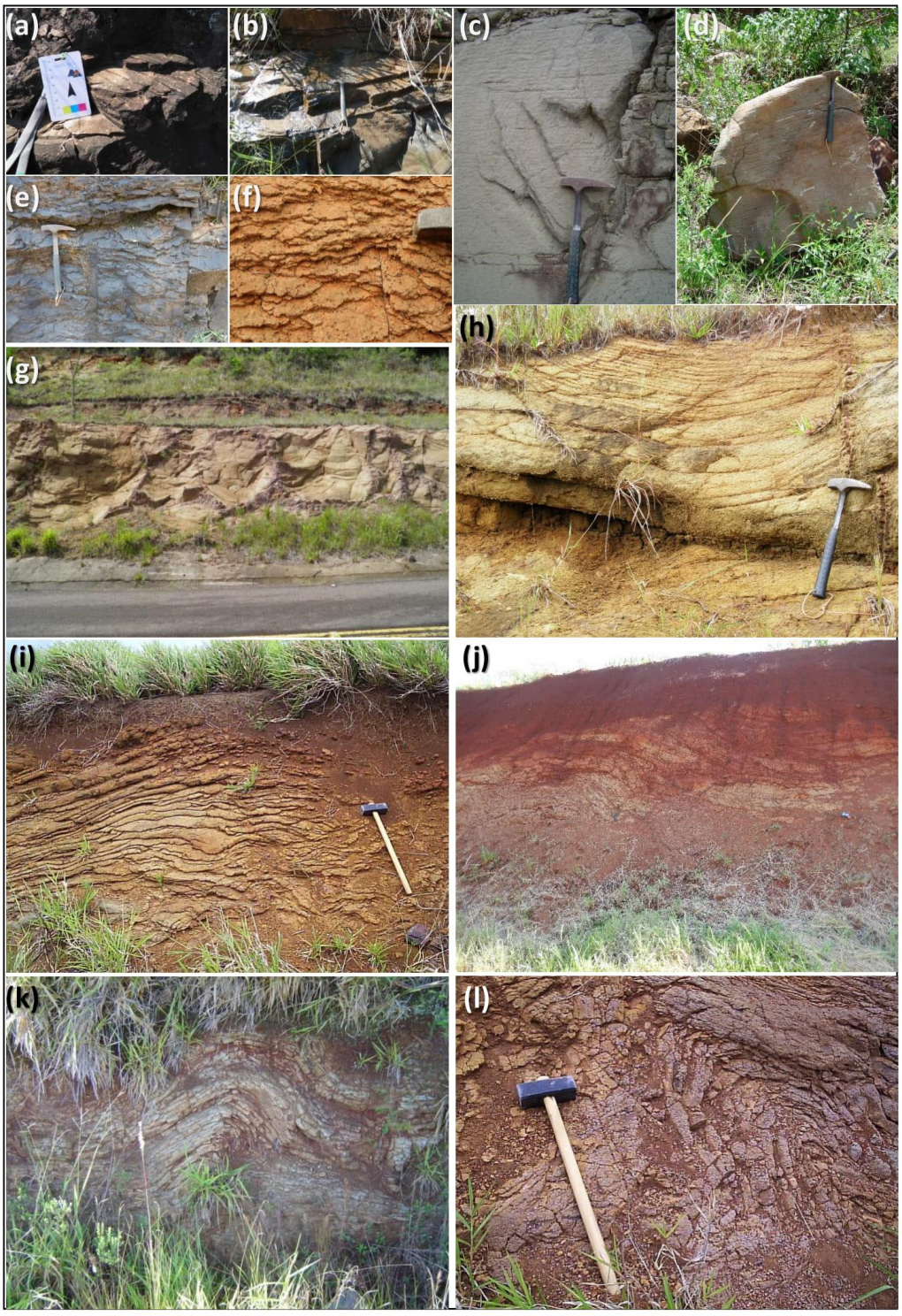

Plate 19 – Upper Zone - Flow lamination: (a) Plane parallel, sub-horizontal flow lamination at the base of a basalt flow. OL 3100; (b) Plane parallel, sub-horizontal at the base of a basalt flow. OL 3941; (c) Flow lamination at the base of a basalt flow, highlighted by weathering. EA-1145;(d) Part of a basalt flow with planar flow lineament, highlighted by weathering. EA-811; (e) Parallel, smootlhly flowing lamination, indicating local changes in the flow regime. OL 3949; (f) Flow lamination on the vesicular zone of a basalt flow, highlighted by weathering. OL 3737; (g) Concave structures due to the channelized flow of several anastomosed basalt lobes, of a compound flow. The superposition and anastomosis of the channeled lobes give the outcrop the appearance of a sedimentary rock with channeled cross-stratification. OL 3126; (h) Detailed view of Picture (g). The concave flow structure of the channelized lobes. OL3018; (i) Flow

lamination of a basalt flow, highlighted by weathering. The scale is ca. 80 cm long. JCC254; (j) Wavy and folded flow lamination reflecting the internal movement of the basalt flow, produced by irregularities and obstacles of the paleo-topography. Features highlighted by weathering. OL 4146; (k) Flow lamination folded probably by an obstacle which hampered the advance of the basalt flow. OL-2110; (l) Top view of a basalt lobe showing its inner flow structure. The scale is ca. 80 cm long. JCC254.

3.4.3.a Flow lamination

The interface between the Core Zone and the Top Zone of the flow, is marked by a region with intense flow lamination (Plate 19 a, 19 b, 19 e, 19 f), composed of oriented minerals, and also stretched glass globules (Plate 19 c, 19 d). Like the platy flow fracturing developed in the lower zone of the flow, the flow lamination is formed by stress due to the diference in the displacement rate that occurs in that upper region. In thinner flows, flow lamination can show folds and other ductile structures produced when overcoming obstacles on the paleo-relief (Plate 19
j, 18 k, 18 l).

A very striking style is the flow lamination shown in some cross sections of sets of composite lobes. In these cases, which are uncommon, the flow lamination takes on the aspect of a cross-chanelled stratification (Plate 19 g, 19 h).

In fresh rock, the flow lamination may not be very evident, but the diferential action of weathering is very efficient in emphasizing it (Plate 19).

3.4.3.b Autoliths

During the displacement of a flow, the upper crust even the vesicular zone, already solidified can be fragmented and these autoliths would be encompassed and partially digested by the flow itself (Plate 20).

Small fragments of lava of a few cm in length, which had been generated by small steam e xplosions at the top of the basalt flow, can occasionally be found. These fragments are projected and are encrustated on the surface of the flow itself or of a neighboring lobe or flow (Plate 24 a).

3.4.3.c Upper vesicular zone

In this portion of the flow concentrate those bubbles formed by gases and fluids, which are dispersed in the flow and that tend to escape to the atmosphere during the lava degassing process.

As the Core Zone cools more slowly because it is insulated and also because it is continuously being lava fed, the larger diameter vesicles and amygdales are located

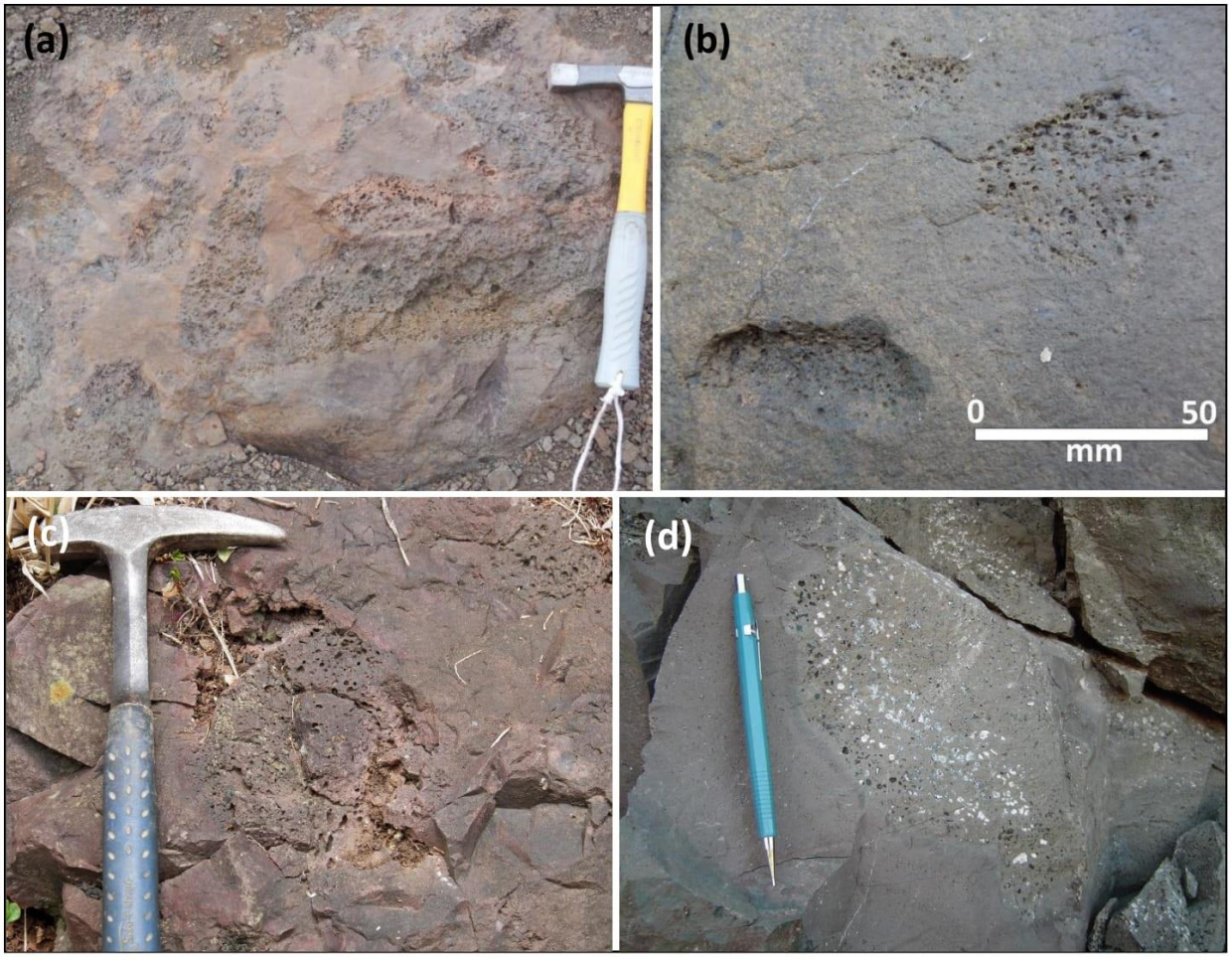

Plate 20 – Upper Zone. Autholiths: (a) Intensely vesiculated fragments, almost scoriaceous, of the cooling flow captured and partially diggested by the still hot and partially fluid lava. OL 3500; (b) Intensely vesiculated fragments of the cooling flow captured and partially diggested by the still hot and partially fluid lava. OL 4122; (c) Vesicular, almost scoriaceous fragments of the cooling flow captured and partially diggested by the still hot and partially fluid lava. OL 3045-03; (d) Intensely vesiculated fragments of the cooling flow itself captured and partially diggested by the still hot and partially fluid lava. Most of the

vesicles are filled with quartz and carbonates, which emphasizes that this process occured while the spill was still in motion, with the degassing of the lava responsible for filling the vesicles and not any subsequent process. EA-1435.

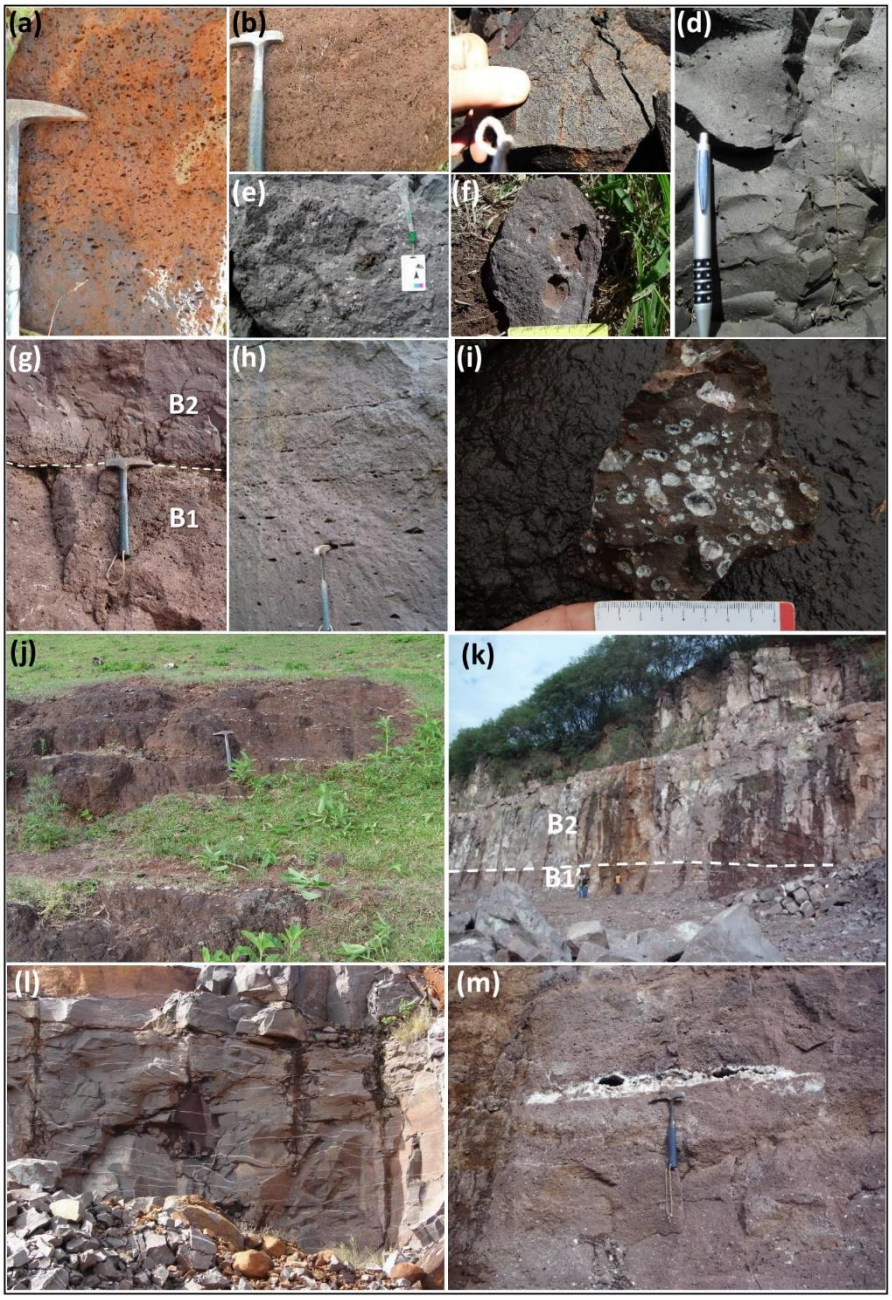

Plate 21 – Upper zone – Vesicular zone: (a) Upper vesicular zone of a thick tabular pāhoehoe basalt flow. Sub-spherical vesicles up to 2 cm in diameter, smoothly aligned along flow lines. OL 3658; (b) Part of the upper vesicular zone of a thick pāhoehoe basalt flow. Sub-spherical vesicles up to 2 cm in diameter. OL 3736; (c) Rare occurence of a vesicular zone in a hypohyaline basalt flow, composed by millimetric vesicles concentrated in the flow's top. OL 3946; (d) The most common situation in hypohyaline basalt, is that the millimeter vesicles are dispersed in the massive and dense flow's body. OL 3172; (e) Portion of the upper vesicular zone of a thick tabular pāhoehoe basalt flow, showing some vesicles filled with zeolites, i.e, amygdales. OL 3160; (f) Vesicles up to 2.5 cm, from the upper vesicular zone of a tabular basalt flow. Hand sample. EA-1209b; (g) Upper vesicular zone of the tabular pāhoehoe basalt flow B1, in contact with the lower vesicular zone of basalt flow B2. The contact between B1 and B2 is sharp, highlighted by the dashed line. EA- 1665; (h) The upper vesicular zone of a tabular pāhoehoe basalt flow, showing stretched and agglutinated vesicles, up to 30 cm along the flow planes. EA-1209; (i) Portion of the upper vesicular zone of a thick tabular pāhoehoe flow. There are empty vesicles, other lined with quartz microcrystals, and amygdales filled with white silica. OL 4024; (j) Up to 2 m long sub-horizontal layers of quartz, formed by the coalescence of vesicles as a function of the diferential stress produced by the movement of the fluid core and

the upper crust already cooled and consolidated. These long quartz layers are aligned according to the flow planes. EA-875; (k) Upper vesicular zone of the basalt flow B1, with up to 3 m long stretched vesicles, partially or completely filled with silica and carbonates. The contact between B1 and B2 is sharp and is highlighted by the dashed line. Geologists Oderson Souza Filho, Tiago M. Esteves and Otavio A.B. Licht. EA-1665; (l) Detail view of picture (k). Upper vesicular zone of flow B1 with streched vesicles up to 3 m long, partially or completely filled with silica and carbonates. EA-1665. (m) Detail view of Picture (l) Stretched vesicle, 120 cm long, partially filled with silica and carbonates, arranged along the flow plan of a tabular basalt flow. EA-1665.

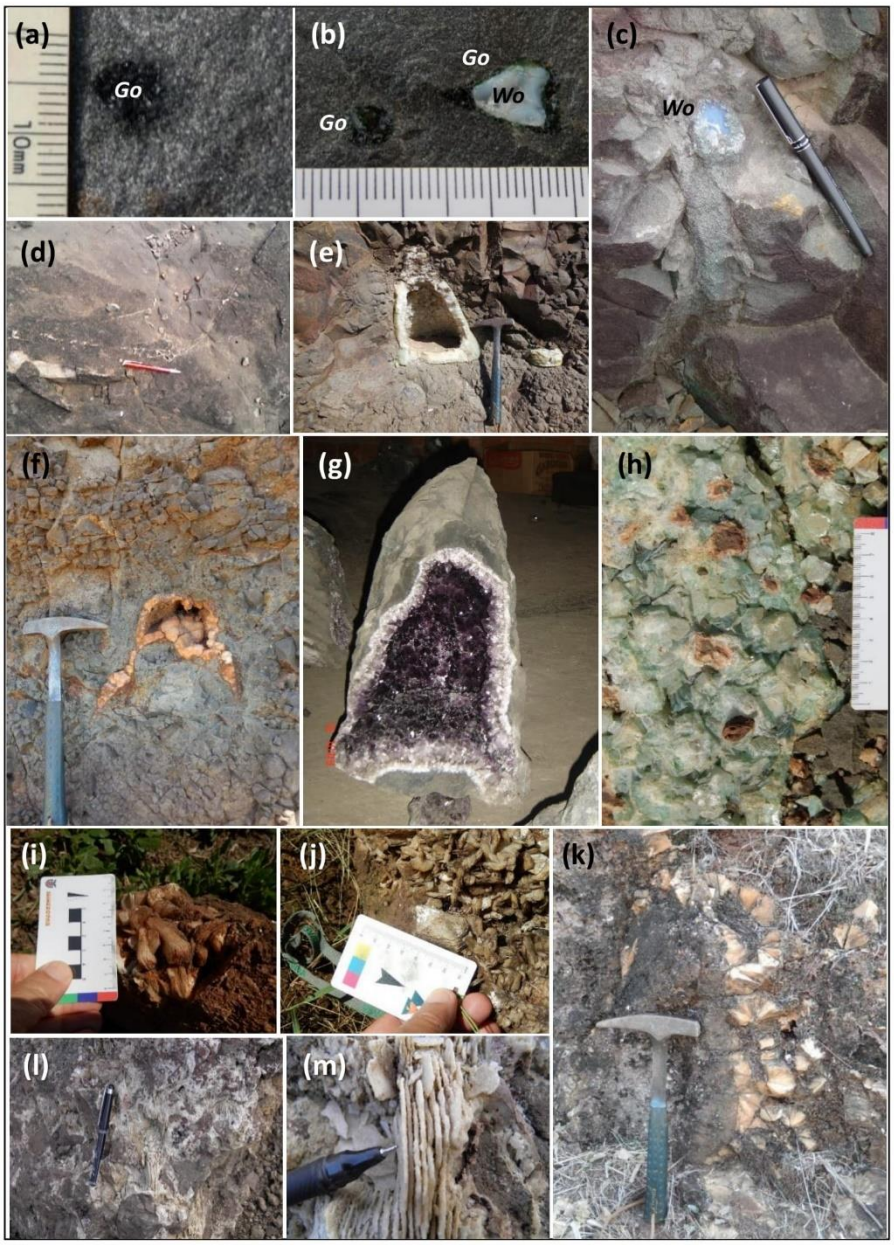

Plate 22 – Minerals filling vesicles and fractures: (a) Detail view of a deep green opal (Go) globule hosted by the core of a massive basalt flow. Scale in millimeters. OL 3751; (b) Detail view of two globules, one entirely fill of deep green opal (Go) and other zoned with a deep green opal rim (Go) surrounding a white opale core (Wo). These globules are hosted by the core zone of a basalt flow. Scale in millimeters. OL 3790; (c) Cylindrical and subvertical pipe filled with bluyish white chalcedony. The photo shows both the cross and the longitudinal section of the tube. EA-859; (d) Veins of amorphous white silica, filling open spaces along fracture planes of the massive core zone of a basalt flow, possibly due to late or post magmatic fluid injection. OL 3010; (e) Typical triangular aspect of the longitudinal section of a geode, also known as chapell. It indicates the difficulty of the bubble to rise and cross the more viscous upper portions of the flow. The geode is lined with white to light purple (amethystine) quartz crystals up to 4 cm long. OL 3777; (f) Enlightening example about the process of rising a large bubble on a thick basalt flow. In this longitudinal section, the largest vesicle, with the greatest amount of volatiles and, therefore, the greatest upthrust rose rapidly, and the two tails, with less volatiles, have been left behind. These geodes are partially filled with white quartz crystals up to 5 cm. OL 3689; (g) Typical triangular aspect of the longitudinal section of a 35 cm high geode. This shape indicates the difficulty of the bubble to rise upwards and cross through the more viscous upper portions of the flow. The geode contains up to 4 cm long amethyst crystals, surrounded by massive silica and celadonite bands, few millimeter thick. EA-1604; (h) Aggregate of green apophyllite

crystals up to 4 cm long, found in basalt geodes. OL 3169; (i) Aggregate of white stilbite crystals up to 5 cm long, found inside geodes of a basalt flow, and showing the typical bow tie penetration-twin. OL 3950; (j) White stilbite cristals up to 3 cm, showing the typical bow tie penetration-twin, found inside geodes of a basalt flow. OL 4098; (k) Veins of fiber-radiated natrolite aggregates, filling fractures on the core zone of a basalt flow. OL 3814; (l) and (m) Brecciated zone of a basalt flow, which sufered percolation of late or postmagmatic fluids, producing cementation by quartz, calcite and microcrystalline silica. EA-1740.

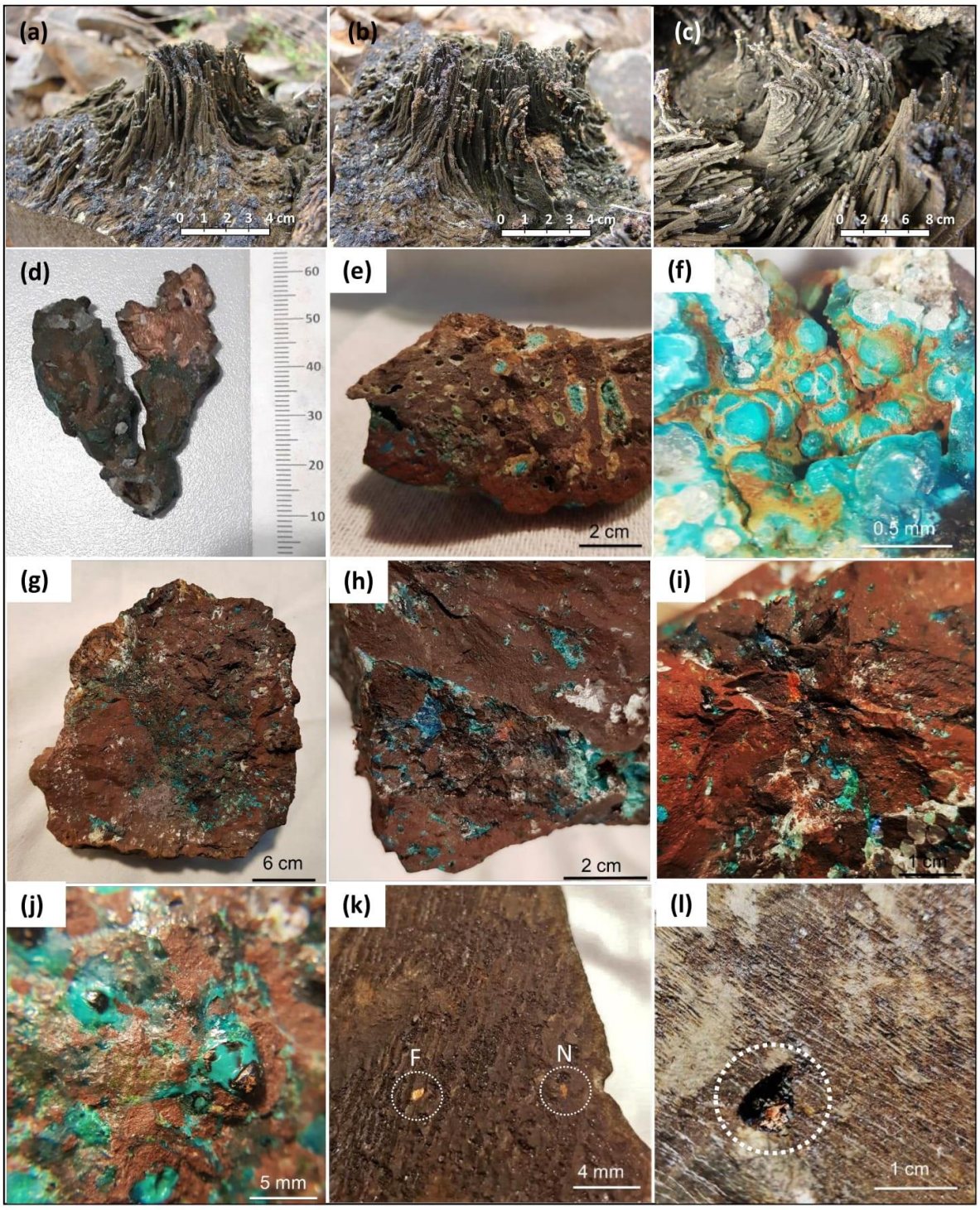

Plate 23 – Minerals filling vesicles and fractures: (a), (b) and (c) Bundles of curved millimeter cylinders, possibly composed of altered basalt glass, grown inside of vesicles of a basalt flow up to 7 cm long. EA-1651; (d) Native copper nugget, 5 cm long, found inside a geode of a thick, tabular basalt flow. Min. Dalmina; (e) Zeolites, celadonite and chrysocolla filling amygdales of the upper vesicular zone of a basalt flow. Hand sample. OL-AP-02; (f) Bothryoidal crysocolla (bluyish green) and zeolite (white), filling an amygdale of the upper zone of a basalt flow. OL-AP-04; (g) Volcanic breccia with venules containing native copper, cuprite, chrysocolla, malachite, zeolites and glass. Hand sample. OL-AP-06; (h) Detail view of (g). Basalt fragment of the breccia, with irregular amygdales filled with zeolites, chrysocolla, cuprite and azurite. Hand sample. OL-AP-06; (i) Detail view of (g). Basalt fragments of the breccia, with irregular amygdales filled with cuprite, malachite, chrysocolla, zeolites and glass. Hand sample. OL-AP-06; (j) Detail view of (g). Amygdales filled with native copper, malachite, chrysocolla and glass. Hand sample OL-AP-06; (k) A joint's

plane coated with glass with striae and slickensides indicating centimeter movement. Over the glass, small native copper flakes are seen, as well as a small native copper nugget (N) along a glass globule is placed filling a cavity. Hand sample. EA-1734; (l) Detail view of (k) The striae are more clearly seen. EA-1734; Pictures from (d) to (l) were provided by Geologist Ana Clara Torres Muller.

near this region. On the contrary, as the Upper Zone undergoes great losses of temperature for the external environment, it will be in less plastic conditions and for that reason the smaller vesicles and amygdales are more frequent (Plate 21).

Vesicles are empty holes, remnants of bubbles contained in the lava, which result from the exsolution of a gas or water vapor dissolved in the magma (Cashman et al. 2000; Spudis et al. 2000) (Plate 21). Amygdales are formed in a similar process to vesicles, but they are partially or totally filled with glass, or low temperature minerals (Plate 22 and Plate 23).

The shape and size of the vesicles or amygdale depend mainly on the amount of fluids, which means internal pressure and upthrust, and the viscosity of the enclosing lava. They may display the form of pipes, empty or filled with minerals such as opal, massive silica, quartz or carbonates. If their cross section is triangular, the vertix opposite to the base always points to the top of the flow (Plate 22 e, Plate 22 g). If they are oblate or prolate, they may have undergone compression by the weight exerted by a new and overlapping flow, or may have been stretched during the flow movement while still in plastic state (Plate 21 h, Plate 21 m). In those flows with excess volatiles, the diferential movements of the Flow's Upper Zone, that are concomitant with the lava degassing, the bubbles may coalesce forming large sub-horizontal layers (Plate 21 k, Plate 21 l, Plate 21 m).

The amygdales may be lined or filled with quartz, amethyst, carbonates, many zeolites species (Plate 22) or by native copper, which is commonly accompanied by cuprite, malachite, chrysocolla and azurite (Plate 23). In one single location the amygdales are filled with bundles of curved tubes up to 7 cm long and few millimeter in diameter, composed of altered basalt glass (Plate 23 a, 23 b, 23 c)

3.4.3.d Filamentous surface

During the movement of the flow or lobe, still in a plastic state, breakouts can occur on active fronts, producing a superficial crust which is covered by a fabric of basalt and/or glass filaments (Plate 24).

3.4.3.e Ropy surface

The ropy upper surface is a typical and diagnostic feature of basalt flows with pāhoehoe morphology. They are curved and parallel wrinkles, which give the top surface a look of rope. They are formed by cooling the lava still in motion.

The half Moon-like curved aspect of each rope indicates the direction of flow in that place (Plate 25c, 25 d, 25 e), although it is possible to obtain divergent measures or that even show the inversion of the direction of flow,

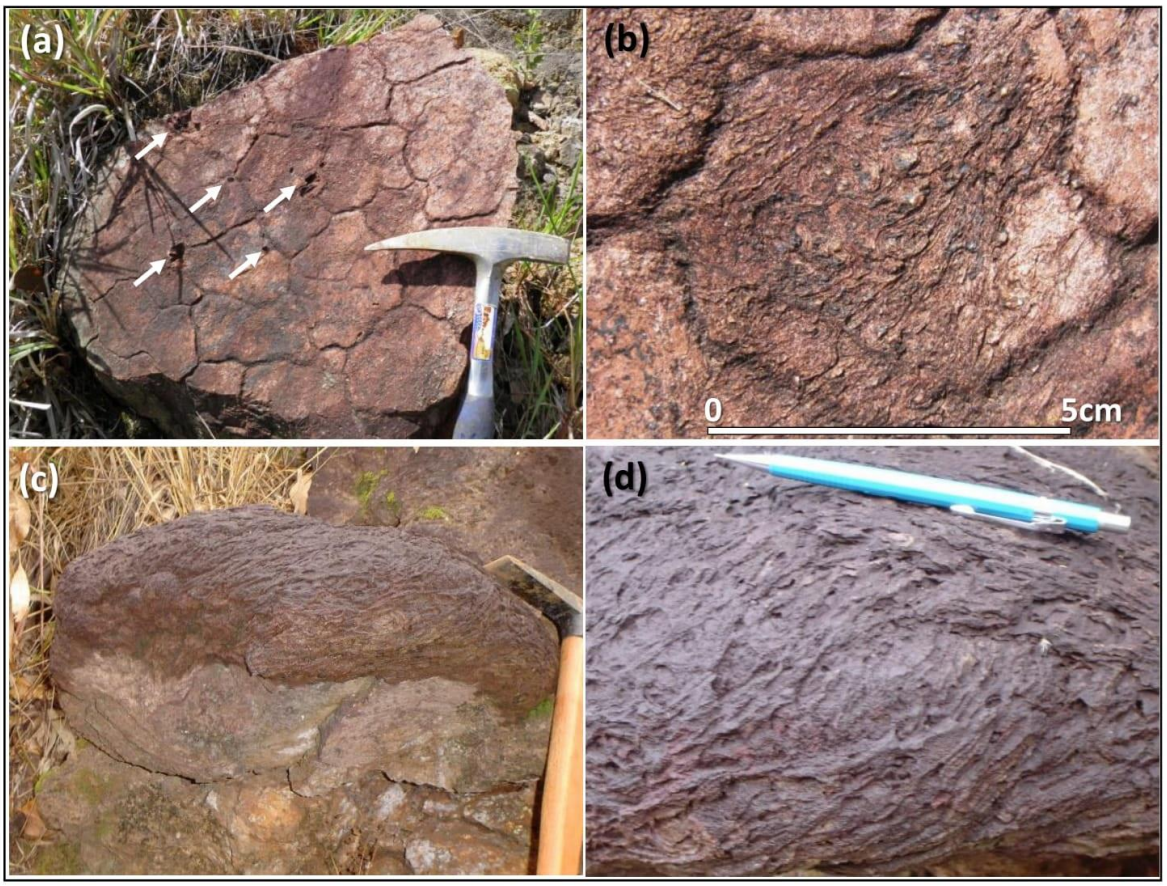

Plate 24 – Upper zone – Top crust: (a) Top crust of a basalt flow surface, composed by irregularly shaped polygons, due to cooling. Some impact marks produced by falling of small lava fragments (arrows) are also preserved. OL 3126; (b) Detail view of (a). The finely rough crust of one of the polygons that make up the surface of the basalt flow. OL 3126; (c) A break-out of an active front of a pāhoehoe basalt flow. The surface

is covered by a web of glassy filaments; (d) Detailed view of (c). The breakout's surface is made up of glass filaments composing a dense and interwoven fabric.

Plate 25 – Upper zone – Ropy Surface: (a) Panoramic view of the floor of a quarry exposing the upper surface of a pāhoehoe basalt flow with a typical ropy structure. Many lobes and breakouts changing the flow direction are observed. OL 3169; (b) The main direction of the major flow (large arrow) and a minor lobe (small arrow) flow convergently. OL 3169; (c) Detail view of a lobe and it typical ropy surface. OL 3169; (d) Detail view of a lobe and its typical ropy surface. OL 3169; (e) Ropy surface on the top of a pāhoehoe flow composed of two lobes, flowing divergently, possibly due to roughness of the paleo-topography. OL 3169; (f) A single lobe showing its massive core (C) and the ropy surface. OL 3169; (g) Spreading ridges of a

pāhoehoe flow. OL 3832; (h) Wavy upper surface of a pāhoehoe flow. OL 3832; (i) Fragments of a pāhoehoe flow crust, showing the typical ropy surface, composing the upper breccia of a rubbly pāhoehoe flow. OL 3035; (j) Part of the ropy upper crust of a pāhoehoe flow. EA-1217.

due to irregularities in the paleo-topography over which the flow was moving. Small breakouts also may diverge from the general direction of the main flow (Plate 25 b). If these features are exposed in very near places, the average of the measurements gives a good and precise indication of the general flow direction. Fragments of rope surfaces were found in several locations, but the most spectacular and didactic is on the floor of the quarry of the Municipality of Bandeirantes in which there are dozens of lobes with a ropy surface, where it is possible to measure the local variations of direction of each breakout, as well as to determine the general flow's direction (Plate 25 b, 25 e).

3.4.3.f Autobreccia

With the contraction due to cooling, the top crust of a flow can fragment and form a mosaic shape surface (Plate 26 a, 26 b, 26 c). In thick or viscous flows, this self-brecciated zone can also be thick and later be filled with minerals deposited by post-magmatic fluids, like white massive silica, carbonates and zeolites (Plate 26 d).

3.5 Mafic Volcaniclastic Deposits – MVD

Aspects of physical volcanology have been obser- ved by many pioneering researchers of the Serra Geral Group (Derby 1878, Oliveira 1889, White 1908, Oliveira 1916, Branner 1919, Baker 1923, DuToit & Reed 1927, Walther 1927, Washburne 1930, Guimarães 1933, Openheim 1934, Miranda ca.1934, Maack 1939, Maack 1947, Gordon Jr. 1947, Leinz 1949, Pichler 1952 e Schneider 1970). They described the compositional differences of the flows, the morphology, the internal structure and facies of the flows, the presence of dikes and sills, the contact with the Botucatu Fm sandstones, and also the presence of pyroclastic deposits. However, the greater emphasis on geochemical aspects produced a gap in the approach to physical volcanology until the late 1990s.

The lack of recent researches presenting the deposits generated by this eruptive model, led Ross et al. (2005) to assume that in the PIP no mafic volcaniclastic deposit (MVD) are found.

Licht (2012), Arioli & Licht (2013), Valore et al (2017), Licht (2018), Licht & Arioli (2018), Valore (2020) identified thick volcaniclastic deposits of hydrovolcanic and strombolian origin, intercalated in the basalt flows all over the Serra Geral Group in the State of Paraná.

In a general view, the volcaniclastic deposits are widely distributed, have great lateral continuity and can reach up to 12 m thick (Plate 27 a). Many features, like

Plate 26 – Upper zone – Autobreccia: (a) Autobreccia composed by fragments of an intensely vesiculated basalt displaying a jigsaw arrangement, with the interstices filled with eolic sand, whose grains are identical to those of the Botucatu Fm. sandstone. Top view. OL 3700; (b) Autobreccia on the flow's top. The interstices are filled with very fine siliciclastic material. Top view. OL 4213; (c) the same description as (b). Top view. OL 3890; (d) Flow breccia on the top of a basalt flow. The interstices are filled with amorphous

and microcrystalline silica, produced by injections of late to post magmatic fluids. Lateral view. EA-1141.

the heterolithic composition of their framework, which comprises typical basalt bombs with their typical internal structure, as well as the siliciclastic composition and the presence of sideromelane shards on the matrix, point to the presence of external water. The proposed model of hydrovolcanic eruptions comprises the contact of the ascending basic magma with aquifer systems (Licht & Arioli 2011, Licht 2012). The high confining pressure in the depth where the contact occured would produce explosive eruptions mixing together siliciclastic material which compose the sedimentary sequence, i.e., the country rock, and basalt fragments, either juvenile and lithics, which represent the ascending magma and previously emplaced flows respectively. Maars, tuff rings and tuff cones would be formed by this process during the evolution of the Serra Geral volcanism (Figure 15).

3.5.1 MVDs - internal structure and facies

Interspersed with basalt and andesi-basalt flows, continuous layers of volcaniclastic deposits are often found, consisting of a breccia in the base, tuff-breccia in the middle and tuff in the top, all in gradational contact. In some places this complete section is observed allowing the identification of a stratigraphy composed of these three main facies. This internal structure is very constant in almost all the expositions visited in the Serra Geral Group. The general structure of the MVD is chaotic, poorly selected and matrix supported (Plate 27b, 27 c, 27 e, 27 h, 28 b, 28 e), but can be locally clast supported (Figure 27 d). The MVDs are heterolytic, consisting of juvenile basalt or basalt-andesitic clasts and reworked breccia in various proportions, immersed in a fine-grained matrix (Plate 27 c, 27 f, 27 g, 27 i, 27h, 28 g, 28 k).

Framework clasts (basalt or andesi-basalt) are angular, subangular to globular, showing 10 to 50% of oblate and prolate vesicles, usually filled with microcrystalline carbonate or silica (Plate 27 i, 27 h, 28 b, 28 c). The diameter of the clasts ranges from 0.2 to 5 cm (ash to lapilli) (Plate 28 s, 28 e, 28 h), to 80-100 cm (blocks and bombs) (Plate 27 c, 27 e, 27 g, 27 j, 28 g, 28 j).

It is important to note that both in the breccia and in the tuff-breccia, the clasts which compose the framework are constituted by fragments of basalt of varying characteristics, representing clasts of juvenile and regional rock, that is, fragments of previously placed basalt flows. The matrix is sandy-silty-clayey (ash to fine lapilli), composed by crystalloclasts of quartz, plagioclase, K-feldspar and accessories like apatite, pyroxene, with a constant presence of sericite, and eventually biotite. The matrix can be vitreous, with subconchoidal fracture; it

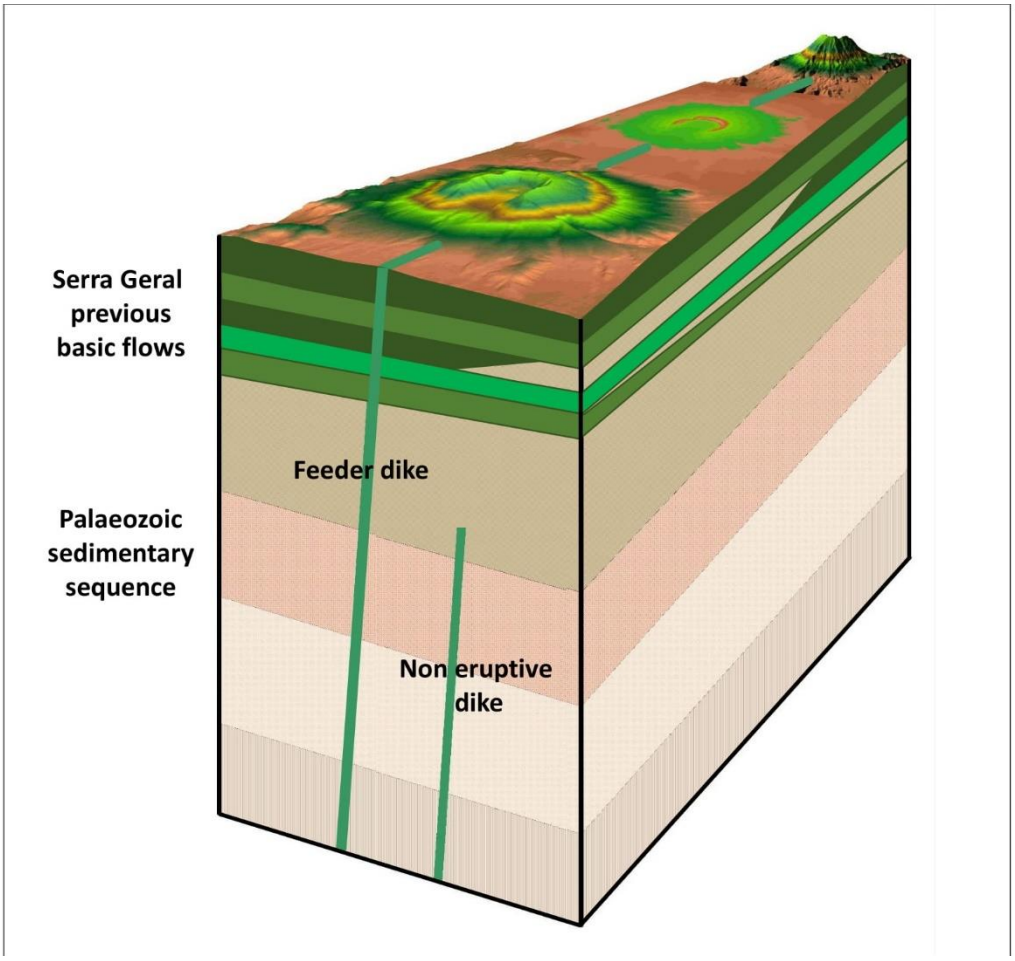

Figure 15 – Idealized model for the hydrovolcanism, which occured during the evolution of the Paraná Igneous Province. After Licht & Arioli (2011).

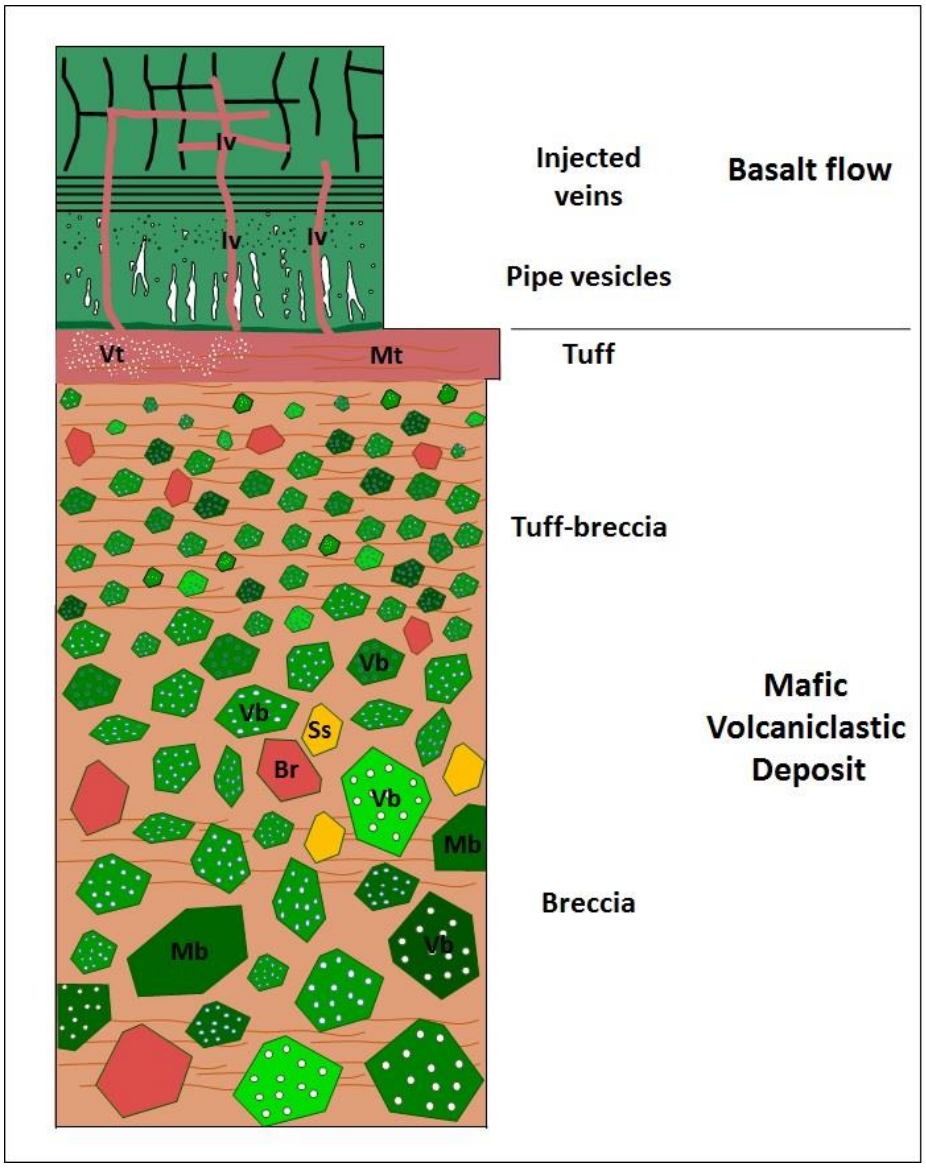

Figure 16 – A schematic and idealized section of a Mafic Volcaniclastic Deposit, showing the three main facies: breccia, tuff-breccia and tuff. The heterolytic character of the framework is highlighted with lapilli to bombs and blocks of massive basalt (Mb), vesicular and/or amygdaloidal basalt (Vb), reworked breccia (Br) and Botucatu Fm. sandstone (Ss). The massive and/or laminated groundmass supports the clasts of the framework. In the upper bed, are identified the vesiculated, the massive and laminated tufff. In the overlying basalt flow, the pipe vesicles represent gases and volatiles released under pressure from the MVD. The injected veins (Iv) are connected to the MVD and their composition is the same as the breccia's and tuff-breccia's groundmass and the tuff as well.

can be intensely vesiculated with the irregular shape vesicles concentrated on top of the tuff layer, close to contact with the overlying basaltic flow. The vesicles could be lined with microcrystalline silica (Plate 29 d, 29 e). The matrix can be also finely laminated, plane-parallel and horizontal, by the alternation of red and dark red laminae (Plate 29 f), with very localized disturbances or ruptures, in contact with clasts of the framework (Plate 28 b). The description of the matrix is very similar to the whole MVD and could be equally applied to breccias, tuff-breccias and tuffs.

It is necessary to emphasize that this is a general and ideal view. Under a detailed observation, there are subdivisions of each major facies, like lense shaped interdigitations and discontinuities and also epiclastic

volcanogenic sediments, as shown by Valore (2020).

3.5.1.1 Breccia

The basal breccia of a MVD range in thickness from a few decimeters to several meters. It has a disordered structure, is poorly selected, and the clast vs. groundmass contacts are difuse and imprecise. The framework is composed by angular clasts, ranging from lapilli to bombs and blocks, majorly made of vesicular to scoriaceous basalt or andesi-basalt. Eventually the clasts can be composed by massive basalt (Plate 27 c, 27 e), reworked reddish breccia (Plate 27 g), and much more rarely of Botucatu Fm sandstone (Plate 27 j).

In many places, elongated basalt clasts with the major axis in a vertical position are observed (Plate 27 c).

In almost all localities, the breccia is matrix supported but some remaining spaces between clasts could be filled with amorphous masses and veinlets of massive or crystallized milky or glassy silica and carbonates.

The groundmass is siliciclastic, ranging from medium ash to fine lapilli, composed of crystalloclasts, i.e. broken crystals of quartz, plagioclase, K-feldspar, apatite, pyroxene, along with sericite and biotite. Isolated ash aggregates are observerd, but they may be concentrated along the poorly defined stratification. The groudmass can be massive, or even show a poorly developed plane-parallel stratification. In a unique site the groundmass shows a fluidal structure and is composed by sub-rounded quartz identical to those of the Botucatu Fm. sandstone (Plate 27 h). Groundmass is often vesiculated and with vesicles lined by quartz microcrystals.

The contact with the underlying basalt flow is always irregular and with the middle tuff-breccia is transitional.

3.5.1.2 Tuff-breccias

The middle portion of an MVD is composed of a tuff-breccia layer, which varies from 50 cm to 4 meters in thickness. It is disorganized, often matrix supported and poorly selected (Plate 28 a, 28 b, 28 c, 28 e, 28 l). The proportion between clast to groundmass varies, and locally the tuff-breccia could be clast supported (Plate 28 d).

The framework is composed of clasts of varying composition but mostly made of basalt or andesi-basalt clasts, vesicular to scoriaceous (Plate 28 b); the vesicles are oblate and prolate, especially those that follow the contour of the clasts, configuring classic round volcanic bombs (Plate 28 j). The clasts have an angular to sub-rounded shape, and their size ranges from a few cm to 30 cm following to the major axis, i.e., lapilli to bombs (Plate 28 b, 28 c, 28 f, 28 g, 28 k).

The siliciclastic groundmass is coarse to medium ash, composed almost exclusively of quartz crystalloclasts, but also with plagioclase, K-feldspar, apatite, pyroxene fragments, along with sericite and biotite. Ash aggregates are often found as well as reddish basalt shard-like fragments, with cuspate countours (Plate 28 h). As a general rule, groundmass use to be massive (Plate 28 a, 28 b) or plane-parallel stratified (Plate 28 h). Lamination disorders, sags due to ballistic impacts, can be eventually seen at the base of some of the clasts (Plate 28 l). The groundmass shows up to 15% of vesicles and the amount grows towards the top of the layer. The vesicles reach 5 mm in diameter, being generally prolate, empty or lined with microcrystalline quartz.

In few places, typical degassing pipes are observed inside the tuff-breccia bed. They are subvertical structures, of badly defined contours, filled only with a clast-suported breccia composed by coarse lapilli and bombs; the matrix must have been ellutriated by rising gases and steam(Plate 28 i).

The contact with the upper tuff layer is transitional.

3.5.1.3 Tuff lenses and beds

The top layer of an MVD consists of a tufff up to 90 cm thick.

The groundmass is glassy and extremely hardened, almost a siliceous sinter, with subconchoidal fracture, dark red in fresh fracture and light pink when weathered (Plate 29 c, 29 d, 29 e).

The tuff may be massive or finely laminated showing horizontal plane-parallel bedding (Plate 29 i), lens-shaped structures, chanelled cross-bedded lamination, evidenced by the alternation of millimeter laminae of a light red and dark color, implying in lesser or greater proportion of ash and secondary iron oxides (Plate 29 f). In close observation, the plane-parallel lamination may be disturbed by slumps which imply in being deposited in a wet environment.

Chaotically distributed, millimetric vesicles, oblate to irregularly shaped are common (30%), either empty or lined with quartz microcrystals (Plate 29 e).

Tuff beds showing cross-chanelled stratification are also found. Some of the internal surfaces become highlighted by deposition of secondary iron oxides. Under petrographic and electronic microscope, spheroids shows radiated internal structure (Plate 29 g, 29 h).

The tuff is composed of ash to fine lapilli, made of fragments of quartz, plagioclase, sericite and biotite, and a great proportion of basalt ash, either as single grains or aggregates resembling clouds. It may contain or be exclusively composed of glass spheroids up to 1 mm Ø, welded by a glassy matrix (Plate 29 m).

The vitroclastic tuff is a very particular variety that participates in the section of some MVDs. It has a clearly plane-parallell or concave stratification, and the aspect on outcrop may lead to misidentification, as it is very similar to an arkose. It consists of glass spheroids (Plate 29 m), up to 1 cm in diameter, which may contain well-formed plagioclase crystals (Plate 29 i). The internal structure shows perlitic fracturing (Plate 29 i). In the deposit, which can reach 1.5 m in thickness, irregularly shaped basalt fragments are common, with the aspect of a bomb since displays vesicles oriented according to the edge (Plate 29 k). The contact with the underlying breccia or tuff-breccia may be transitional or sharply erosive (Plate 29 j). It was identified in many locations, which were connected along a profile of at least 70 km (Licht et al. 2015).

3.5.1.4 Injection veins

In basalt and basalt-andesitic flows that cover MVDs, isolated or interconnected veins are often found (Plate 30). These veins have a dark pink to dark red color, a clay-silty-sand grain size and a quartz-feldspar-micaceous composition, which is in every way identical to the groundmass of the underlying MVD.

As the veins fill contraction fractures and disjunctions due to simple cooling or by combining cooling with the movement of the flow, the veins can be unique and isolated (Plate 30 c), or compose complex systems (Plate 30 a, 30 g). Thus, the attitude of the veins can vary from sub-vertical to sub-horizontal, having from a few mm to 30-40 cm thick and from a few cm to a few meters long.

Sub-parallel and sub-horizontal veins can be interconnected to a subvertical one that feeds the system and which is rooted in the underlying tuff or tuff-breccia layer (Plate 30 a; 30 b).

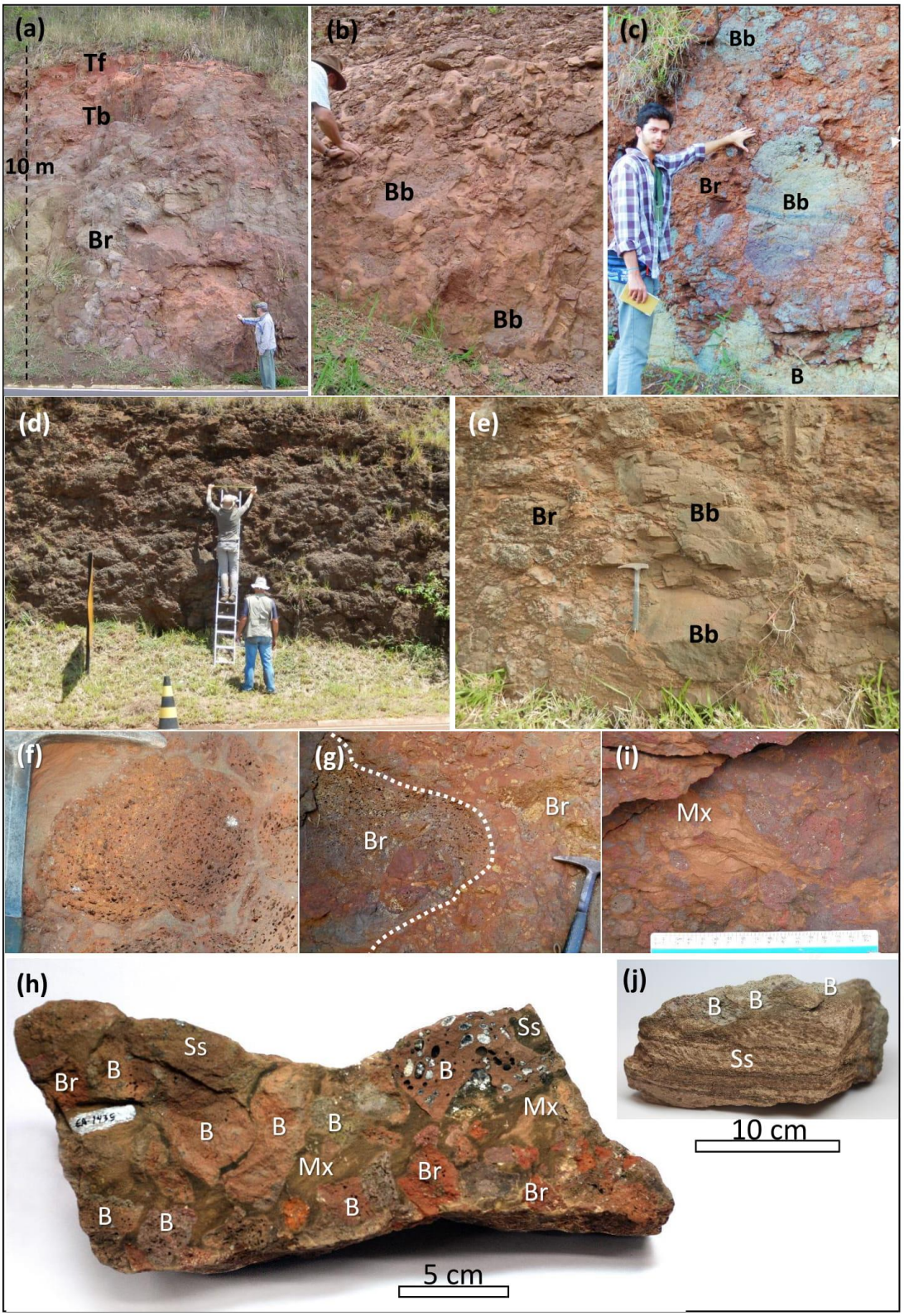

Plate 27 – Mafic Volcaniclastic Deposits – Breccia: (a) Full section of a mafic volcaniclastic deposit up to 10 m thick, composed of a lower breccia, a middle tuff-breccia and an upper tuff bed. Geologist Edir E. Arioli. EA-1205; (b) The lower breccia of a MVD. The coarse fraction, lapilli to bombs and blocks is heterolithic since it is composed of a great diversity of basalt either juvenile and lithics. The basalt blocks are highly vesiculated, sub-angular to sub-rounded, up to 50 cm in diameter. The matrix is siliciclastic, mostly massive but in some places is stratified, intensely hardened and weathering resistant. Geologist Edir E. Arioli. EA-839; (c) The lower breccia of a MVD. The presence of massive basalt bombs and blocks (Bb) up to 1 m in

diameter, indicates a very proximal position in relation to the eruptive center which was not found to date. It overlays a basalt flow (B). Geologist Allan Gomes. OL 3136 -1; (d) The breccia of a MVD. It is composed by many breccia sets, either clast-supported and matrix-supported. The overall description is very similar to (b) and (c). Thus, even considering the great distance between these outcrops, their overall similarity indicates a persistence of the processes and the same source of their components. In this field work the breccia's coarse components are being measured. Geologists Lucas A. Valore and Otavio A. B. Licht OL 3802; (e) Detail view of the same breccia of (d). Many massive basalt blocks up to 1m in diameter indicate a very proximal position in relation to the eruptive center. OL 3802; (f) Detail view of a basalt bomb showing the typical orientation of stretched vesicles, following the clast limits. OL 3728; (g) Detail view of the breccia of Picture (a) focusing a 1 m diameter bomb composed by reworked breccia. EA-1205; (h) Detail view of a complex breccia composed by heterolithic coarse fraction, comprising basalt (B) of many types, reworked brecia (Br) and Botucatu sandstones (Ss), surrounded by a sandy groundmass, with fluidal structure. This is an enlightening example of the hydrovolcanism that occured in the Serra Geral Group. EA-1435; (i) Detail view of the same breccia as (h), emphasizing the finely laminated sandy groundmass. EA-1435; (j) close-up of a bomb, composed of Botucatu sandstone, with primary sedimentary structures still preserved. In this site, the Botucatu sandstone is located ca. 270 m below surface, meaning that the hydrovolcanic eruption occured at least at this depth or even deeper. OL 1435.

Plate 28 – Mafic Volcaniclastic Deposits – Tuff-brecia: (a) Tuff-breccia, the middle portion of a Mafic Volcaniclastic Deposit (MVD). The groundmass supported framework is composed of highly angular coarse lapilli and bombs, mostly of intensely vesiculated basalt, surrounded by a siliciclastic matrix. OL 3130; (b) Tuff-breccia composed of coarse lapilli and bombs of highly vesiculated basalt supported by a siliciclastic groundmass. Many of the framework composing fragments are erratically distributed, including some vertically positioned, indicating a highly energetic process of transport and an abrupt deposition, similar to ash and block fall. OL 3045-17; (c) Tuff breccia composed by coarse lapilli and bombs of highly vesiculated basalt supported by a siliciclastic groundmass. Many of the framework composing fragments are erratically distributed, including some vertically positioned, indicating a highly energetic process of transport and an abrupt deposition, similar to ash and block fall. EA-1683; (d) Commonly, the MVD's framework is highly heterolithic and the clasts are highly angular, relecting the efects of the explosive fragmentation. OL 3130; (e) A typical view of a MVD's tuff-breccia. Coarse lapilli to bombs, mostly of intensely vesiculated basalt from diferent compositions. The overall structure is fully unorganized and matrix supported. The groundmass is siliciclastic, massive or laminated. OL 3001; (f) Tuff-breccia whose framework is composed of highly vesiculated basalt bombs immersed in a massive siliciclastic groundmass. OL 3888; (g) A 20 cm long bomb of intensely vesiculated basalt, composing the framework of a tuff-breccia. OL 3075; (h) The transition from a tuff-breccia to the laminated tuff. Note the cuspate or highly angular basalt lapilli surrounded by the

siliciclastic groundmass which compose the tuff-breccia. OL 3085; (i) Part of a degassing chimney. During its scape, the highly pressured gases contained in the MVD, elutriated the groundmass and finer fractions, lefting behind the coarser fraction. OL 3130; (j) The typical internal structure of a 10 cm basalt bomb surrounded by the siliciclastic matrix, composing the tuff-breccia's framework. OL 3130; (k) An elongated 5 cm bomb of intensely vesiculated basalt. OL 3931; (l) When exposed to wheatering, the basalt fragments do not resist, become altered and are slowly removed. On turn, being much more stable and resistant to the wheathering agents, the siliciclastic matrix, remains intact for much longer. OL 3045-17.

Plate 29 – Mafic Volcaniclastic Deposits – Tuff: (a) The upper tuff bed (T) of a volcaniclastic deposit, covered by a basalt flow (B). The contact is neat, following a smoothly wavy surface. A continuous open space, found along the contact between both lithologies, is possibly due to the contraction of the tuff bed by dehydration and cooling. The upper crust of the tuff bed shows tiny flow wrinkles, marking the displacement of the basalt flow. Min. Tec. Clovis Fonseca. EA-1205; (b) A neat contact between the upper tuff bed (T) of a volcaniclastic deposit and a basalt flow (B). The contact, (highlighted by the white dotted line), is made by an open space, which separates both lithotypes. OL 3890; (c) Conchoidal fracture of a massive, glassy, siliciclastic tuff on top of a volcaniclastic deposit. OL 3045-07; (d) Tuff bed showing alternance of light pink and deep red thin beds, reflecting compositional variation. The tuff is intensely vesiculated, relecting the abundance of hot fluids. EA-885; (e) intensely vesiculated tuff bed on top of a volcaniclastic deposit. The vesicles are lined with hyaline quartz microcrystals. OL 3043; (f) A tuff bed composed of alternance of light pink and deep red thin laminae, reflecting compositional variation. EA-1225b; (g) Two thick tuff beds composing a mafic volcaniclastic deposit, separated by an erosive surface (highlighted by the white dotted line). The lower bed (A) is massive, possibly an ash fall deposit, but due to the intense weathering is now altered into caolinite. The upper bed (T), possibly a surge deposit, is composed by many channelled cross

stratification sets. Min. Tec. Clovis Fonseca. OL 3073; (h) Detail view of the tuff bed, with channelled cross stratification. Under petrographic and electronic microscope, spheroids showing radiated internal structure, similar to glass spheroids, are observed. OL 3073; (i) Bedded tuff showing plane-parallel dipping stratification. One of the beds is a lapili tuff, clast supported, containing spheroids up to 1 cm in diameter. EA -1436; (j) Well stratified vitroclastic tufff (V) deposited over a breccia (B) whose framework is composed of platy basalt fragments and a mixed matrix of basalt and siliciclastic ash. The concave contact surface is erosive (highlighted by a white dashed line). OL 3500; (k) Detail view of (i). In the base of the vitroclastic bedded tuff (V), massive basalt bombs (B) up to 25 cm in diameter are found. The bedding and the extreme energy contrast between vitroclasts and bombs suggest a genetic process similar to a surge. The major bombs are delimited by white dotted lines. OL 3500; (l) Detail view of a spherical vitroclast, axiolithic texture, glass spicles produced by devitrification, and containg an euhedral plagioclase crystal. Thin plate // light. EA-610; (m) Glassy groundmass of the vitroclastic tuff showing the subspherical and prolate vitroclasts. The scale is 100 μm. SEM image. EA-610

Plate 30 – Injected veins on basalt flows: (a) The pink to reddish veins (V) are siliclastic in composition (quartz-feldspar / plagioclase-mica), ash to lapilli, filled open cooling joints and fractures in the overlying flow (B). A sub-vertical feeder vein (F), connects the system to the mafic vulcaniclastic deposit (shown in (b), mostly the upper tuff layer. OL 3089; (b) the 1.5 m thick tuff and tuff-breccia layer (T) which feeds the vein system shown on (a). OL 3089; (c) massive and interconnected vein system (V), hosted by the vesicular zone of a basalt flow (B). EA-1216a; (d) Detail view of an intensely vesiculated vein (V). The irregularly shaped pores and vesicles (dashed yellow circles) are empty, indicating that the injected material was enriched in volatiles. OL 4116; (e) detail view of a vein (V) which encloses angular fragments (F) of the host vesicular basalt (B), indicating the injection was produced under high pressure. OL 3089; (f) Detail view of a vein showing compositional zoning. The core (C) is made of white and massive sílica and the external rim (R) have a siliciclastic composition. It was hosted by a vesicular basalt (B). OL 3018; (g) vein system composed by three injection phases. The first phase (1) is composed by reddish siliclastic material, the second (2) is represented by a swarm of parallel and vertical thin white sílica veins. The third (3) is made of thin late silica veins cutting the previous ones. The system is hosted by vesicular basalt (B). OL 3089; (h) clast of vesicular basalt surrounded by a reddish siliclastic groundmass of a tuff-breccia layer. Those vesicles conected to the border of the clast were filled with the same material which constitutes the groundmass (white arrows). EA-

1226; (i) detail view of a vein (highlitghted) injected through a cooling fracture of a vesicular basalt (B). OL 3087; (j) detail view of the same outcrop showing unusual veins composed by vesicular basalt (V), filling the same fracture system as the siliciclastic veins, shown in Picture (i). OL 3087.

The veins must have been produced by injections of groundmass in suspension and/or emulsion into the fluids and steam hosted by the MVD.

The mixture of water-steam-solids, practically a hydrothermal solution, was injected into the open spaces of the cooling joints and disjunctions of the overlying basalt flow. Due to the pressure and speed of the injection, fragments of the host flow may have been included and transported along with the mixture, forming a vein breccia (Plate 30 e).

Depending on the availability of fractures that will act as conduits, pressure and fluid availability, the injection process may have occured in successive pulses with fracture bundles which may be sub-parallel or discordant, and have different compositions (Plate 30 g). Remnants of the pressured and hot fluids which served as transport media to the solid particles which compose de injection veins, had produced clouds of irregular and empty vesicles inside the veins (Plate 30 b).

The veins can show longitudinal and transversal compositional zonality, which would represent the geochemical halos generated by the migration process as well the distribution of the fluid-solid mixture inside the fracture. Similarly, the geochemical reaction of the fluids responsible for the injection against the host rock, are expressed as contact halos (Plate 30 f).

A plane-parallel and sub-horizontal lamination which is often observed in thicker veins (Plate 30 c, 30 e), would have been produced by a gravitational process. After the pressure and turbulence due to the injection movement ceased, the suspended sandy-silty-clay material was deposited in the open space of the fracture, giving rise to a thin sub-horizontal lamination.

3.6 Acidic flows

In the state of Paraná, the acidic rocks of the Serra Geral volcanism, were firstly identified as "porphiritic andesites on the top of the trapp flows" (Maack 1953). The acidic volcanics in the northern portion of the PIP, within the limits of the State of Paraná, were characterized as "latiandesites or similar rocks" (Ruegg 1975).

Further researches classified the acidic volcanic that occur in the region of Palmas (Bellieni et al 1986) as well as in the region of Guarapuava and Ourinhos (Peate et al 1992) as rhyolites. Actually, when examined in detail, these acidic rocks are represented by a wide range of acidic rocks, such as dacite, rhyodacite, quartz-latite, trachydacite, and rhyolite, but totalling less than 10% in area of the Serra Geral Group in the State of Paraná (Nardy 1994, Nardy et al 1995, Licht & Arioli 2018).

3.6.1 Contact between the acidic flows with the Botucatu sandstones and the basalt flows

The contact between acidic volcanics and the sandstones, may occur in a similar way that those already described for the basic flows, i.e., neat (Plate 31 b) and brecciated (Plate 31 c).

The contact between acidic flows and Botucatu Fm. sandstones reveals a fundamental fact in the complex evolution of the Serra Geral volcanism, that is: neither all acidic rocks are in the top of the volcanic sequence. It is a fact that the acidic flows may be located in places of higher altitude, but this does not mean that they are at the top of the volcanic sequence or that they represent final events, related to a normal sequence of magmatic differentiation. The occurrence of acidic lava flows, covered by a sandstone layer, stress this statement (Plate 31 e).

Contacts between acid lava over basalt flows can be brecciated (Plate 31 h), be it a vitrophyre (Plate 31 g) or a pitchstone (Plate 31 f). The breccia has a plane-parallel structure to the contact region, showing stretched vesicles and angular fragments of massive and glassy rhyodacite or rhyolite along large K-felpdspar broken crystals.

3.6.2 Acidic flows - internal structure

The internal structure of the acidic flows, independently of its chemical composition, rhyolitic, rhyodacitic or trachidacitic, follows the scheme proposed by Besser et al. (2018) for the rhyolite flows of the São Joaquim Plateau, in the neighbor State of Santa Catarina (Figure 17).

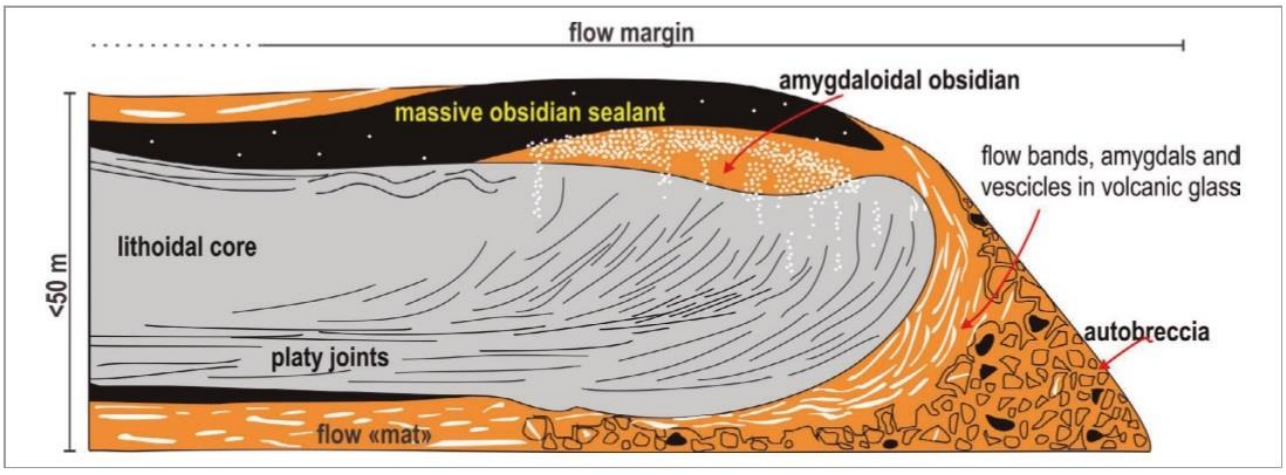

Figure 17 – Schematic section of a rhyolite or rhyodacitic flow (Besser et al. 2018).

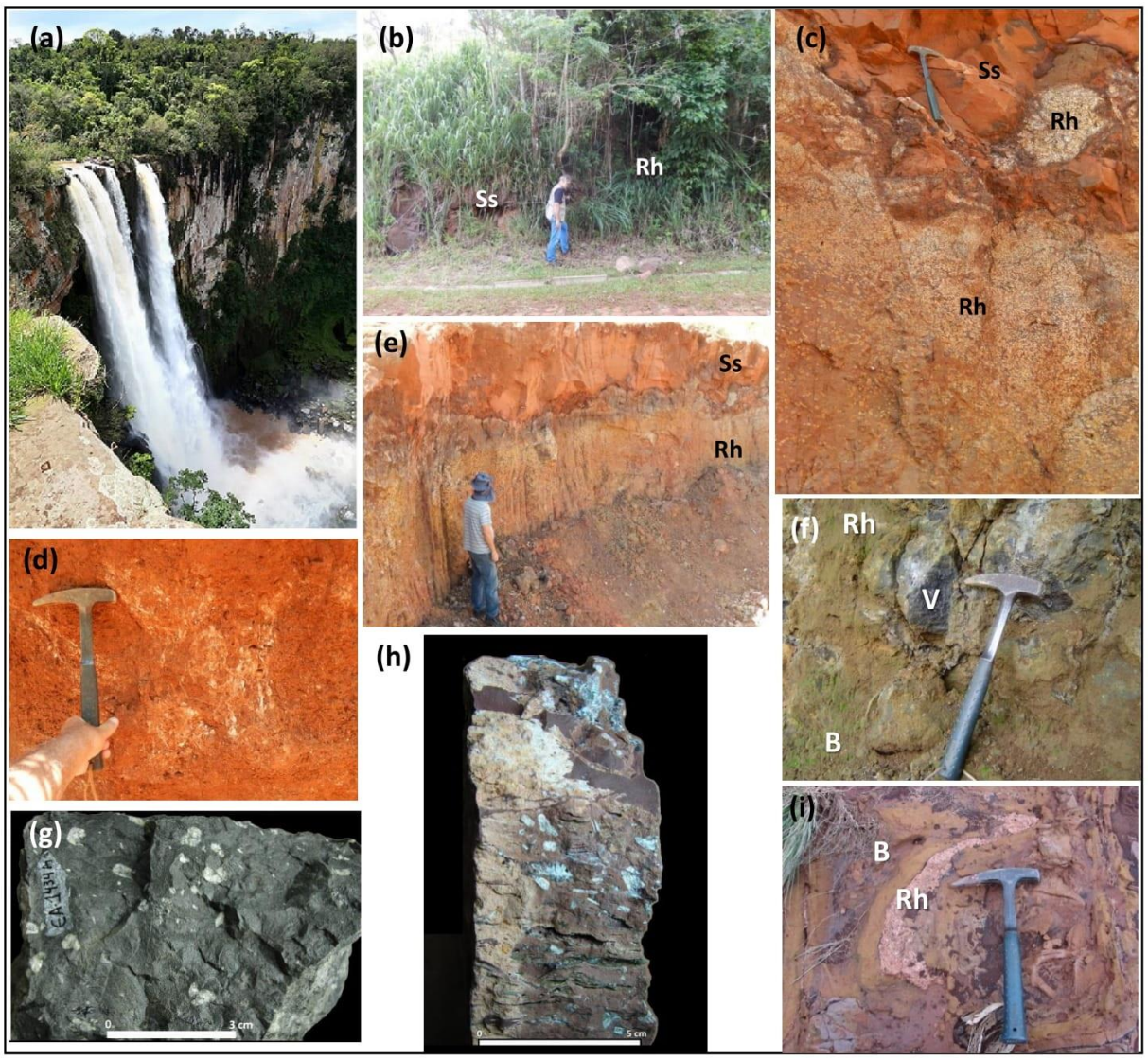

Plate 31 – Acidic flows – Contact: (a) Salto do Apucaraninha waterfall. The cliff is ca. 70 m high, made up of a sequence of porphyry rhyodacite flows OL 4046; (b) Contact between, the Botucatu Fm. sandstones (Ss) overlayed by porphyry rhyodacite flow (Rh). OL 4046; (c) Brecciated contact – porphyry rhyodacite injections (Rh) between blocks of the Botucatu Fm. sandstone (Ss) which became darkened near the contact. OL 3967; (d) Argillitized flow structure (clear strips) of the porphyry rhyodacite, injected between the blocks of the Botucatu Fm. sandstone (reddish mass). OL 3964; (e) same description as (c). OL 3620; (f) vitrophyre (V) in the contact between a basalt flow (B) which is overlayed by a porphyry rhyodacite flow (Rh). EA-1434; (g) detail view of the vitrophyre containing up to 0.75 cm long oligoclase phenocrysts. Hand sample. EA-1434; (h) Flow breccia composed of fragments of brownish massive rhyolite, vitrophyre with white oligoclase phenocrysts, and stretched empty spaces. It occurs in the base of the porphyry rhyodacitic flow. Hand sample. EA-1434; (i) Injections of rhyolite (Rh) filling spaces, fractures and disjunctions on the basalt flow (B). EA-407.

The effect of the weathering highlights the internal structure of the acidic flows, increasing the contrast between the fluidal core and the upper crust composed by massive and almost glassy rhyolite or rhyodacite (Plate 32 a, 32 j). The upward injections from the flow's core, crossing and involving fragments of the upper crust are very characteristic (Plate 32 b, 32 c, 32 d). These injections are marked by groups of many fusiform and hydrodynamic stretched silica bodies, that are aligned along the flow lines. In fresh rock, the glassy acidic lava host these silica bodies which may be observed either in longitudinal and cross section (Plate 32 f, 32 g, 32 h, 32i). Marking the chilled border of some small vertical conduits, pitchstone and/or vitrophyre are observed (Plate 32 d, 32 e). In some sites, the flow's front is defined by a characteristic autobreccia (Plate

33 o).

3.6.3 Acidic flows – flow structure and banding

The flow structures of the acidic flows may be present as different patterns: sub-horizontal (Plate 33 a, 33 b, 33 l, 33 m) to vertical planes (Plate 33 k), wedging planes (Plate 33 c, 33 d, 33 n), convex surfaces (Plate 33 e, 33f),

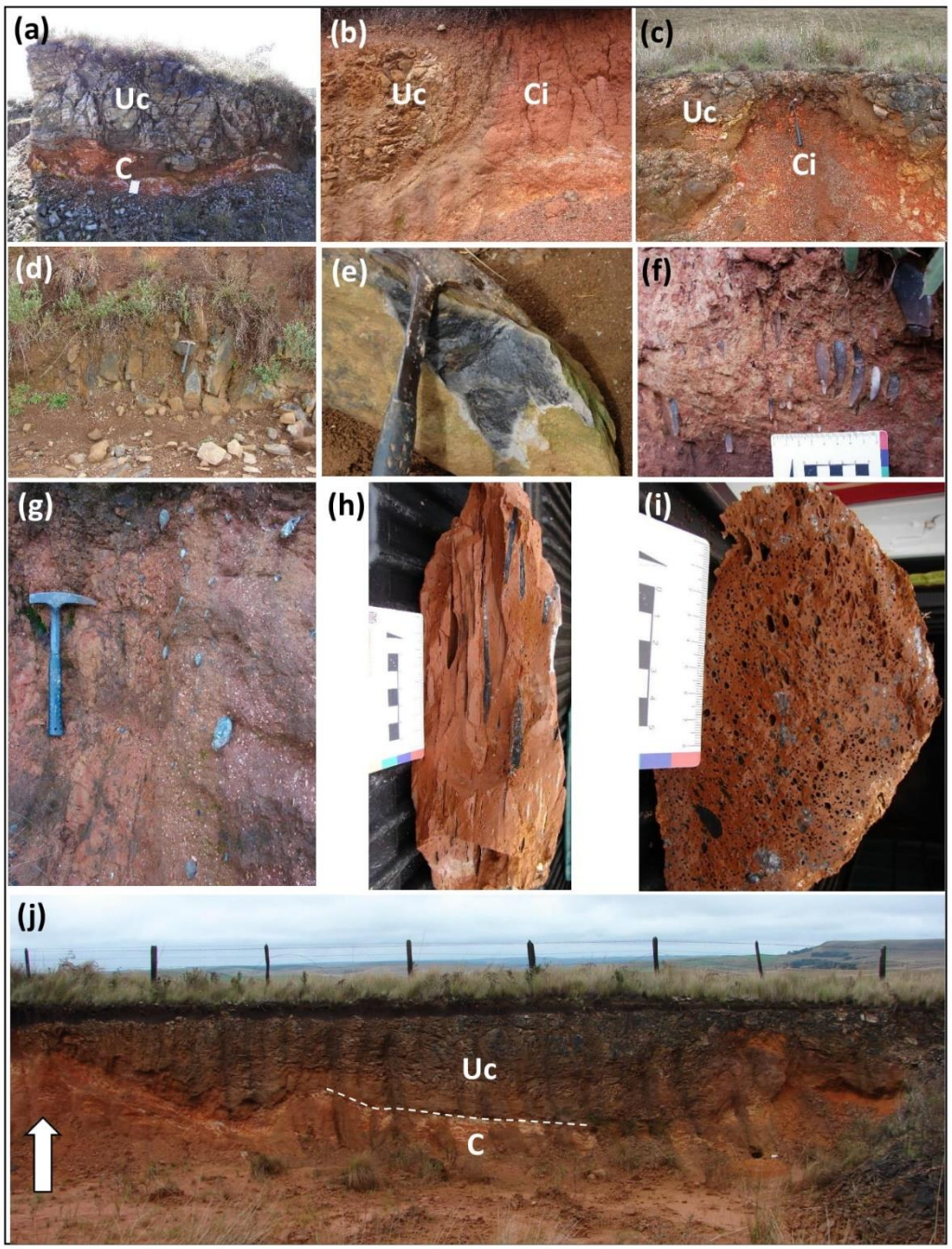

Plate 32 – Acidic flows – Internal structure: (a) Illustrative cross section of the rhyolite flow's inner structure, showing the upper crust, made of massive gray rhyolite (Uc), and the core (C), intensely venulated and showing complex flow structures, intensely weathered. EA-461; (b) A remnant of the rhyolite flow's upper crust (Uc) involved by an upward injection of the flow's core (Ci). EA-442; (c) An upward injection from the rhyolite flow's core (Ci), crossing the upper crust (Uc). These injections are metric to decametric in diameter. They seem to make up a field of rhyolite vents crossing the overlying rhyolite EA-461; (d) and (e) Pitchstone and/or vitrophyre is found in many of the vents, both at the walls of the conduit and on top of the roof, allways associated to glassy rhyolite. EA-456; (f) Within the conduit, fusiform segregations of massive silica, like stretched amygdules, point in the sense of the flow. The reddish material that fills the conduit is intensely altered and weathered. EA-456; (g) The same description for another conduit. EA-432; (h) and (i) The reddish rhyolite that fills the duct is aphanitic, and rich in stretched segregations of massive silica with hydrodynamic shape. The shape and position of these silica segregations indicate the direction of flow, towards the vent. Both pictures are of the same sample: (h) longitudinal section and (i) cross section. EA-455; (j) Longitudinal section of a rhyolite flow, exposing the upper crust (Uc) made of glassy rhyolite and the core

(C) which is intensely weathered. White strips and fusiform silica segregations mark the flow lines in the flow's core. In the left (white arrow) a core's swell almost break the upper crust to form a small vent. The limit between the upper crust and the core is partially highlighted by the dashed white line. EA-442.

Plate 33 – Acidic fows – Flow banding and lamination: (a) dipping flow planes of a rhyolite flow. EA-313; (b) Laminated rhyolite flow. Geologist Edir E. Arioli. EA-442; (c) Wedged flow lamination of a rhyolite flow. EA-439; (d) Truncated wedge lamination in laminated rhyolites, highlighted by weathering. EA-431; (e) Convex surfaces due to contraction by cooling, highlighting the rhyolite flow's front. Frontal view. Prof. Eleonora M.G. Vasconcellos. LC-40; (f) Convex surfaces due to contraction by cooling, highlighting the rhyolite flow's front. Lateral view. LC-40; (g) Lenticular and sigmoidal banding due to the interference of devitrified, crystalline (light) and glassy, hypohyaline (dark) bands on a phaneritic (oligoclase crystals) rhyolite flow. EA-1098; (h) and (i) Rhyolite flow. Intercalation of crystalline (light) and glassy (dark) levels. Due to some obstacle the flow should overpass, the flow lamination became intensely folded, showing closed, stretched, intra-foliated and other ductile patterns. EA-362; (j) Frontal surface of trachydacite lobe, showing folded flow structures. Flow direction to the left. OL 3570; (k) Subvertical flow lamination due to

the high viscosity of the rhyolite and perhaps some obstacle encountered by the flow. OL 4043; (l) An intense sub-horizontal, paralel, flow lamination of a porphyry rhyodacite flow. The weathering highlighted the flow structure as a platy flow fracturing. OL 4043; (m) Rhyolite flow lamination highlighted by weathering. OL 4055; (n) Folded flow structures of a trachydacite flow. OL 3558; (o) Rhyodacite flow front highlighted by an autobreccia. OL 4043.

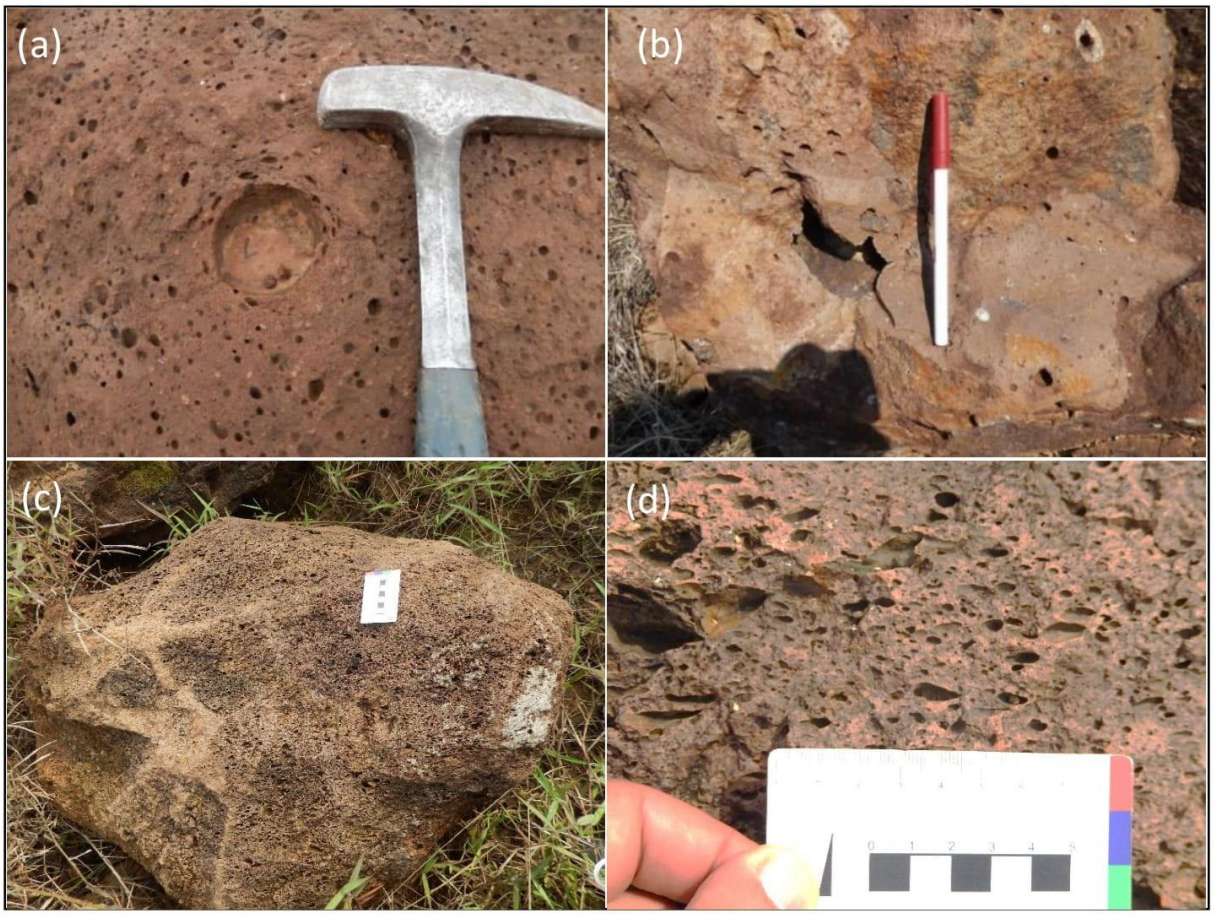

Plate 34 – Acidic flows – Vesicles and amygdales: (a) A 6 cm diameter spherical vesicle, in the vesicular zone of a trachydacite flow. OL 3553; (b) Empty and partially filled with quartz vesicles composing the vesicle zone of a rhyolite flow. OL 3560; (c) The vesicular zone of a porphyry rhyodacite flow. It is intensely vesiculated, up to 40 %, and the vesicles are mostly stretched but also irregular to subspherical. Veins of massive rhyolite intertwine. OL 4043; (d) Detail view of (c) to stress the stretched vesicles up to 2 cm, composing the vesicle zone of a porphyritic rhyodacite flow. OL 4043.

intercalation of lenticular hypohyaline and phaneritic bands (Plate 33 g), intercalation of intensely deformed glassy and crystalline levels, showing ductile patterns like closed, stretched and intrafoliated folds (Plate 33 h, 33 i), and smooth folding in the lobe front (Plate 33 j).

3.6.4 Acidic flows – vesicles and amygdales zones

The vesiculation of the acidic flows is not a very commonly observed feature. However, it is present in some places as sub-spherical vesicles up to 6 cm in diameter surrounded by many small vesicles which are aligned following very subtle flow planes (Plate 34 a). The vesicles are most commonly totally empty, but eventually could be lined or partially filled with massive white silica to millimeter long quartz crystals (Plate 34 b). The vesicular zone could be well developed, with up to 40% stretched vesicles, marking the flow (Plate 34 c, 34 d).

3.7 Basic dikes

Very often diabase and basalt dikes are found cutting the basalt and andesi-basalt flows (Plate 35).

These intrusive bodies follow the general N45°W direction, known as the Ponta Grossa Arch Dike Swarm, which is conspicuously exposed in the State of Paraná (Maack 1953; Pinese 1989; Piccirillo et al 1990). These dikes are easily identified by the magnetometric signal (Ferreira 1982; Raposo & Ernesto 1989) as well clearly observed in many remote sensing images, e.g. Landsat (Figure 18), Aster and Google Earth, as isolated dikes or the swarm itself.

Thicker dikes develop coarse phaneritic textures, while in the thinner ones the texture is of a fine basalt or even glass in those of few cm thick (Plate 35 f, 35 g). The contact zone of the thicker dikes with the basalts can present an intense fracturing, parallel to the direction of the intrusive body (Plate 35 a, 35 b, 35 e).

Less commonly, the contact zone may be a brecciated band composed of basalt fragments immersed on a basalt matrix (Plate 35 d).

The contact zone can also be glassy, due to the rapid temperature loss for the enclosing basalt flow that was already completely cooled (Plate 35 f, 35 i).

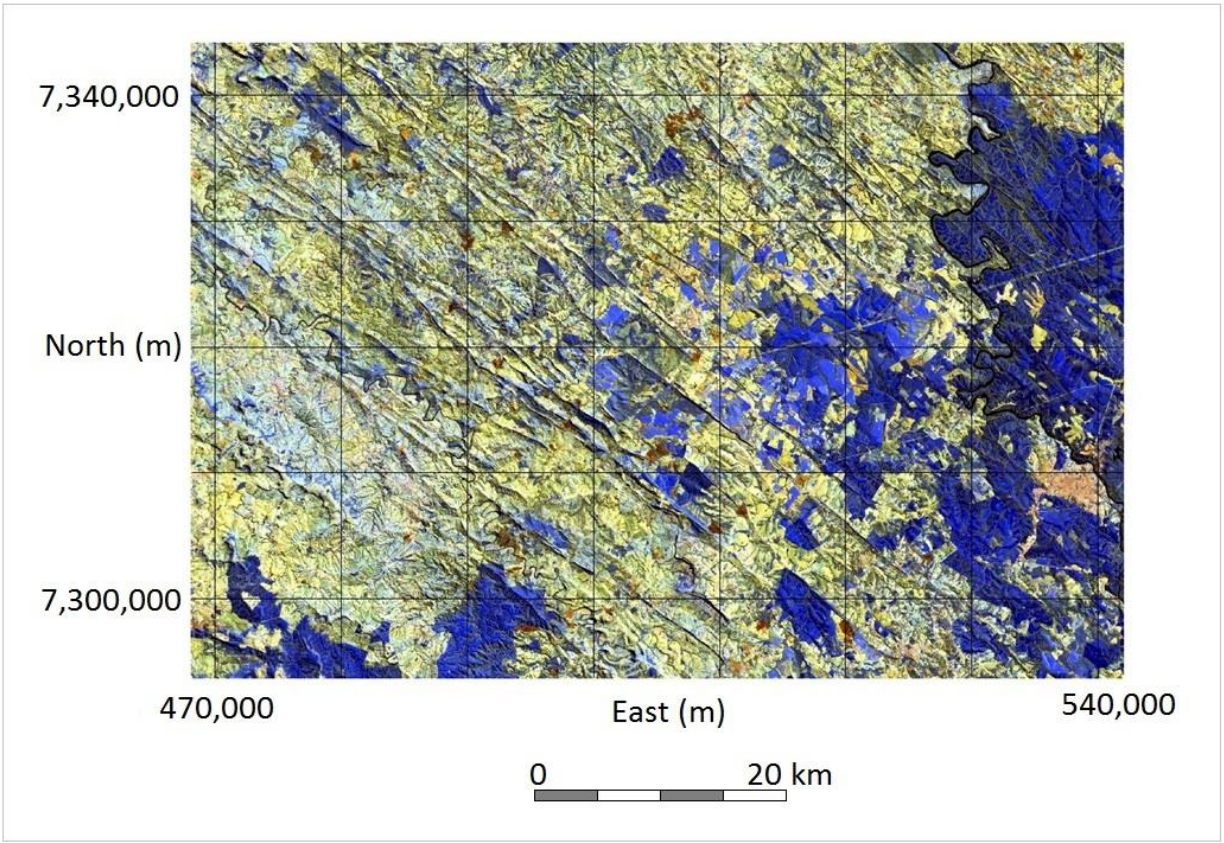

Figure 18 – Partial view of the N45°W Ponta Grossa Arch Dike Swarm (Composite image Landsat TM RGB 754; UTM SAD69, central meridian -51°W. (Modif. Rostirolla S. unpublished)

The efforts and tensions due to the dike's intrusion process can accentuate the internal flow structures of an already cooled basalt flow, transforming them into ruptile structures whose spatial position stress the disturbance caused by the intrusion (Plate 35 c).

3.8 Contact between the Serra Geral Group basic flows and the Bauru Group sandstones

The younger basalt flows that are placed at the top Serra Geral Group, are covered by the sedimentary rocks of the Caiuá Group and the Bauru Group in erosive and abrupt contact, a disconformity.

In some places, the basalt flows are directly covered by lenses of polymitic conglomerates (Plate 36 b, 36 f, 36 f) with pebbles of chalcedony, basalt and sandstone (Plate 36 d) round to oblates, with up to 10 cm in the maximum length, showing imbrication (Plate 36 e). These lenses, which range from a few dm to 2-3 m thick, reflect highly energetic fluvial transport and deposition processes, and are included in the sequence of sandstones and microconglomerates (Plate 36 f), which make up the Bauru Group and the Caiuá Group, which in the State of Paraná reach ca. 120 m thick.

4. Conclusions

The geologic mapping of the Serra Geral Group in the State of Paraná allowed the unravelling of many lithological and faciological features that are critical to the genetic and paleogeographical interpretation of this continental igneous province. Some of these features deserve further highlight. The authors deem it most important the evidence of abundant water in the igneous system, provided both by the underlying Paleozoic aquifers and surface sources. Abundant water should have a role in the origin of the extensive and thick layers of mafic volcaniclastic deposits MVDs, 'peperites', hydrovolcanic and hydrothermal features not attributable to final magmatic fluids. This component of the whole magmatic system has been persistently overlooked by previous studies in the Paraná Igneous Province. The identification of the various styles of lava flows, namely lobate, S- and P-type, rubbly and inflated lows, is a contribution to the knowledge of the volcanic history of the province that this project duly achieved. The occurrence of mafic pegmatites, lava tubes and degassing chimneys in the thicker basalt flows is another finding that deserves mentioning, due to their abundance and genetic meaning in this portion of the province. Moreover, the amount of lithological and faciological evidence provided by this Photographic Atlas is hoped to assist for and bring about the future studies that this important prominent unit of the South American geology deserves hosting.

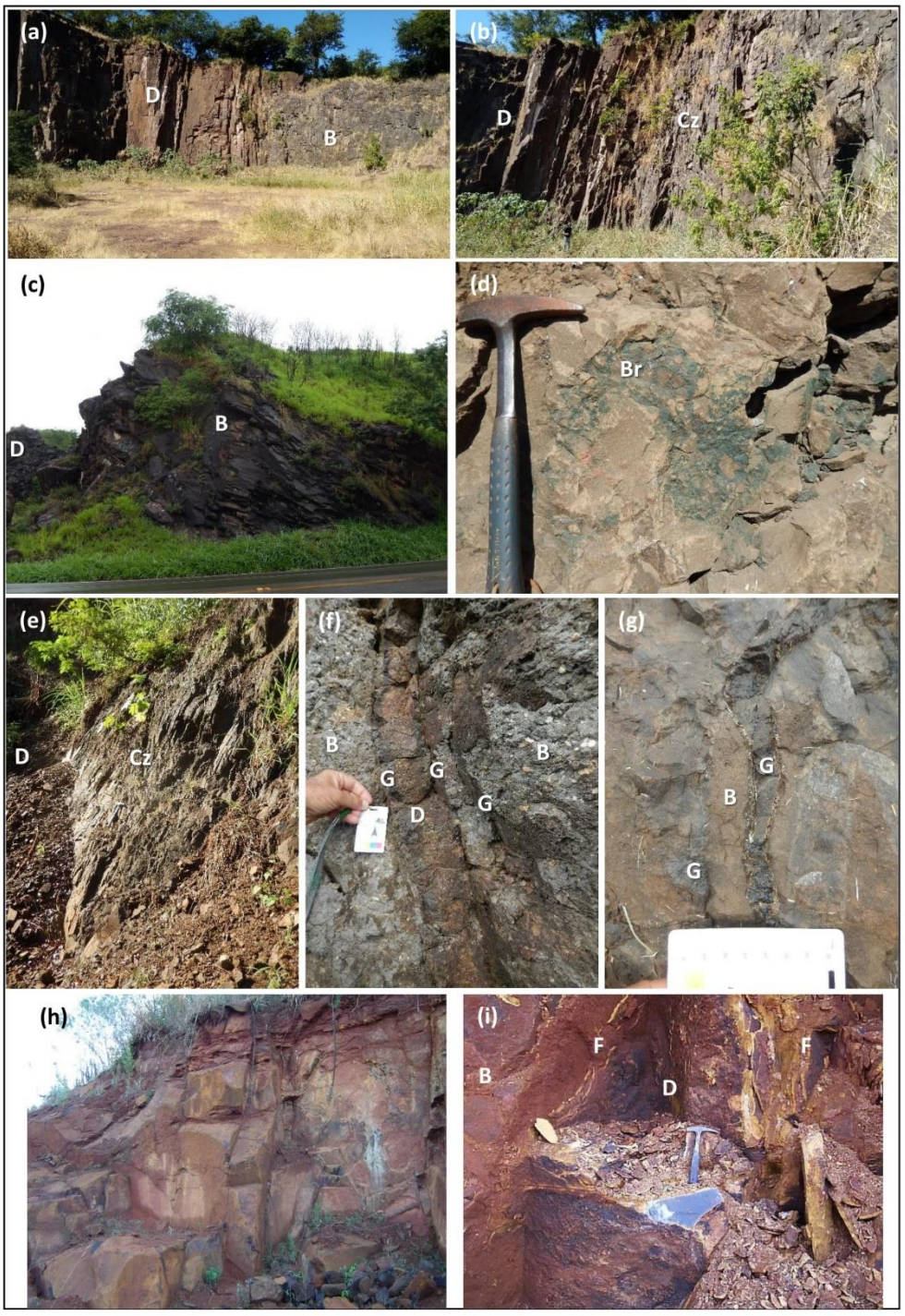

Plate 35 – Diabase and basalt dikes: (a) Contact between a diabase dike (D) and the enclosing basalt flow (B). Vertical fracturing is due to the stress during intrusion. OL 4162; (b) Detail view of a diabase dike (D) and the contact zone (Cz) between the enclosing basalt flow. The dense sub-vertical fracturing is due to the stress during intrusion. OL 4162; (c) The intrusion of a large diabase dike (D) produced a tilt of the basalt flow (B) close to the contact. Tilting is highlighted by the dip of the flow lamination and the platy fracturing, both originally sub-horizontal. OL 4029; (d) Contact breccia (Br) formed during the intrusion of a diabase dike into a basalt flow. It is composed by angular fragments of basalt supported by an intensily chloritized matrix. OL 4192; (e) Detail view of the contact between a diabase dike (D) and the enclosing basalt flow. The dense sub-vertical fracturing (Cz) is due to the stress during intrusion. OL 4097; (f) A ca. 20 cm thick dike of vesicular basalt (D), intruded the vesicular zone of a basalt flow (B). The chilled margins are made of glass (G). OL 4140; (g) Two 1 – 2 cm thick dikes were intruded on a basalt flow (B). Temperature and pressure losses were so rapid, that the injected magma was quickly chilled and the outer border transformed on basalt

glass (G). OL 4138; (h) Massive aspect of a ca. 10 m thick diabase dike, and its internal vertical fracturing due to differential stress during intrusion and contraction during cooling. EA- 1177; (i) Detail view of a ca. 1 m thick diabase dike (D) intruded on a basalt flow (B). The rock is dark bluish gray, massive and phaneritic. A dense subvertical plane-parallel fracturing (F) follows the contact zone between the dike and the hosting basalt flow. JCC214.

Plate 36 – Contact between the Serra Geral Gp. and the Bauru Gp.: (a) The neat contact (disconformity) between the uppermost basalt flow of the Serra Geral Group, exposed on the floor, and the early fluvial sediments of the Bauru Group on the wall. Geologist Allan Gomes. OL 3879; (b) Detail view. Sedimentary sequence of the Bauru Group composed of lenses of coarse fluvial conglomerate hosted by sandstone. OL 3879; (c) Detailed view. Vesicular zone of the uppermost basalt flow, just below the neat contact (disconformity) with the basal sandstones and conglomerates of the Bauru Broup. OL 3879; (d) Detail view of an unusual sandstone clast (Ss), showing high sphericity and roundness, and composing the framework of a fluvial conglomerate lens of the Bauru Group. OL 3879; (e) Detailed view of a coarse fluvial conglomerate lens, showing imbricated, well rounded and low sphericity basalt and calcedony clasts. OL 3879; (f) Neat contact (disconformity) of fluvial conglomerate lens hosted by sandstone, deposited over the uppermost

basalt flow of the Serra Geral Group. OL 3906; (g) Detail view of the uppermost basalt flow of the Serra Geral Group, showing flow structure. OL 3906.

Acknowledgements

The data and photos that make up this paper were collected by the authors, during the Serra Geral Group's Geological Mapping Project in the State of Paraná, which was sponsored by the Paraná Geological Service (MINERAIS DO PARANÁ S.A. – MINEROPAR, and later Instituto de Terras, Cartografia e Geologia – ITCG) to which the authors were affiliated from the 1980's to 2018.

The authors acknowledge the colleagues Eleonora Maria Gouvea Vasconcellos (Universidade Federal do Paraná), Lucas Albanese Valore (Universidade Federal do Paraná), Dianne Silveira Höfig (University of Texas), Luanna Chmyz (Universidade de São Paulo), Allan Gomes (University of Queensland) and Birgir Óskarsson (Icelandic Institute of Natural History), for the discussions we held in the field and office meetings. Thanks are due to two anonimous reviewers of Boletim Paranaense de Geociências for their criticisms and suggestions that contributed to the improvement of the draft.

Acknowledgements are due to Eduardo Salamuni, Editor-in-Chief of the Boletim Paranaense de Geociências for the invitation to the authors to write and compose the present article.

References

ARIOLI E.E., LICHT O.A.B. 2013. Mapeamento geológico do Grupo Serra Geral no Estado do Paraná. Relatório Interno. Mineropar. Curitiba, 2v.

BAKER C.L. 1923. The lava fields of the Paraná Basin, South America. Journal of Geology, 31(1): 66-79.

BATIZA R., W HITE J.D.L. 2000. Submarine lavas and hyaloclastite. In Sigurdsson H., Houghton B., McNutt S.R., Rymer H., Stix J. (eds.) Encyclopedia of Volcanoes. Academic Press, San Diego.p361-382

BELLIENI G., COMIN-CHIARAMONTI P., MARQUES L.S., MELFI A.J., NARDY A.J.R., PAPATRECHAS C., PICCIRILLO E.M., ROISENBERG A., STOLFA D. 1986. Petrogenetic aspects of acid and basaltic lavas from the Paraná Plateau (Brazil): geological, mineralogical and petrochemical aspects. Journal of Petrology 27(4):915-944p.

BESSER M.L., VASCONCELLOS E.M.G., NARDY, A.J.R. 2018. Morphology and stratigraphy of Serra Geral silicic lava flows in the northern segment of the Torres Trough, Paraná Igneous Province. Braz. J. Geol. 48(2):201-219.

BONDRE N.R., DURASWAIMI R.A., DOLE G. 2004. A brief comparison between the lava flows from the Deccan Volcanic Province and the Columbia-Oregon Flood Basalts: implications for models of flood basalt emplacement. In: SHETH, H.C.; PANDE, K. (eds). Magmatism in India through time. Proceedings of the Indian Academy of Sciences (Earth and Planetary Sciences), v. 113, p. 809-817.

BRANNER J.C. 1919. Outlines of the geology of Brazil to accompany the geological map of Brazil. Bulletin of the Geological Society of America, 30:189-338.

BROOKS E.R., WOOD M.M., GARBUTT P.L. 1982. Origin and metamorphism of peperite and associated rocks in the Devonian Elwell Formation, northern Sierra Nevada, California Geolog ical Society of America Bulletin, 93:1208-1231

BRYAN, S., ERNST, R.E. 2008. Revised definition of Large Igneous Provinces (LIPs). Earth-Science Reviews, 86: 175–202.

BUSBY-SPERA, C.J., WHITE, J.D.L., 1987. Variation in peperite textures associated with difering host-sediment properties. Bull. Volcanol. 49:765-775.

CAS R.A.F., WRIGHT J.V. 1988. Volcanic successions Modern and Ancient: A geological approach to proces ses and successions. London, Chapman & Hall, 527p

CASHMAN K.V., MANGAN M.T. 2014. A century of studying efusive eruptions in Hawaii. In: POLAND M.P., TAKAHASHI T.J., LANDOWSKI C.M. (eds), Characteristics of the Hawaiian volcanoes U.S. Geological Survey Prof. Paper 1801, chap. 9.

CASHMANN K. V., STURTEVANT B., PAPALE P., NAVON O. 2000. Magmatic fragmentation. In: SIGURDSSON, H (ed.) Encyclopedia of volcanoes. San Diego: Academic Press. p. 421-430.

COFFIN, M.F., ELDHOLM, O. (1994). Large igneous provinces: crustal structure, dimensions, and external consequences. Review of Geophysics, 32: 1–36.

COMIN-CHIARAMONTI P. 1988. Petrographical Notes. Appendix. In: PICCIRILLO E.M., MELFI A.J. (eds) The Mesozoic flood volcanism of the Paraná Basin. IAG - Univ São Paulo. 1988

CORSARO R.A., MAZZOLENI P. 2002. Textural evidence of peperites inside pillow lavas at Acicastello Castle Rock (Mt. Etna, Sicily). Journal of Volcanology and Geothermal Research 114:219-229

COSTA J. 2011 Modelo geológico-descritivo da sequência de lavas dos derrames da Província Magmática do Paraná na região da Usina de Itaipu, PR. Tese (Doutor), Prog. Pós -Graduação Geologia, UFPR. Curitiba.

COUTINHO J.M.V. 2008. dike swarms of the Paraná Triple Junction, Southern Brazil. Rev. Inst. Geociênc. USP Geol. USP Série Cientif. 8 (2), 29–52.

CPRM - SERVIÇO GEOLÓGICO DO BRASIL. 2001. Mapa geológico, tectônico, recursos minerais e recursos minerais industriais e energéticos do Brasil. São Paulo, CPRM. 1:2.500.000. CD-ROM.

DADD K.A., WAGONER N.A. VAN. 2002. Magma composition and viscosity as controls on peperite texture: an example from Passamaquoddy Bay, southeastern Canada. Journal of Volcanology and Geo thermal Research 114:63-80.

DERBY O.A. 1878, A geologia da região diamantífera da Província do Paraná no Brasil. Rio de Janeiro. Archivos do Museu Nacional do Rio de Janeiro, III (3/4): 87-98.

DONAIRE T., SÁEZ R., PASCUAL E. 2002. Rhyolitic globular peperites from the Aznalcollar mining district (Iberian Pyrite Belt, Spain): physical and chemical controls. Journal of Volcanology and Geothermal Research 114:119-128.

DU TOIT A., REED F.R.C. 1927. Geological comparison of South America with South Africa. Washington: Carnegie Institution of Washington, (Publ. 381) (reprint 1952).

ERNST R.E. 2014. Large Igneous Provinces. Cambridge Univ. Press. Cambridge. 667p.

FERREIRA F.J.F. 1982. Integração de Dados Geofísicos e Geológicos: Configuração e Evolução Tectônica do Arco de Ponta Grossa. Dissertação (Mestrado). Univ. São Paulo.

FORBES A.E.S, BLAKE S., TUFFEN H. 2014. Entablature: fracture types and mechanisms. Bull Vulcanol 76:820-833.

FRANK, H.T., GOMES M.E.B., FORMOSO M.L.L..2009. Review of the arealextent and the volu- me of the Serra Geral Formation, Paraná Basin, South America. Pesquisas em Geociencias, 36 (1): 49-57.

GIFKINS C.C., MCPHIE J., ALLEN R.L. 2002. Pumiceous rhyolitic peperite in ancient submarine volcanic successions. Journalof Volcanology and Geothermal Research 114:181-203.

GOËR DE HERVE A., VINCENT P.-M., CAMUS G. 1998. Must we still use the term ‘‘peperite’’? A review of the type peperites of Scrope, in Limagne, France. IAVCEI International Volcanological Congress, Cape Town, pp. 16

GORDON Jr. M. 1947. Classification of the Gondwanic rocks of Paraná, Santa Catarina and Rio Grande do Sul. Rio de Janeiro: DNPM, Divisão de Geologia e Mineralogia, 1-19 (Notas Preliminares e Estudos, 38a).

GOURGAUD A. 2019. Pépérites. In: Histoire de la découverte géologique du Massif central français. SHNA, Mémoire n°8. p 90-94

GUIMARÃES D. 1933. A província magmática do Brasil meridional. Belo Horizonte, Departamento dos Serviços Geographico e Geologico, Monographia 1, 65 p.

HANSON R.E., HARGROVE U.S. 1999. Processes of magma/wet sediment interaction in a large scale Jurassic andesitic peperite complex, northern Sierra Nevada, California. Bull. Volcanology 60:610-626.

HANSON R.E., WILSON T.J. 1993. Large-scale rhyolite peperites (Jurassic, Southern Chile). Journal of Volcanology and Geothermal Research. 54:247-264

HARTLEY M.E. ,THORDARSON T. 2009. Melt segregations in a Columbia River Basalt lava flow: A possible mechanism for the formation of highly evolved mafic. Lithos, v. 112, n. 3-4, p. 434–446.

HON K., KAUAHIKAUA J., DENLINGER, R., MACKAY K. 1994, Emplacement and inflation of pāhoehoe sheet flows; observations and measurements of active lava flows on Kilauea Volcano, Hawaii: Geological Society of America Bulletin, v. 106, no. 3, p. 351–370, doi:10.1130/0016-7606(1994)106<0351:E-AIOPS>2.3.CO;2.

HOOTEN J.A., ORT M.H. 2002. Peperite as a record of early-stage phreatomagmatic fragmentation processes: an example from the Hopi Buttes volcanic field, Navajo Nation, Arizona, USA. Journal of Volcanology and Geothermal Research, 114:95-106.

JERRAM D.A., STOLLHOFEN H. (2002). Lava-sediment interaction in desert settings; are all peperite-like textures the result of magma-water interaction? Journal of Volcanology and Geotherma l Research 114:231-249.

JERRAM D.A., MOUNTNEY N., HOLZFÖRSTER F., STOLLHOFEN H. 1999. Internal stratigraphic relationships in the Etendeka Group in the Huab Basin, NW Namibia: understanding the onset of flood volcanism. Journal of Geodynamics, Amsterdam, v. 28, n. 4 5, p. 393-418.

JOHNSTON D.A., DONNELLY-NOLAN J.M. 1981. Guides to some volcanic terranes in Whashington, Idaho, Oregon and Northern California. Us GS Circ 838. Available at https://pubs.er.usgs.gov/publication/cir838. Access 10, July, 2020

JUTRAS P., MACRAE A., OWEN J.V., DOSTAL J., PRÉDA M., PRICHONNET G..2006. Carbonate melting and peperite formation at the intrusive contact between large mafic dikes and clastic sediments of the upper Palaeozoic Saint-Jules Formation, New-Carlisle, Quebec. Geological Journal 41:23-48

KERR A.C., MENZIES M.A. 2004. Phanerozoic volcanism. London: Cardif University, Royal Holloway University of London.

KOKELAAR, B.P., 1982. Fluidization of wet sediments during the emplacement and cooling of various igneous bodies. J. Geol. Soc. London. 139: 21-33.

LAVINE A., AALTO K.R. 2002. Morphology of a crater-filling lava lake margin, The Peninsula tufff cone, Tule Lake National Wildlife Refuge, California: implications for formation of peperite te xtures. Journal of Volcanology and Geothermal Research 114:147-163.

LEINZ V. 1949. Contribuição à geologia dos derrames basálticos do sul do Brasil. São Paulo: Universidade de São Paulo, Faculdade de Filosofia, Ciências e Letras, 61 p. (Boletim 103, Geologia 5-6).

LICHT O.A.B. 2018. A revised chemo-chrono-stratigraphic 4-D model for the extrusive rocks of the Paraná Igneous Province. Journal of Volcanology and Geothermal Research 355 (2018) 32–54

LICHT O.A.B., ARIOLI E.E. 2011. Evidências de eventos explosivos – hidrovulcanismo – na Formação Serra Geral, Estado do Paraná, Brasil. V Simp. Vulcanismo e Ambientes Associados, SBG, Goiás. Anais... CD-ROM

LICHT O.A.B., ARIOLI, E.E. 2018. Mapeamento geológico do Grupo Serra Geral no Estado do Paraná. Nota Explicativa. ITCG, Curitiba. 318 p.

LICHT O. A. B., VALORE L. A., SZATMARI P. 2015. Faciology and stratigraphy of Mafic Volcaniclastic Deposits (MVDs), Serra Geral Group, Saudade do Iguacu-Coronel Vivida region, State of Parana, Brazil. In: VI SIMPOSIO DE VULCANISMO E AMBIENTES ASSOCIADOS, 2015, São Paulo, SP. Boletim de Resumos https://sites.google.com/site/ visvaa2015. Sao Paulo: SBG.

LICHT O.A.B. 2012. Estudo de produtos hidrovulcânicos no sudoeste do Paraná. MINEROPAR, Curitiba (192 pp. Available: https://www.researchgate.net/publication/235940955_Estudo_de_Produtos_Hidrovulcanicos_no_Sudoeste_do_Parana_In_Portuguese. Acesso 10/01/2018

LONG P.E., WOOD B.J. 1986. Structures, textures, and cooling histories of Columbia River basalt flows. Geological Society of America Bulletin, v. 97, p. 1144-1155.

LORENZ V., ZIMANOWSKI B., BUETTNER R. 2002. On the formation of deep-seated subterranean peperite-like magma-sediment mixtures. Journal of Volcanology and Geothermal Research 114:107:118.

MAACK R. 1939. Exploração geográfica e geológica em Santa Catarina (Brasil). Traduzido do original Geographische und Geologische Forschung in Santa Catarina (Brasilien) por Alvim G.F. Div. Geol. Mineralogia. Dep. Nac. Prod. Mineral, Min. Agricultura. Rio de Janeiro

MAACK R. 1947. Breves notícias sôbre a geologia dos Estados do Paraná e Santa Catarina. Curitiba. IBPT. Archivos de Biologia e Tecnologia, vol. II, art. 7.

MAACK R. 1953. Mapa Geológico do Estado do Paraná. Serv Geologia, Inst. Biologia e Pesquisas Tecnológicas. Curitiba, esc 1:740.000

MACDONALD G.A. 1953. Pāhoehoe, Aa and block lava. American Journal of Science, 251: 169-191.

MANO V.G.T. 1987. Estudos geológicos e geotécnicos das descontinuidades rochosas, “pillow lavas” e paleocanal nos basaltos da fundação da barragem de Nova Avanhandava, Rio Tietê (SP). Dissertação de Mestrado. Instituto de Geociências, Universidade de São Paulo.

MARQUES FILHO P.L., CORREIA P.C., LEVIS P., ANDRADE C.A.V. 1981. Características usuais e aspectos peculiares do manto de alteração e transição solo-rocha em basaltos. In: CONGRESSO BRASILEIRO DE GEOLOGIA DE ENGENHARIA, 3., 1981. Itapema. Anais... São Paulo: ABGE, 1981. v. l2, p. 53-72.

MARTIN B.S., PETCOVIC H.L., REIDEL S.P. 2005. Goldschmidt Conference 2005: Field trip guide to the Columbia River Basalt Group. Richland (WA): U.S. Department of Energy, Pacific Northwest National Laboratory, 2005. 62 p.

MARTIN, U., NÉMETH, K., 2007. Blocky versus fluidal peperite textures developed in volcanic conduits, vents and crater lakes of phreatomagmatic volcanoes in Mio/Pliocene volcanic fields of Western Hungary. Journal of Volcanology and Geothermal Research 159:164–178.

MASULILI F. 2019. Geological and petrological studies of peperite related to fault movement. Thesis (Master of Sciences). Ehimi University, Japan Available athttps://www.researchgate.net/publication/340952112_Geological_and_petrological_studies_of_peperite_related_to_fault_movement. Access September, 10th, 2020.

MCCLINTOCK M.K., WHITE J.D.L. 2002. Granulation of weak rock as a precursor to peperite formation: coal peperite, Coombs Hills, Antarctica. Journal of Volcanology and Geothermal Research 114:205-217.

MENZIES M.A., KLEMPERER S.L., EBINGER C.J., BAKER J. (eds) 2002. Characteristics of volcanic rifted margins. Geological Society of America, Special Paper. v.362, p. 1-14.

MENZIES M.A., EBINGER, C.J. 2000. Volcanic rifted margins. Geological Society of America, GSA Today, p. 8 11.

MIRANDA J. 1934 (aprox.). Notas geológicas sobre o Municipio de Taquara, Rio Grande do Sul. Rio de Janeiro: Serviço Geologico e Mineralogico, 38 p. (Boletim, 83).

MORAES L.C. de, SEER H.J. 2017. Pillow lavas and fluvio-lacustrine deposits in the northeast of Paraná Continental Magmatic Province, Brazil. Journal of Volcanology and Geothermal Research. http://dx.doi.org/10.1016/j.jvolgeores.2017.03.024

NARDY A.J.R., OLIVEIRA M.A.F.de., AGLINSKAS R.S., LOPES R.P. 1994. Geologia e estratigrafia do vulcanismo Mesozoico de região central da Bacia do Paraná. 38° Cong. Brasil. Geologia, SBG, Camboriu. Anais... v1:97-99.

NARDY A.J.R., OLIVEIRA M.A.F. de., AGLINSKAS R.S. 1995. Proposição formal dos Membros Palmas e Chapecó como unidades litoestratigráicas da Formação Serra Geral. IV Simp. Geologia do Sudeste, SBG, Aguas de Lindóia. Boletim. p73

NARDY A.J.R., ROSA, M.C., LUCHETTI, A.C.F., FERREIRA, M.L.C., MACHADO, F.B., OLIVEI RA, M.A.F. 2011. Parâmetros físicos pré-eruptivos do magmatis mo ácido da Província Magmática do Paraná: resultados preliminares. São Paulo, UNESP. Geociências 30 (4), 575–588

NELSON C.E., JERRAM D.A., HOBBS R.W. 2009. Flood basalt facies from borehole data: implications for prospectivity and volcanology in volcanic rifted margins. Petroleum Geoscience, 15:313-324.

NICHOLS R.I. 1936. Flow units in basalt. The Journal of Geology, 44(5):617-630

OLIVEIRA, E.P. 1916. Geologia do Estado do Paraná. Rio de Janeiro: Ministério da Agricultura, Industria e Commercio, 1: p. 67-143 (Boletim, 5)

OLIVEIRA, F de P. 1889. Reconhecimento geologico do Valle do Rio Paranapanema. São Paulo: Commissão Geographica e Geologica da Provincia de S. Paulo, p. 3-31 (Boletim, 2).

OPPENHEIM, V. 1934. Sobre a bacia sedimentária gonduanica na República do Uruguay. Anais da Academia Brasileira de Ciências, 3(6): 143-155.

ÓSKARSSON, B.V. 2005. Lava-rise structures in pāhoehoe and ‘A’ā: Examples from the Hrútagjá lava shield and Kapelluhraun ‘A’ā flow field on the Reykjanes peninsula. Univ. of Iceland. Reykjavik. BSc Thesis. 126p

PEATE, D.W., HAWKESWORTH, C.J., MANTOVANI, M.S.M. 1992. Chemical stratigraphy of the Paraná lavas (South America): classification of magma types and their spatial distribution. Bull. Volcanol. 55, 119-139.

PICCIRILLO E.M., BELLIENI G., CAVAZZINI G., COMIN-CHIARAMONTI P., PETRINI R., MELFI A.J., PINESE J.P.P., ZANTADESCHI P. DE MIN A. 1990 Lower Cretaceous tholeiitic dike swarms from the Ponta Grossa Arch (southeast Brazil): Petrology, Sr-Nd isotopes and genetic relationships with the Paraná flood volcanics. Chemical Geology, 89:19-48.

PICHLER, E. 1952. Diques de arenito em Salto Grande, Rio Paranapanema. Boletim da Sociedade Brasileira de Geologia, v1, n1, pp. 20-21.

PINESE J.P.P. 1989. Caracterização petrológica e geo-química dos diques do Arco de Ponta Grossa. Dissertação (Mestrado). Univ. São Paulo. São Paulo. 208p.

PUFFER J.H., HORTER D.L. 1993. Origin of pegmatitic segregation veins within flood basalts. Geol. Soc. of America Bull. 105:738-748.

RAPOSO M.I.B., ERNESTO M. 1989. Rochas intrusivas básicas do Arco de Ponta Grossa: resultados paleomagnéticos preliminares. Simp. Geologia do Sudeste, SBG, Rio de Janeiro, Boletim de Resumo, p 179.

ROSS P.-S., UKSTINS PEATEI., MCCLINTOCK M.K., XU Y.G., SKILLING I.P., WHITE J.D.L., HOUGHTON B.F. 2005. Mafic volcaniclastic deposits in flood basalt provinces: A review. Journal of Volcanology and Geothermal Research. 145, p 281-314.

ROSSETTI L., LIMA E.F., WAICHEL B.L., HOLE M.J., SIMÕES M.S., CHERER C.M.S. 2017. Lithostratigraphy and volcanology of the Serra Geral Group, Paraná-Etendeka Igneous Province in Southern Bra- zil: Towards a formal stratigraphical framework. J. Volcanol. Geotherm. Res. 355:98-114.

RUEGG N.R. 1975. Modelos de variação química na Província Basáltica do Brasil Meridional. Características de teor, distribuição geográica e diferenciação. Tese (Livre docência), Inst. Geociências, Univ. São Paulo, SP. 2vol.

SADOWSKI G.R. 2012. A short review on the importance of colonnades, entablatures and “fault joints” for the excavation of basaltic rocks. Soils and Rocks, São Paulo, 35(3): 297-302.

SCHMINCKE H.U. 2004. Volcanism. Springer Verlag. 324 p.

SCHNEIDER A.W. 1970. Vulcanismo basáltico da Bacia do Paraná: perfil Foz do Iguaçu - Serra da Esperança. XXIV Cong. Bras. Geol. Brasília. Anais... Soc. Bras. Geologia.

SELF S., JAY A.E., WIDDOWSON M., KESZTHELYI L.P. 2008. Correlation of the Deccan and Rajahmundry Trap lavas: are these the longest and largest lava flows in the Earth ? Journ. Volcanol. Geotherm. Research 172: 3-19.

SELF S., THORDARSON T., KESZTHELYI, L. 1997. Emplacement of continental lood basalts flows. In: Mahoney J.J., Coin M. (Eds.). Large Igneous Provinces. American Geophysical Union, 100:381-410.

SELF S., KESZTHELYI L., THORDARSON T. 1998. The importance of pāhoehoe. Annual Review of Earth Planetary Sciences, v. 26, p. 81-110.

SEM B., SABALE A.B. 2011. Flow-types and lava emplacement history of Rajahmundry Traps, West of River Godavari, Andhra Pradesh. Journ. Geol. Soc. India 78(5): 457:467.

SOUZA JR. N.N.O. 1992. O "entablamento" em derrames basálticos da Bacia do Paraná: aspéctos genéticos e caracterização geotécnica. Tese de Doutorado. Escola de Engenharia de São Carlos, USP. 263p.

SPRY A. 1962. The origin of columnar jointing, particularly in basalt flows. Journal of the Geological Society of Australia, 8:2, 192-216.

SPUDIS P.D. 2000. Volcanism on the Moon. In: SIGURDSSON, H (ed) Encyclopedia of volcanoes. San Diego: Academic Press. p. 697-708.

SQUIRE R.J., MCPHIE J. 2002. Characteristics and origin of peperite involving coarse-grained host sediment. Journal of Volcanology and Geothermal Research 114:45-61.

SWANSON D.A., WRIGHT T.L. 2006. Guide to Geologic Field Trip between Lewiston, Idaho and Kimberly Oregon, emphasizing the Columbia River Basalt Group.

TARDUNO J.A., DUNCAN R.A., SCHOLL D.W., 2002. Proceedings of the Ocean Drilling Program, Init ial Reports. V 197. doi:10.2973/odp.proc.ir.197.2002. Available at http://www-odp.tamu.edu/publications/197_IR/197TOC.HTM. AccessApril, 23, 2002

THIEDE D. S., VASCONCELLOS P. M. 2010. Paraná flood basalts: Rapid extrusion hypothesis confirmed by new 40Ar/ 39Ar results. Geology. v 38, n 8, p 747-750.

TOMKEIEFF S. 1940. The basalt lavas of the Giant's Causeway district of Northern Ireland. Bull Volcanol 6(1):89–143.

VALORE L.A., 2020. Estratigrafia e evolução geológica dos depósitos interderrames de Sertanópolis – PR, Província Ígnea do Paraná. Dissertação de Mestrado. Dep. Geologia , Setor Ciencias da Terra, UFPR, Curitiba.

VALORE L.S., LICHT O.A.B. 2015. Evidences of the dynamic interaction between Botucatu sandstones and a Serra Geral basic flow, Jacarezinho, State of Paraná, Brazil. VI Simp. Vulcan. Ambientes Associados. SBG, São Paulo. Anais... CD-Rom.

VA LORE L.S., LICHT O.A.B., HOFFIG D.F., VAS - CONCELLOS E.M.G., UKSTINS-PEATE I., ÓSKARSON B.V. 2017. Mafic Volcaniclastic Deposits of the Paraná Igneous Province and their correla tion to chemostratigraphy – State of Paraná, Brazil. X Simp. Sul-Brasileiro de Geologia, SBG, Curitiba. Available at http://ssbg2017anais.siteoicial.ws/ST/ st8/ST821.pdf. Access September, 10th, 2020.

VINCENT P.M., KIEFFER G., BOIVIN P., CAMUS G., GOURGA UD A., DE GÖER A., MERGOIL J. 1982. A propos des diatremes et du phreatomagmatisme: le terme "peperite" doit-il être conserve ?. International Kimberlite Conference: Extended Abstracts, 3, 206-206. https://doi.org/10.29173/ikc2262

WALKER G.P.L., 1989. Spongy pāhoehoe in Hawaii: a study of vesicle-distribution patterns in basalt and their significance. Bull Volcanol., 51:199-209

WAICHEL B.L., LIMA E.F. de., SOMMER C.A., LUBACHESKY R. 2007. Peperite formed by lava flows over sediments: an exa mple from the central Paraná Continental Flood Basalts, Brazil. Journ. Volcanol. Geotherm. Research, 159:343-354

WALTHER K. 1927. Contribución al conocimiento de las rocas 'basalticas' de la formacion de Gondwana en la America del Sur. Boletim del Instituto Geologico y Perforaciones, 9, 41 p.

WASHBURNE C.W. 1930. Petroleum geology Comissão Geográfica e Geológica do Estado de São Paulo, 282p. (Boletim, 22)

WHITE I.C. 1908. Comissão de Estudos das Minas de Carvão de Pedra do Brazil – Relatório Final. Imprensa Nacional, Rio de Janeiro. Re-impressão - Edição Comemorativa: 100 anos do Relatório White, CPRM, 2008, Belo Horizonte, 617 p.

WHITE R., MCKENZIE D. 1989. Magmatism at rift zones: The generation of volcanic continental margins and flood basalts, J. Geophys. Res., 94, 7685 – 7729.

WHITE, J.D.L., MCPHIE, J., SKILLING, I.P., 2000. Peperite: a useful genetic term. Bull. Volcanology, 62,65-66.

WILMOTH R.A., WALKER G.P.L. 1993, P-type and S-type pāhoehoe ; a study of vesicle distribution patterns in Hawaiian lava flows: Journal of Volcanology and Geothermal Research, v. 55, n. 1–2, p. 129– 142, doi:10.1016/0377-0273(93)90094-8.

WOHLETZ K. 2002. Water/magma interaction: some theory and experiments on peperite formation. Journal of Volcanology and Geothermal Research 114:19-35.

WRIGHT T.L., TAKAHASHI T.J. 1989. Observations and interpretation of Hawaiian volcanism and seismicity 1779–1955: an annotated bibliography and subject index. University of Hawaii Press, Honolulu, Hawaii.

Annex

In this Annex, the reader will ind 39 tables classified by morphology, facies and other remarkable features. The tables contain 174 selected field stations considered to have the more representative features. The first and second columns of each table, refer respectively to the Plate and the picture, the third column contains the the field station code, and the two last columns contain the geographic coordinates of the field station.

They will be useful to compose didactic field classes or geotouristic routes to visit 174 selected locations from the 3,704 sites the authors surveyedduring the Project Geological Mapping of the Serra Geral Group in the State of Paraná, supported by the Government of the State of Paraná. The pictures were selected fromthe photographic data- base of the Project and the respective locations from Licht (2012), Arioli and Licht (2013) and Licht and Arioli(2018).

Plate	Picture	Field Station	Latitude (WGS84)	Longitude (WGS84)
01	a	OL 3633	-23.026900	-49.914690
01	b	OL 3620	-23.264990	-49.846450
01	c	OL 3702	-23.286720	-50.070950
01	d	EA-1426	-25.700390	-51.215070
01	e	OL 3752	-23.232850	-50.139020
01	f	OL 3752	-23.232850	-50.139020

Table 01 – Selected field stations with representative examples of the contact between basalt lava flows and sandstones, i.e., Serra Geral Group over the Botucatu Formation.

Plate	Picture	Field Station	Latitude (WGS84)	Longitude (WGS84)
02	a	EA-867	-26.208360	-53.405310
02	b	EA-863	-26.271030	-53.454550
02	c	OL 3981	-23.394300	-50.812870
02	d	OL 3162	-23.256518	-51.038736
02	e	OL 3889	-23.008030	-51.076230

02	f	EA-1211c	-25.099080	-52.896560

Table 02 – Selected field stations with representative examples of the compound lava flows.

Plate and Picture	Picture	Field Station	Latitude (WGS84)	Longitude (WGS84)
03	a	EA-802	-26.442390	-53.266740
03	b	EA-1162	-25.194340	-52.277480
03	c	EA-546	-26.250080	-51.508470
03	d	OL 3714 a	-23.272070	-50.165550
03	e	EA-1695	-24.987610	-53.472030

Table 03 – Selected field stations with representative examples of the single, tabular flows.

Plate	Picture	Field Station	Latitude (WGS84)	Longitude (WGS84)
02	c	OL 3981	-23.394300	-50.812870
02	d	OL 3162	-23.256518	-51.038736
02	e	OL 3889	-23.008030	-51.076230
04	a	EA-955	-26.053290	-53.326600
04	b	OL 3748	-23.149140	-50.150310
04	c	OL 3755	-23.219430	-50.156160
04	d	EA-1735	-24.734070	-53.091280
04	e	OL 3748	-23.149140	-50.150310
04	f	OL 3748	-23.149140	-50.150310

Table 04 – Selected field stations with representative examples of the thin flows.

Plate	Picture	Field Station	Latitude (WGS84)	Longitude (WGS84)
05	a	OL 4196	-23.836220	-51.536460
05	b	OL 4196	-23.836220	-51.536460
05	c	OL 3120	-26.413240	-52.384530
05	d	OL 3120	-26.413240	-52.384530
05	e	OL 3120	-26.413240	-52.384530
05	f	EA-968	-26.060770	-53.101100

Table 05 – Selected field stations with representative examples of the Type-S lobes.

Plate	Picture	Field Station	Latitude (WGS84)	Longitude (WGS84)
06	a	EA-1163	-25.144700	-52.278490
06	b	JCC254f	-25.119170	-52.719970
06	c	EA-1217	-25.242720	-53.973470
06	d	EA-1217	-25.242720	-53.973470
06	e	EA-1163	-25.144700	-52.278490
06	f	OL 4254	-23.192880	-51.489360
06	g	OL 4254	-23.192880	-51.489360

Table 06 – Selected field stations with representative examples of the P-type lobes.

Plate	Picture	Field Station	Latitude (WGS84)	Longitude (WGS84)
07	a	OL 3647 a	-23.158499	-50.002648
07	b	OL 3647 a	-23.158499	-50.002648

Table 07 – Selected field stations with representative examples of the ponded lava flows.

Plate	Picture	Field Station	Latitude (WGS84)	Longitude (WGS84)
03	a	EA-0802	-26.442390	-53.266740
03	b	EA-1162	-25.194340	-52.277480
03	c	EA-546	-26.250080	-51.508470
03	d	OL 3714 a	-23.272070	-50.165550
03	e	EA-1695	-24.987610	-53.472030
13	a	OL 4112	-23.653990	-51.505700
14	a	EA-0848	-26.243840	-53.280990
14	h	EA-1210	-25.110160	-52.835290

Table 08 – Selected field stations with representative examples of the inflated lava flows.

Plate	Picture	Field Station	Latitude (WGS84)	Longitude (WGS84)
08	a	EA-1073	-25.420760	-51.666850
08	b	EA-1073	-25.420760	-51.666850
08	c	EA-1073	-25.420760	-51.666850
08	d	OL 3173	-23.061700	-50.125110
08	e	OL 3640	-23.064600	-50.103500
08	f	EA-1346	-25.291030	-51.812980

Table 09 – Selected field stations with representative examples of the hypohyaline flows.

Plate	Picture	Field Station	Latitude (WGS84)	Longitude (WGS84)
09	a	OL 4117	-23.596650	-51.661090
09	b	OL 3082	-24.902090	-54.195750
09	c	OL 3082	-24.902090	-54.195750
09	d	OL 3082	-24.902090	-54.195750
09	e	EA-1217	-25.242720	-53.973470
09	f	OL-2147	-25.599028	-53.771250
09	g	OL 4161	-23.733330	-51.848430

Table 10 – Selected field stations with representative examples of the rubbly pāhoehoe flows.

Plate	Picture	Field Station	Latitude (WGS84)	Longitude (WGS84)
10	a	OL 3647	-23.154950	-50.001810
10	b	OL 3169	-23.109690	-50.412270
10	c	OL 3169	-23.109690	-50.412270
10	d	OL 3169	-23.109690	-50.412270
10	e	OL 3169	-23.109690	-50.412270

Table 11 – Selected field stations with representative examples of the flow peperite.

Plate	Picture	Field Station	Latitude (WGS84)	Longitude (WGS84)
11	a	OL 3033	-26.151030	-53.322220
11	b	EA-886	-26.188270	-53.396290
11	c	OL 3029	-26.173530	-53.329810
11	d	EA-911	-26.294910	-53.192180
11	f	OL 3029	-26.173530	-53.329810

Table 12 – Selected field stations with representative examples of the contact of a flow covering a volcaniclastic deposit.

Plate	Picture	Field Station	Latitude (WGS84)	Longitude (WGS84)
12	a	EA-948	-26.039180	-53.313520
12	b	EA-1139	-25.406530	-52.091020
12	c	EA-776	-26.442560	-53.352450
12	d	EA-1617	-25.912100	-52.404190
12	e	OL 4071	-23.587480	-51.419510
12	f	OL 3795	-23.112480	-50.408040

Table 13 – Selected field stations with representative examples of the contact between flows.

Plate	Picture	Field Station	Latitude (WGS84)	Longitude (WGS84)
08	a	EA-1073	-25.420760	-51.666850
08	b	EA-1073	-25.420760	-51.666850
08	c	EA-1073	-25.420760	-51.666850
08	e	OL 3640	-23.064600	-50.103500
11	d	EA-911	-26.294910	-53.192180
12	b	EA-1139	-25.406530	-52.091020
12	f	OL 3795	-23.112480	-50.408040

Table 14 – Selected field stations with representative examples of the platy flow fracturing.

Plate	Picture	Field Station	Latitude (WGS84)	Longitude (WGS84)
05	a	OL 4196	-23.836220	-51.536460
05	c	OL 3120	-26.413240	-52.384530
06	f	OL 4254	-23.192880	-51.489360
06	g	OL 4254	-23.192880	-51.489360

Table 15 – Selected field stations with representative examples of the lower vesicular zone.

Plate	Picture	Field Station	Latitude (WGS84)	Longitude (WGS84)
13	a	OL 4112	-23.653990	-51.505700
13	b	OL 4112	-23.653990	-51.505700
13	c	OL 4186	-23.837690	-51.702940
13	d	OL 4186	-23.837690	-51.702940
13	e	OL 3948	-23.286370	-50.878970
13	f	OL 4186	-23.837690	-51.702940
13	g	EA-1188	-24.941670	-51.384780

Table 16 – Selected field stations with representative examples of the lower colonnade.

Plate	Picture	Field Station	Latitude (WGS84)	Longitude (WGS84)
08	a	EA-1073	-25.420760	-51.666850
08	b	EA-1073	-25.420760	-51.666850
08	c	EA-1073	-25.420760	-51.666850
14	a	EA-848	-26.243840	-53.280990
14	b	OL 4254	-23.192880	-51.489360
14	c	OL 4063	-23.742830	-51.281520
14	d	OL 3070	-25.148520	-53.586970
14	e	EA-1139	-25.406530	-52.091020
14	f	EA-612	-26.041230	-52.593390
14	g	EA-612	-26.041230	-52.593390
14	h	EA-1210	-25.110160	-52.835290
14	i	OL 4063	-23.742830	-51.281520

Table 17 – Selected field stations with representative examples of the entablature.

Plate	Picture	Field Station	Latitude (WGS84)	Longitude (WGS84)
03	b	EA-1162	-25.194340	-52.277480
08	f	EA-1346	-25.291030	-51.812980

Table 18 – Selected field stations with representative examples of the chisel marks.

Plate	Picture	Field Station	Latitude (WGS84)	Longitude (WGS84)
15	a	OL 3142	-26.282350	-51.106380
15	b	OL 4071	-23.587480	-51.419510
15	c	OL 4160	-23.873740	-51.864660
15	d	OL 3517	-25.963090	-52.771990
15	e	EA-631	-26.257730	-53.619020
15	g	OL 3949	-23.279010	-50.860810
15	h	OL 4119	-23.653900	-51.684620

Table 19 – Selected field stations with representative examples of the convex surfaces.

Plate	Picture	Field Station	Latitude (WGS84)	Longitude (WGS84)
16	a	EA-1230	-25.375940	-53.574960
16	b	OL 4254	-23.192880	-51.489360
16	c	OL 3153	-23.996830	-51.085580
16	d	EA-1230	-25.375940	-53.574960
16	e	OL 4146	-23.547820	-51.689010

Table 20 – Selected field stations with representative examples of the degassing chimneys.

Plate	Picture	Field Station	Latitude (WGS84)	Longitude (WGS84)
17	a	OL-2011	-25.750389	-53.327694
17	b	OL-2011	-25.750389	-53.327694
17	c	OL-2140	-25.681790	-53.811590
17	d	OL-2011	-25.750389	-53.327694
17	e	OL-2140	-25.681790	-53.811590
17	f	EA-1054	-26.258110	-53.618810

Table 21 – Selected field stations with representative examples of the basic pegmatites.

Plate	Picture	Field Station	Latitude (WGS84)	Longitude (WGS84)
18	a	OL 3161	-23.488730	-51.630800
18	b	OL 4139	-23.779990	-51.642940
18	c	OL 4107	-23.769020	-51.438580
18	d	OL 4165	-23.704030	-51.874050
18	e	OL 4126	-23.668290	-51.704760
18	f	OL 4165	-23.704030	-51.874050

Table 22 – Selected field stations with representative examples of the lava tubes.

Plate	Picture	Field Station	Latitude (WGS84)	Longitude (WGS84)
19	a	OL 3100	-26.864280	-52.181750
19	b	OL 3941	-23.360840	-50.855500
19	c	EA-1145	-25.369980	-52.376140
19	d	EA-811	-26.416090	-53.389770
19	e	OL 3949	-23.279010	-50.860810
19	f	OL 3737	-23.088250	-50.069810
19	g	OL 3126	-26.409770	-53.012520
19	h	OL 3018	-26.243470	-53.633940
19	i	JCC254	-25.119170	-52.719970
19	j	OL 4146	-23.547820	-51.689010
19	k	OL-2110	-25.170278	-52.673250
19	l	JCC254	-25.119170	-52.719970

Table 23 – Selected field stations with representative examples of the flow lamination.

Plate	Picture	Field Station	Latitude (WGS84)	Longitude (WGS84)
20	a	OL 3500	-25.692332	-52.620972
20	b	OL 4122	-23.698120	-51.712310
20	c	OL 3045-03	-26.032780	-53.320750
20	d	EA-1435	-25.986210	-51.358240

Table 24 – Selected field stations with representative examples of the autoliths.

Plate	Picture	Field Station	Latitude (WGS84)	Longitude (WGS84)
21	a	OL 3658	-22.931790	-50.067580
21	b	OL 3736	-23.076980	-50.070580
21	c	OL 3946	-23.284280	-50.950350
21	d	OL 3172	-23.053700	-50.120720
21	e	OL 3160	-23.477660	-51.942860
21	f	EA-1209b	-25.114080	-52.821080
21	g	EA-1665	-24.752460	-53.774970
21	h	EA-1209b	-25.114080	-52.821080
21	i	OL 4024	-23.536210	-51.135820
21	j	EA-875	-26.176250	-53.479690
21	k	EA-1665	-24.752460	-53.774970
21	l	EA-1665	-24.752460	-53.774970
21	m	EA-1665	-24.752460	-53.774970

Table 25 – Selected field stations with representative examples of the upper vesicular zone.

Plate	Picture	Field Station	Latitude (WGS84)	Longitude (WGS84)
22	a	OL 3751	-23.236710	-50.126960
22	b	OL 3790	-23.083130	-50.568760
22	c	EA-859	-26.117470	-53.436410
22	d	OL 3010	-26.055360	-53.648860
22	e	OL 3777	-23.192890	-50.330390
22	f	OL 3689	-23.029520	-50.206890
22	g	EA-1604	-25.916990	-52.434480
22	h	OL 3169	-23.109690	-50.412270
22	i	OL 3950	-23.27867	-50.84511
22	j	OL 4098	-23.769720	-51.388790
22	k	OL 3814	-23.097150	-50.713090
22	l	EA-1740	-25.33424	-54.20040
22	m	EA-1740	-25.33424	-54.20040
23	a	EA-1651	-26.073300	-52.859150
23	b	EA-1651	-26.073300	-52.859150
23	c	EA-1651	-26.073300	-52.859150
23	d	Trevo quarry	-24.354239	-54.144390
23	e	OL-AP-02	-24.65541477	-52.69752591
23	f	OL-AP-04	-24.65541477	-52.69752591
23	g	OL-AP-06	-25.59160494	-53.70269186
23	h	OL-AP-06	-25.59160494	-53.70269186
23	i	OL-AP-06	-25.59160494	-53.70269186
23	j	OL-AP-06	-25.59160494	-53.70269186
23	k	EA-1734	-24.748280	-53.061780
21	l	EA-1734	-24.748280	-53.061780

Table 26 – Selected field stations with representative examples of the minerals that fill vesicles.

Plate and	Picture	Field Station	Latitude (WGS84)	Longitude (WGS84)
09	a	OL 4117	-23.59665	-51.66109
09	c	OL 3089	-24.96007	-54.05629
24	a	OL 3126	-26.409770	-53.012520
24	b	OL 3126	-26.409770	-53.012520

Table 27 – Selected field stations with representative examples of the filamentous surface of breakouts and protrusions.

Plate	Picture	Field Station	Latitude (WGS84)	Longitude (WGS84)
25	a	OL 3169	-23.109690	-50.412270
25	b	OL 3169	-23.109690	-50.412270
25	c	OL 3169	-23.109690	-50.412270
25	d	OL 3169	-23.109690	-50.412270
25	e	OL 3169	-23.109690	-50.412270
25	f	OL 3169	-23.109690	-50.412270
25	g	OL 3832	-23.209430	-50.685620
25	h	OL 3832	-23.209430	-50.685620
25	i	OL 3035	-26.144720	-53.305280
25	j	EA-1217	-25.242720	-53.973470

Table 28 – Selected field stations with representative examples of the ropy surface.

Plate	Picture	Field Station	Latitude (WGS84)	Longitude (WGS84)
26	a	OL 3700	-23.023440	-50.101880
26	b	OL 4213	-23.438210	-51.428280
26	c	OL 3890	-22.991780	-51.089220
26	d	EA-1141	-25.377480	-52.266340

Table 29 – Selected field stations with representative examples of the top autobreccia.

Plate	Picture	Field Station	Latitude (WGS84)	Longitude (WGS84)
27	a	EA-1205	-25.234700	-52.646600
27	b	EA-0839	-26.167640	-53.334370
27	c	OL 3136-1	-25.234780	-52.646430
27	d	OL 3802	-23.174000	-50.617010
27	e	OL 3802	-23.174000	-50.617010
27	f	OL 3728	-23.073880	-50.126310
27	g	EA-1205	-25.234700	-52.646600
27	h	EA-1435	-25.986210	-51.358240
27	i	EA-1435	-25.986210	-51.358240
27	j	EA-1435	-25.986210	-51.358240

Table 30 – Selected field stations with representative examples of the breccias of the Mafic Volcaniclastic Deposits - MVDs

Plate	Picture	Field Station	Latitude (WGS84)	Longitude (WGS84)
28	a	OL 3130	-24.801750	-54.054660
28	b	OL 3045-17	-26.039440	-53.313610
28	c	EA-1683	-24.782060	-54.011980
28	d	OL 3130	-24.801750	-54.054660
28	e	OL 3001	-26.068000	-53.721000
28	f	OL 3888	-22.914280	-51.214420
28	g	OL 3075	-25.141220	-54.197070
28	h	OL 3085	-24.912750	-54.157310
28	i	OL 3130	-24.801750	-54.054660
28	j	OL 3130	-24.801750	-54.054660
28	k	OL 3931	-22.932960	-51.307430
28	l	OL 3045-17	-26.039440	-53.313610

Table 31 – Selected field stations with representative examples of the tuff-breccias of the Mafic Volcaniclastic Deposits - MVDs.

Plate	Picture	Field Station	Latitude (WGS84)	Longitude (WGS84)
29	a	EA-1205	-25.234700	-52.646600
29	b	OL 3890	-22.991780	-51.089220
29	c	OL 3045-07	-26.033670	-53.319170
29	d	EA-885	-26.145710	-53.316880
29	e	OL 3043	-26.104330	-53.161330
29	f	EA-1225b	-25.371830	-54.268560
29	g	OL 3073	-25.027510	-53.555400
29	h	OL 3073	-25.027510	-53.555400
29	i	EA-1436	-25.995740	-51.380160
29	j	OL 3500	-25.692332	-52.620972
29	k	OL 3500	-25.692332	-52.620972
29	l	EA-610	-26.039130	-52.606930
29	m	EA-610	-26.039130	-52.606930

Table 32 – Selected field stations with representative examples of tuff beds and lenses of the Mafic Volcaniclastic Deposits - MVDs.

Plate	Picture	Field Station	Latitude (WGS84)	Longitude (WGS84)
30	a	OL 3089	-24.960070	-54.056290
30	b	OL 3089	-24.960070	-54.056290
30	c	EA-1216a	-25.216260	-53.951390
30	d	OL 4116	-23.592720	-51.651850
30	e	OL 3089	-24.960070	-54.056290
30	f	OL 3018	-26.243110	-53.633860
30	g	OL 3089	-24.960070	-54.056290
30	h	EA-1226	-25.340760	-54.212960
30	i	OL 3087	-24.905280	-54.181380

Table 33 – Selected field stations with representative examples of veins injected from the Mafic Volcaniclastic Deposits on the basalt flows.

Plate	Picture	Field Station	Latitude (WGS84)	Longitude (WGS84)
31	a	OL 4046	-23.751410	-50.898980
31	b	OL 4046	-23.751410	-50.898980
31	c	OL 3967	-23.702910	-50.653560
31	d	OL 3964	-23.730270	-50.642790
31	e	OL 3620	-23.264990	-49.846450
31	f	EA-1434	-25.710550	-51.340530
31	g	EA-1434	-25.710550	-51.340530
31	h	EA-1434	-25.710550	-51.340530
31	i	EA-407	-26.109680	-52.276290

Table 34 – Selected field stations with representative examples of the contacts of the acidic flows.

Plate	Picture	Field Station	Latitude (WGS84)	Longitude (WGS84)
32	a	EA-461	-26.480970	-51.671860
32	b	EA-442	-26.588460	-51.563390
32	c	EA-461	-26.480970	-51.671860
32	d	EA-456	-26.523540	-51.674530
32	e	EA-456	-26.523540	-51.674530
32	f	EA-456	-26.523540	-51.674530
32	g	EA-432	-26.585180	-51.806960
32	h	EA-455	-26.548950	-51.660880
32	i	EA-455	-26.548950	-51.660880
32	j	EA-442	-26.588460	-51.563390

Table 35 – Selected field stations with representative examples of the internal structure of the acidic flows.

Plate	Picture	Field Station	Latitude (WGS84)	Longitude (WGS84)
33	a	EA-313	-26.588460	-51.563390
33	b	EA-442	-26.581200	-51.698610
33	c	EA-439	-26,581200	-51,698610
33	d	EA-431	-26.577130	-51.748390
33	e	LC-40	-26.581299	-51.700326
33	f	LC-40	-26.581299	-51.700326
33	g	EA-1098	-25.321430	-51.504200
33	h	EA-362	-26.065920	-52.111470
33	i	EA-362	-26.065920	-52.111470
33	j	OL 3570	-23.109740	-49.750560
33	k	OL 4043	-23.753480	-50.905620
33	l	OL 4043	-23.753480	-50.905620
33	m	OL 4055	-23.869970	-51.054330
33	n	OL 3558	-23.118070	-49.813810
33	o	OL 4043	-23.753480	-50.905620

Table 36 – Selected field stations with representative examples of the flow structure and banding of the acidic flows.

Plate	Picture	Field Station	Latitude (WGS84)	Longitude (WGS84)
34	a	OL 3553	-23.090760	-49.847330
34	b	OL 3560	-23.109280	-49.801650
34	c	OL 4043	-23.753480	-50.905620
34	d	OL 4043	-23.753480	-50.905620

Table 37 – Selected field stations with representative examples of the vesicles and amygdales of the acidic flows.

Plate	Picture	Field Station	Latitude (WGS84)	Longitude (WGS84)
35	a	OL 4162	-23.743000	-51.858940
35	b	OL 4162	-23.743000	-51.858940
35	c	OL 4029	-23.649350	-51.108510
35	d	OL 4192	-23.715650	-51.511740
35	e	OL 4097	-23.753160	-51.344740
35	f	OL 4140	-23.820540	-51.661630
35	g	OL 4138	-23.746400	-51.640670
35	h	EA-1177	-25.305280	-52.542420
35	i	JCC214	-25.366670	-52.697150

Table 38 – Selected field stations with representative examples of the diabase and basalt dikes.

Plate	Picture	Field Station	Latitude (WGS84)	Longitude (WGS84)
36	a	OL 3879	-22.867900	-51.251580
36	b	OL 3879	-22.867900	-51.251580
36	c	OL 3879	-22.867900	-51.251580
36	d	OL 3879	-22.867900	-51.251580
36	e	OL 3879	-22.867900	-51.251580
36	f	OL 3906	-22.681020	-51.640480
36	g	OL 3906	-22.681020	-51.640480

Table 39 – Selected field stations with representative examples of the contact between the Serra Geral Gp. basic flows and the Bauru Gp. sandstones.